TALLINN UNIVERSITY OF TECHNOLOGY
SCHOOL OF ENGINEERING
Department of Electrical Power Engineering and Mechatronics

POWER HARDWARE-IN-THE-LOOP SETUP FOR RESEARCH AND DEVELOPMENT OF ISLANDED MICROGRID CONTROL SCENARIOS

REAALAJASIMULAATORI RAKENDUS SAARTALITLUSES MIKROVÕRGU JUHTIMISSTRATEEGIATE UURIMISEKS JA ARENDAMISEKS

MASTER THESIS

Student: Jaak Lepik

Student code: 204337AAAM

Supervisor: Tobias Häring

Co-supervisor: Argo Rosin, Professor

Tallinn 2022

(On the reverse side of title page)

AUTHOR'S DECLARATION

Hereby I declare, that I have written this thesis independently.
No academic degree has been applied based on this material. All works, major viewpoints and data of the other authors used in this thesis have been referenced.

"....." ..... 202…..

Author: .....
/ signature /

Thesis is in accordance with terms and requirements

"....." ..... 202…..

Supervisor: .....
/ signature /

Accepted for defence

"....."..... 202… .

Chairman of theses defence commission .....
/ name and signature /

Non-exclusive Licence for Publication and Reproduction of Graduation Thesis[1]

I, Jaak Lepik hereby

1. grant Tallinn University of Technology (TalTech) a non-exclusive license for my thesis Power hardware-in-the-loop setup for research and development of islanded microgrid control scenarios,

supervised by Tobias Häring and Argo Rosin,

1.1 reproduced for the purposes of preservation and electronic publication, incl. to be entered in the digital collection of TalTech library until expiry of the term of copyright;

1.2 published via the web of TalTech, incl. to be entered in the digital collection of TalTech library until expiry of the term of copyright.

1.3 I am aware that the author also retains the rights specified in clause 1 of this license.

2. I confirm that granting the non-exclusive license does not infringe third persons' intellectual property rights, the rights arising from the Personal Data Protection Act or rights arising from other legislation.

_____ (*date)*

[1] *The non-exclusive licence is not valid during the validity of access restriction indicated in the student's application for restriction on access to the graduation thesis that has been signed by the school's dean, except in case of the university's right to reproduce the thesis for preservation purposes only. If a graduation thesis is based on the joint creative activity of two or more persons and the co-author(s) has/have not granted, by the set deadline, the student defending his/her graduation thesis consent to reproduce and publish the graduation thesis in compliance with clauses 1.1 and 1.2 of the non-exclusive licence, the non-exclusive license shall not be valid for the period.*

ABSTRACT

Author: Jaak Lepik *Type of the work:* Master Thesis

Title: Power hardware-in-the-loop setup for research and development of islanded microgrid control scenarios

Date: 18.05.2022 106 *pages*

University: Tallinn University of Technology

School: School of Engineering

Department: Department of Electrical Power Engineering and Mechatronics

Supervisor(s) of the thesis: Early Stage Researcher Tobias Häring, Professor Argo Rosin

Consultant(s): Tarmo Korõtko

Abstract:

The aim of this thesis is to develop a power hardware-in-the-loop (PHIL) setup that enables to study the effects of flywheel energy storage, PV-system, and different loads on islanded mode duration and the battery's cyclic lifetime in a microgrid.

First, a state-of-the-art overview of microgrids and PHIL setups is given. Various distributed energy sources and energy storage systems are compared and analyzed. The existing TalTech PHIL setup is then investigated, and suitable changes to the testbench are proposed according to the state-of-the-art findings. After adding a controllable PV-system and necessary protective devices to the existing testbench with the FESS, suitable Matlab/Simulink models for the PHIL simulations were researched and developed. Battery energy storage system, PV-generation and load consumption profiles were modelled.

With the upgraded testbench it was possible to develop the PLC programs and researched scenarios. These scenarios include a base scenario consisting of a load and BESS, a scenario with additional PV-system and a scenario with additional PV-system and FESS. The performance of the controller was validated as the Matlab/Simulink and PHIL simulation results were identical during simulations with a 1 second time-step. The PHIL simulation results showed that the PV-system increases the microgrids islanding mode time duration by 11 to 19 hours while also reducing the number of cycles the battery must perform by 26%. The FESS was found to affect the microgrid islanded duration and battery's cyclic lifetime in a negative way due to high inefficiency and low energy storage capacity. The FESS used in this thesis lost on average ~97.26% of the energy used to charge.

Keywords: Microgrid, battery energy storage, flywheel energy storage, power hardware-in-the-loop, battery lifetime, Real time simulation, Simulink

LÕPUTÖÖ LÜHIKOKKUVÕTE

Autor: Jaak Lepik *Lõputöö liik:* Magistritöö

Töö pealkiri: Reaalajasimulaatori rakendus saartalitluses mikrovõrgu juhtimisstrateegiate uurimiseks ja arendamiseks

*Kuupäev:*18.05.2022 106 *lk*

Ülikool: Tallinna Tehnikaülikool

Teaduskond: Inseneriteaduskond

Instituut: Elektroenergeetika ja mehhatroonika instituut

Töö juhendaja(d): Doktorant-nooremteadur Tobias Häring, professor Argo Rosin

Töö konsultant (konsultandid): Tarmo Korõtko

Sisu kirjeldus:

Lõputöö eesmärgiks on luua mikrovõrgu reaalajasimulaatori (PHIL) katsesüsteem, mille abil oleks võimalik uurida hooratasenergiasalvesti, PV-süsteemi ja erinevate koormuste mõju mikrovõrgu saartalitluse ajalisele kestusele ja akusalvesti tsüklilisele elueale.

Kõigepealt anti tänapäevane ülevaade mikrovõrkudest ja PHIL süsteemidest. Võrreldi ja analüüsiti erinevaid hajatootmisüksusi ja energiasalvesteid. Seejärel uuriti olemasolevat TalTech PHIL katsesüsteemi ning pakuti välja muudatused süsteemi täiendamiseks. Muudatuste raames lisati olemasolevale katsesüsteemile juhitav PV-süsteem, tehti vajalikud muudatused kaitseahelates ning seejärel arendati PHIL simulatsioonide jaoks sobilikud Matlab/Simulink mudelid. Modelleeriti akusalvesti ning PV-süsteemi toodangu ja koormuse tarbimise profiilid.

Täiendatud katsesüsteemiga oli võimalik arendada PLC programme ja uurida loodud stsenaariume. Loodud stsenaariumid hõlmasid baas-stsenaariumi, mis koosnes koormusest ja akusalvestist, täiendavast stsenaariumist, kus lisati PV-süsteem ning lisaks stsenaarium, kus lisati PV-süsteem ja hooratasenergiasalvesti. Matlab/Simulink ja PHIL simulatsioonide tulemuste põhjal sai valideeritud, et antud kontroller on võimeline jooksutama 1-sekundilise ajasammuga PHIL simulatsioone. PHIL simulatsioonide tulemused näitasid, et PV-süsteem pikendab mikrovõrgu saartalitluse ajalist kestust 11 kuni 19 tunni võrra ning vähendab akusalvesti poolt tehtavate tsüklite arvu 26% võrra. Leiti, et kasutatud hooratasenergiasalvesti mõjutab negatiivselt mikrovõrgu saartalitluse ajalist kestust ja akusalvesti tsüklist eluiga suurte energiakadude ja madala energiamahtuvuse tõttu. Antud töös kasutatud hooratasenergiasalvesti kaotas ~97.26% laadimisele kulunud energiast.

Märksõnad: Mikrovõrk, akusalvesti, hooratasenergiasalvesti, aku eluiga, saartalitluse ajaline pikkus, reaalajasimulaator, Simulink

THESIS TASK

Thesis title:	**Power hardware-in-the-loop setup for research and development of islanded microgrid control scenarios**	
Student:	**Jaak Lepik, 204337**	
Programme:	**Energy Conversion and Control Systems**	
Type of the work:	**Master Thesis**	
Supervisor of the thesis:	**Tobias Häring**	
Co-supervisor of the thesis:	**Argo Rosin**	
Validity period of the thesis task:	2021/2022	2021/2022 Spring
Submission deadline of the thesis:	**18.05.2022**	

_____	_____	_____	_____
Student (signature)	Supervisor (signature)	Co-supervisor (signature)	Head of programme (signature)

1. Reasons for choosing the topic

Estonia has decided to decisively reduce carbon emission by 2050. This means that the use of fossil energy sources must be reduced, and the share of renewable energy must increase. Renewable energy sources are unpredictable and intermittent, and this can cause problems with grid balancing. Microgrids could be used for grid balancing but nevertheless, there might be mismatches and the ability to operate in islanded mode is important to increase the system's security of supply. The duration of the microgrids islanded mode is mainly determined by its energy storage systems, thus, extending the lifetime of batteries is important. Developing a microgrid system with these properties can be time-consuming and expensive. PHIL setups can be used in this case for faster and cheaper development, as it is possible to use digital twins instead of real devices. This thesis contributes to the research on improving microgrids islanded mode duration and increasing the cyclic lifetime of microgrid batteries.

2. Thesis objective

The aim of the thesis is to develop a power hardware-in-the-loop setup (PHIL) that enables to study the effects of flywheel energy storage, PV-system, and different loads on islanded mode duration and battery's cyclic lifetime in a microgrid.

3. List of sub-tasks:

1. Classification of microgrids and overview of power hardware-in-the-loop (PHIL) setups.

2. Development of the proposed PHIL Setup's electrical and control schematics.
3. Modelling of necessary devices for proposed PHIL setup in MATLAB/Simulink.
4. Development of control strategies and scenarios to increase islanded mode duration and battery lifetime in a microgrid.
5. Validation of MATLAB simulations with the developed PHIL setup and analysis of the results.

4. Basic data:

- Previous student Theses
- Datasheets, manuals from manufacturers.
- Scientific papers in ResearchGate, Scopus.
- Solar irradiation data in Estonia / measured data of existing TalTech 1 kW PV-System.
- Estonian electrical installation standards.
- Load profiles.

5. Research methods

Commercial devices are researched to develop MATLAB Simulink models based on their datasheets. The control strategies for increased battery lifetime and microgrid's islanding time duration are developed, implemented, and tested in MATLAB. MATLAB Real-time simulations are used with the developed PHIL setup to test and validate the models and control strategies. The results are analysed to give recommendations.

6. Graphical material

Graphical materials are used in both the main part of the work and appendixes. The graphical materials include block diagrams, electrical schematics, MATLAB Simulink models, MATLAB simulation results, PHIL simulation results, comparison tables and figures.

7. Thesis structure

Introduction

1. State of The Art
   1.1. Microgrids
   1.2. Power Hardware-In-The-Loop setups
2. Development of the PHIL Setup
   2.1. Existing setup
   2.2. Proposed new system
3. Modelling of objects
   3.1. Battery
   3.2. Programmable load profiles
   3.3. PV-generation profiles
4. Development of control strategies and scenarios
   4.1. Basic device control

4.2. Scenarios

5. Results and validation of control strategies and scenarios

5.1. Error analysis

5.2. Comparison of results

Summary

8. References

- T. Häring, "Research and development of thermal storage control models", Tallinn, 2018.
- F. Plaum, "Development of power conditioning control strategies for flywheel storage in microgrid", Tallinn, 2019.
- N. Cinay, „Research and development of control strategies for energy storages in an islanded microgrid", Tallinn, 2020.
- Datasheets of flywheel, PV-emulator, PV-inverter, battery storage system, Siemens PLC, measurement devices.
- Scientific journals, conferences
- Various web resources

9. Thesis consultants

Tarmo Korõtko

10. Work stages and schedule

State of the art (03.11.2021)

Development of the PHIL Setup (19.11.2021)

Modelling of objects (05.12.2021)

Development of control strategies and scenarios (25.12.2021)

Results and validation of control strategies and scenarios (01.02.2022)

Summary/Conclusions (06.04.2022)

Final version of the thesis (10.05.2022)

CONTENTS

APPLICATION IN ENGLISH

18.05.2022

From: Jaak Lepik (204337AAAM)

To: Ivo Palu

Application

I, Jaak Lepik would like to request the permission to write this Master Thesis in English due to the following reasons:

The main supervisor of this Thesis does not natively speak Estonian, thus there would be a language barrier.

Writing the Master Thesis in English is good preparation for possible doctoral studies in TalTech.

Thank you for your understanding.

Jaak Lepik

PREFACE

This thesis was derived from the research of PhD student Tobias Häring into microgrids.

This thesis topic was provided to me by my supervisors, early-stage researcher Tobias Häring, and Professor Argo Rosin from the Microgrids and Metrology research group. I would like to extend my gratitude to my supervisors for the consistent support and guidance during the development of the thesis.

Furthermore, I would like to thank research scientist Tarmo Korõtko and the rest of the members of the Microgrids and Metrology research group who provided invaluable technical consultations for this thesis.

Jaak Lepik

List of abbreviations and symbols

BESS	Battery energy storage system
DER	Distributed energy resources
DoD	Depth of discharge
DRTS	Digital real time simulator
EOL	End of life (batteries)
FB	Function block
FC	Function
FESS	Flywheel energy storage system
HIL	Hardware in the loop
HUT	Hardware under test
LFP	Lithium Ferrophosphate
NCA	Lithium Nickel Cobalt Aluminium Oxide
NMC	Nickel Manganese Cobalt Oxide
OB	Organization block
PCC	Point of common coupling
PHIL	Power hardware-in-the-loop
PI	Power interface
PLC	Programmable logic controller
PLL	Phase locked loop
RMS(E)	Root mean square (error)
rpm	Rotations per minute
SIL	Software in the loop
SoC	State of charge
TIA	Totally Integrated Automation
LXI	LAN eXtensions for Instrumentation

INTRODUCTION

Climate change and environmental degradation are considered an existential threat to Europe and the world. To overcome these challenges, the European Green Deal was created. The EU Green Deal will attempt to transform Europe into the first climate neutral continent by 2050. The energy sector is estimated to be responsible for more than 75% of EU greenhouse gas emissions. Various actions have been proposed to help reduce the emissions of greenhouse gases in the EU. Notable proposed actions include increasing the share of renewable energy sources at the expense of fossil energy sources, increasing the capacity of energy storages, and integrating energy systems. [1, 2]

As policies and technologies evolve, power systems have become increasingly complex and difficult to design and operate. A major change in the energy sector is the large-scale integration of power electronics based renewable energy sources. Renewables are often considered the main solution to mitigate the effects of climate change. However, the amount of power generated from renewable energy sources is unpredictable and intermittent, and this can cause mismatches between power demand and generation. Mismatches between power demand and generation can lead to reduced power quality and reduced security of power supply. Microgrids could be used to mitigate these problems, but there might still be mismatches, and the ability of microgrids to operate in islanded mode is important for maintaining security of power supply. [3]

The price of power electronics and energy storage systems has dropped drastically in the last decades. Although various sources present different numbers, it is estimated that the price of Li-Ion batteries has fallen by as much as 97% since 1991 [1]. This has increased the economic viability of using Li-Ion batteries in smart and microgrids. Battery energy storage systems (BESS) generally set the maximum islanded mode time duration of 'green' microgrids. As battery energy storage systems are still quite expensive, extending the lifetime of batteries can be incredibly beneficial. [4]

The systems used in the energy sector are becoming more intelligent and complex. For example, developing a microgrid system can be time-consuming and expensive. This has led to increased demand for laboratory testing facilities to reduce product development time and costs. As a result, there is increasing demand for PHIL setups. PHIL is a real-time simulation environment that consists of real physical electrical devices and digital twins of real devices. Programmable power supplies and programmable loads are typically used in PHIL simulations to emulate real-world electrical generation units and loads. PHIL systems allow for faster and cheaper

development, and they provide the means to simulate scenarios that are difficult to achieve in the real world. [5]

The aim of this thesis is to develop a power hardware-in-the-loop setup (PHIL) that enables to study the effects of flywheel energy storage, PV-system, and different loads on islanded mode duration and the battery's cyclic lifetime in a microgrid.

The master thesis has been divided into five main chapters. The first chapter presents a state-of-the-art overview of microgrids, renewable energy sources, energy storage systems, and power hardware-in-the-loop (PHIL) setups. The second chapter focuses on the development of the PHIL setup. Existing TalTech PHIL setup is described, and an upgraded PHIL setup is proposed. Electrical schematics of the proposed PHIL setup are created. The third chapter pivots around Matlab/Simulink modelling and the development of object models for the PHIL setup. The battery energy storage system is modelled on the basis of the datasheet of a chosen real device. PV-generation and load-consumption profiles with a 1 second time-step are also modelled. The fourth chapter focuses on the development of PLC programs and simulation scenarios. Device control and data processing are also described in this chapter. The final chapter focuses on the results of PHIL-simulations. Results are compared, analyzed, and conclusions are drawn.

1. STATE OF THE ART

1.1 Microgrid

A microgrid (MG) is, in essence, a small, compressed version of the main electrical grid [6]. The design of a microgrid is fundamentally similar to the design of the main electrical grid, as both must ensure the security of the supply of electricity to consumers. Microgrids can be connected to the main grid but also have the functionality to operate independently of the main grid. The microgrids connected to the grid are connected to the main grid through a Point of Common Coupling (PCC). Microgrids typically consist of a central controller, smart energy meters, distributed energy sources (solar, wind, hydrogen etc), energy storage systems (batteries, flywheels etc), and electrical loads. The goal of the microgrid system is to provide electricity in a sustainable, safe, and economical manner with intelligent monitoring and control technologies [7]. The general concept of the microgrid and its common system elements are shown in Figure 1.1.

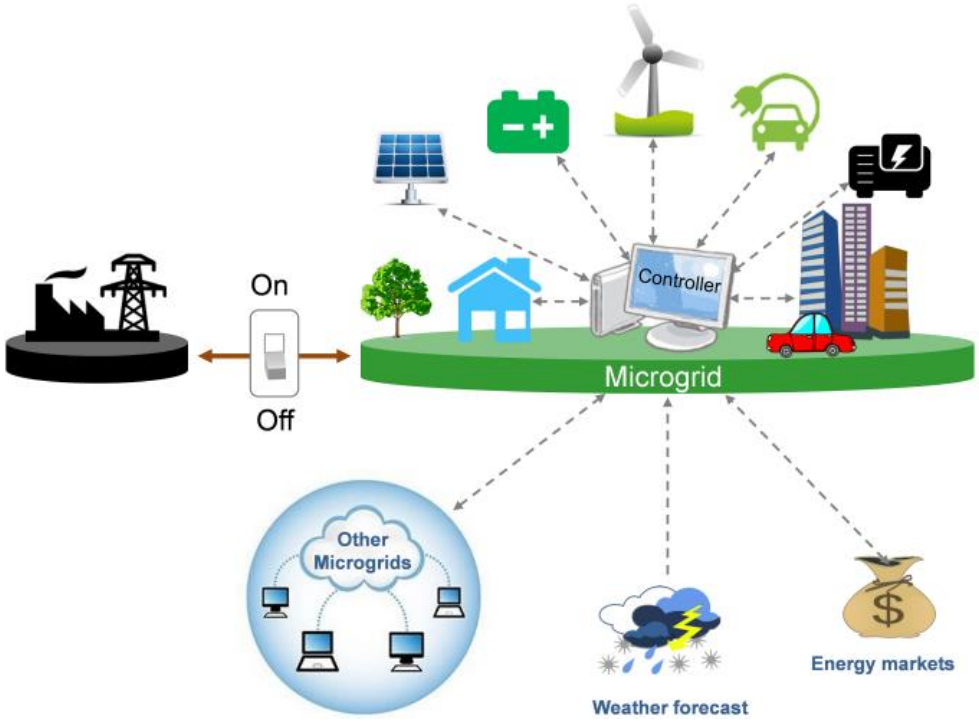

Figure 1.1 Concept of microgrid [8]

Microgrids are especially useful for main grid operators, hospitals, and other critical service providers to increase the security of supply as they cannot tolerate any power disruptions. Additionally, households, commercial buildings, and even districts can benefit from microgrid solutions. It is important to understand why microgrids are so important. Implementing microgrids and accompanying technologies offers several key benefits [9, 10, 11]:

- Improved security of supply and stability for the local grid and the main grid.

- Potential to help balance the main grid: microgrids are controllable prosumers from the point of view of the main grid operators.
- Reduced grid congestion and peak loads.
- Easier integration and better optimized control of renewable energy sources, energy storages, and flexible loads.
- Reduced costs for both energy producers and customers by reducing transmission losses and offering more efficient energy management solutions.
- Possibility to offer new life-enhancing ancillary services to customers.
- Possibility to generate revenue by participating on the power market or providing additional flexibility services to the main grid.
- Microgrids promote 'environmentally friendly' energy solutions.

Managing a microgrid can be quite difficult, especially in islanded mode, due to a lack of inertia and the high penetration of power electronics-based converters. Power electronics-based converters play a vital role in microgrids, but they do not provide natural inertia. The low inertia of the islanded microgrid reduces the stability of the system and increases the difficulty of frequency control. The frequency and overall power quality can fluctuate a lot, and this means that microgrids need to have an adaptive protection system that is able to react faster and better than traditional protective and switching devices.

1.1.1 Classification of microgrids

The requirements (management, protection system etc) of a microgrid depend on the type of microgrid under consideration. It is possible to classify various microgrids based on various variables: parameters, functionalities, and capabilities. For this thesis the most relevant classifications of microgrids are based on [11, 12]:

- Mode of operation
- System topology
- Implemented energy sources

Figure 1.2 presents the used classification of microgrids in this thesis.

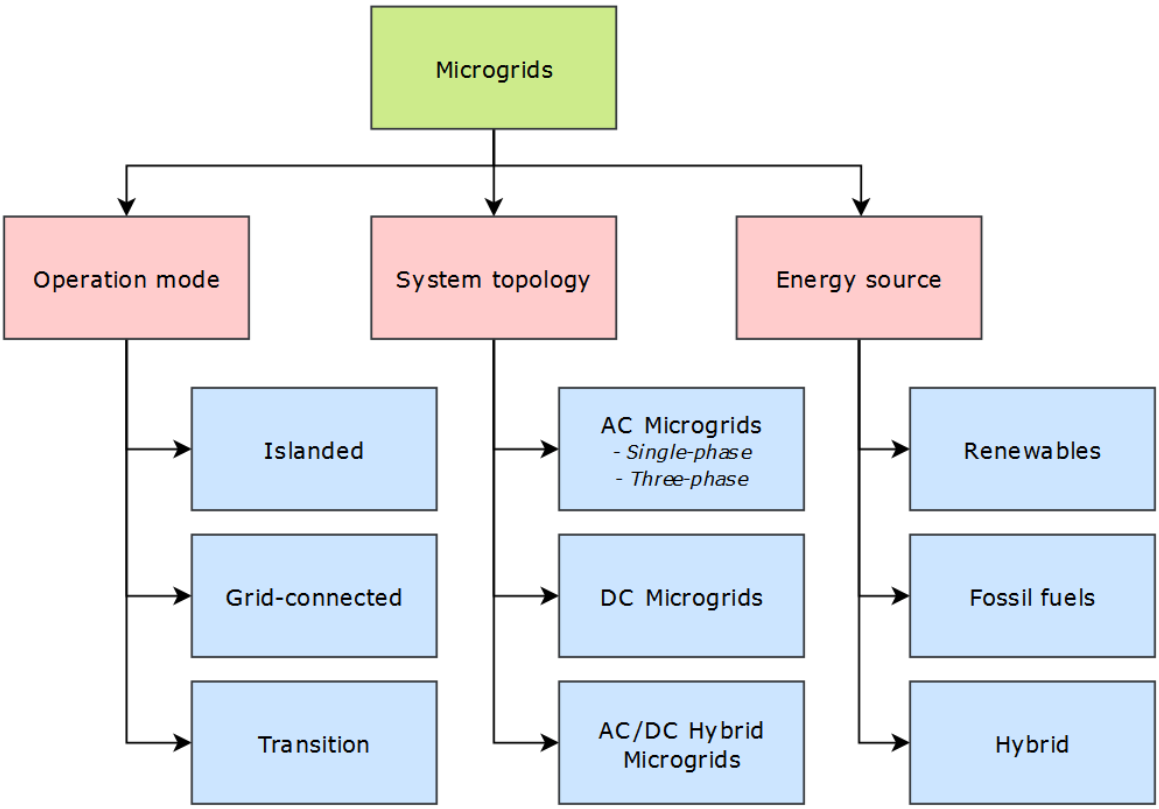

Figure 1.2 Classification of microgrids

Operation mode of microgrid

As presented in Figure 1.2, microgrids can operate in either grid-connected or islanded mode. There is also an additional temporary transition mode that occurs as the microgrid switches between grid-connected and islanded modes.

In grid-connected mode, the microgrid is connected to the main grid. This means that the microgrid acts as a prosumer from the view of the main grid and the whole stability-balancing aspect of the microgrid is quite simple as the microgrid is synchronized with the main grid. There are usually no problems with surplus and deficit of energy in grid-connected microgrids, as the main grid can either soak up all the surplus energy or, in case of energy deficit, the energy can be imported from the main grid. Grid-connected microgrids are often cheaper than isolated islanded microgrids as energy storage systems are optional and can be downscaled. This is because grid-connected microgrids often only need to be able to operate in islanded mode for a limited time duration or not at all. Figure 1.3 shows a grid-connected AC microgrid topology [7].

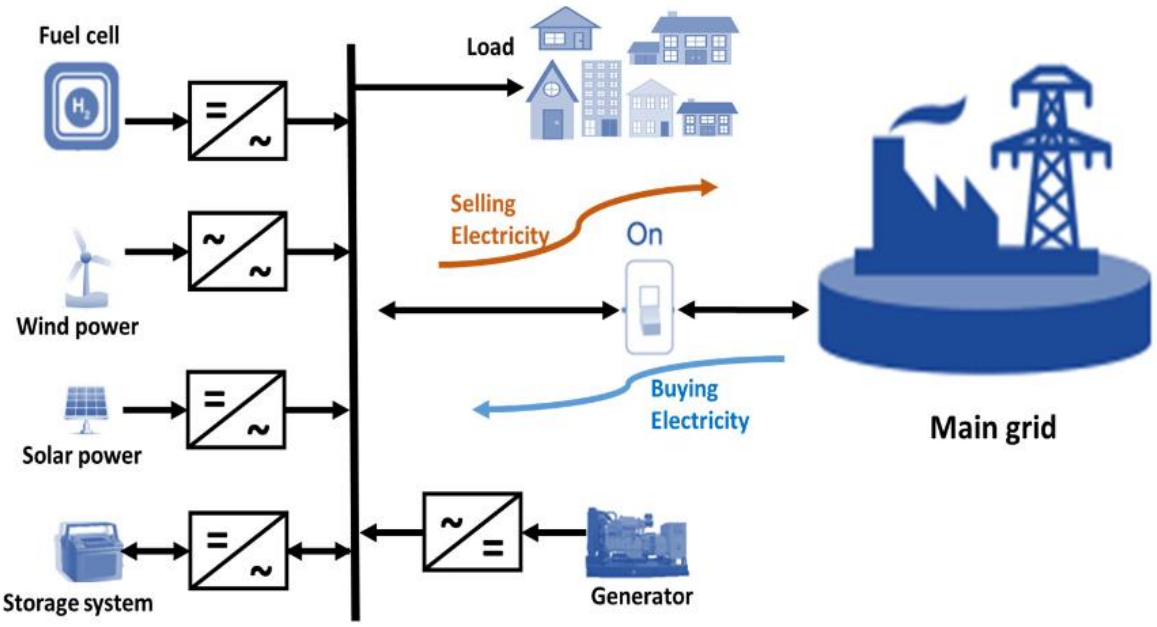

Figure 1.3 Grid-connected microgrid topology [7]

In islanded mode the microgrid is not connected to the main grid. Operating microgrid in islanded mode is much more complex as it requires more advanced devices and controls to ensure the stability of the system. There must be at least one grid-forming device to emulate the electrical grid, a real-time measurement system, and an advanced control system. In this mode, the microgrid acts like UPS and is load-following. The topology of an islanded AC microgrid is presented in Figure 1.4 [7].

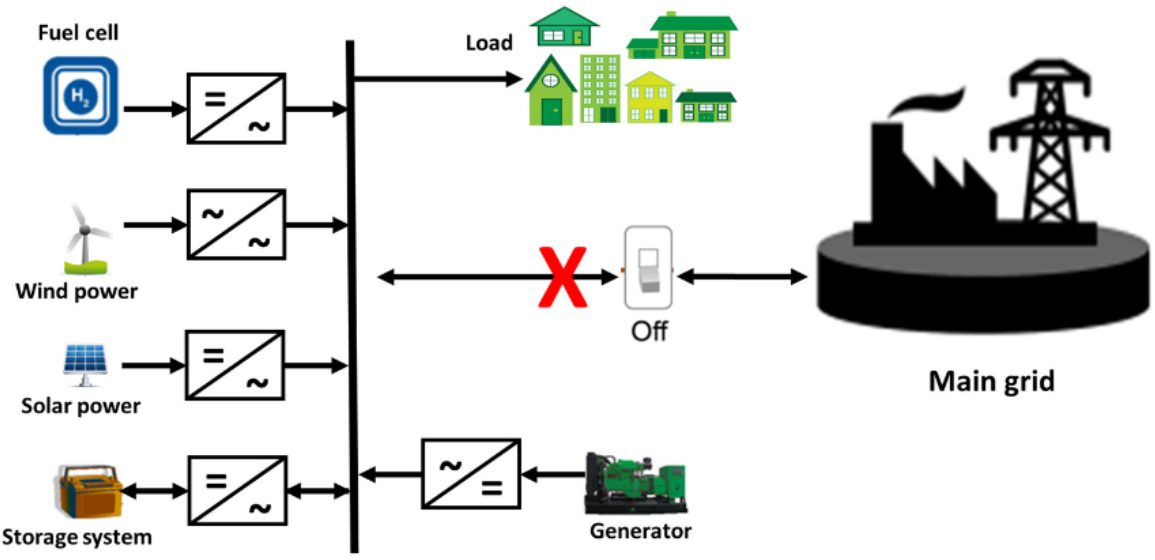

Figure 1.4 Islanded microgrid topology [7]

Microgrid system topology

Based on the distribution system's topology (voltage characteristics), microgrids can be classified as AC, DC, or hybrid AC/DC microgrids. Each system has its own advantages and disadvantages:

AC microgrids are the most conventional microgrids. They use AC voltage for distribution and provide simple integration with the main grid. Due to the popularity of AC distribution networks, there are also many proven and inexpensive AC voltage devices available. There are also several issues regarding AC microgrids: reduced system stability and power quality, synchronization issues, higher control complexity. These issues often require complex control algorithms to keep the system balanced and frequency within allowed limits. AC microgrids can be classified by the configuration of the distribution system:

- Single-phase microgrids
- Three-phase microgrids

Single-phase microgrids (SP-MG) use 230V phase-to-neutral voltage single-phase distribution system. Such microgrids are becoming increasingly popular due to declining cost of battery storages and single-phase hybrid inverters. Single-phase microgrids are most viable for small households in a remote location. The main disadvantage of SP-MGs is the inability to provide power to three-phase consumers.

Three-phase microgrids (TP-MG) use 400V phase-to-phase voltage three-phase distribution system. The main advantages of TP-MGs are the ability to integrate larger renewable energy sources and power both three-phase and single-phase consumers. TP-MGs are more common in larger applications such as military complexes, commercial buildings, etc. The main disadvantage of TP-MG is the increased complexity of the control system.

DC microgrids have emerged due to widespread application of power electronic devices and increased availability of environmentally friendly DC-based energy sources. These microgrids use DC voltage and offer improved efficiency compared to AC microgrids. The increased efficiency comes from fewer power conversion stages as energy storage systems and many renewable energy sources such as PV panels are DC-based. There are also several issues regarding DC microgrids: protective systems are complex and expensive, and DC microgrids are suited for less popular DC loads. The main differences between the AC and DC microgrids are presented in Table 1.1 [13].

Hybrid AC/DC microgrids use both AC and DC distribution networks. Hybrid microgrids are supposed to complement the best of AC and DC microgrids. This results in improved distribution efficiency and reliability of the system and better integration options. The main problems with hybrid AC/DC microgrids are the complexity of network structure and that managing such a microgrid requires very advanced control methods and algorithms.

Table 1.1 Comparison of AC and DC microgrids [13]

Factors	**AC microgrid**	**DC microgrid**
Conversion efficiency	Multiple energy conversions reduce efficiency	Fewer conversion processes increase efficiency
Transmission efficiency	Continuous reactive current loss reduces efficiency	Absence of reactive components increases efficiency
Stability	Affected by external disturbances	Free from external effects
Synchronization	Synchronization required	No synchronization issues
Power supply reliability	Supply can be affected during seamless transfer	Power supply generally reliable
Microgrid controls	Complex control process due to frequency	Simple control approach
Protection system	Simple, cheap, and mature protection schemes	Complex, costly, and immature protection components
Suitability	AC loads	DC loads

1.1.2 Microgrid energy sources

Microgrids can be categorized based on the energy sources implemented. Microgrids may consist of only renewable energy sources or of only fossil energy sources, or a combination of both [14].

Renewables-only microgrids are becoming increasingly popular as technology and society have evolved. These microgrids generate power from renewable energy sources, such as solar and wind, and store it in energy storage systems for later use. Historically such microgrids were nearly impossible to develop as energy generation and storage systems were not as evolved, and their pricing wasn't competitive enough. Renewables-only based microgrids are typically more expensive to develop but have lower running costs. The increased cost of development is because a renewables-only microgrid with good security of supply would need to have either an overdimensioned energy storage or incredibly versatile renewables generation. The reduction in running costs is due to the lack of need to buy fossil energy sources such as diesel fuel. [15]

Fossil fuel based microgrids are currently the most widespread according to [16]. This is because diesel generators and combined heat and power (CHP) plants are reliable

and require smaller initial investments. These microgrids however have negative effect on the climate and high running costs.

Hybrid-powered microgrids use both renewables and fossil fuels as energy sources. Integration of renewables and fossil fuels creates an opportunity to develop economically viable microgrids that have a high security of supply and reduced environmental footprint [15, 14]. All the mentioned microgrids can be easily developed and optimized in software like HomerPRO [17].

Distributed generation (DG) units

The most common generation sources used in microgrids are diesel generators, CHP plants, Solar PV, hydro plants, and wind turbines [16]. These generation sources are different and thus they have their own pros and cons. It is important to note that the selection of energy source(s) needs to be based on the specific microgrid and its needs. The energy sources in microgrids can be classified according to [18, 19]:

- their availability
- output voltage characteristics
- controllability
- type of interface
- power flow control

PV-systems, wind turbines and micro-hydro plants are all considered to be environmentally friendly. However, they are dependent on geographical location and are mostly uncontrollable. Wind turbines and micro-hydro plants are not viable in Tallinn, Estonia due to the urban area limitations, low mean wind speed and the lack of suitable rivers [20].

As diesel generators are not environmentally friendly, they will not be considered for investigation in this work. CHP with a natural gas generator could be a great option to increase the reliability of microgrid system, but due to the economies of scale, the pricing is quite uneconomical for small (<15 kW) installations. It is important to note that the price of natural gas has jumped up nearly 900% in 2021, which currently further reduces the economic viability of natural gas-based generators. [21]. In Table 1.2 the investigated microgrid generation sources are compared based on the classifications above.

Table 1.2 Characteristics of common microgrid generation sources [19, 14]

Characteristics	PV-System	Wind	Micro-Hydro
Availability	Dependent on geographical location	Dependent on geographical location	Dependent on geographical location
Output voltage	DC	AC	AC
Control	Uncontrollable	Uncontrollable	Uncontrollable
Typical interface	Power electronic converter (DC-DC-AC)	Power electronic converter (AC-DC-AC)	Synchronous of induction generator
Power flow control	MPPT, DC link voltage control	MPPT, pitch and link voltage control	Controllable

In conclusion, the best environmentally friendly generation source for Tallinn, Estonia is solar (PV-system). This is because of the competitive pricing of PV-systems, and the fact that they do not require additional space. They can be installed on rooftops.

1.1.3 Energy storage systems

Microgrids should have some form of energy storage to balance the power supply and demand. Energy storage systems are also responsible for providing emergency power supply in islanded mode operation for grid-tied microgrids. The process of energy storge is not perfect and there are energy losses included, although these losses are minimal for modern systems compared to the value that the storage systems can deliver. The main energy losses typically occur during the charging and discharging (round trip efficiency) of the energy storage. Storing losses (self-discharge) vary greatly depending on the type of energy storage and its surrounding environment. [19]

The energy storage systems are usually chosen based on the size of the microgrid and the requirements for the storages reaction time and microgrid islanded mode duration. Figure 1.5 describes the various energy storage systems used in microgrids. Batteries and flywheels are the preferred storage method as their power ratings are best suited for small microgrids. Additionally, they are usually more compact and have lower initial investment requirements compared to other energy storage technologies such as hydro-based storage. Based on Figure 1.5 and market research, it can be concluded that Li-Ion and lead-acid Batteries are the best battery chemistries for microgrids as they are widely available and have suitable power ratings. [19]

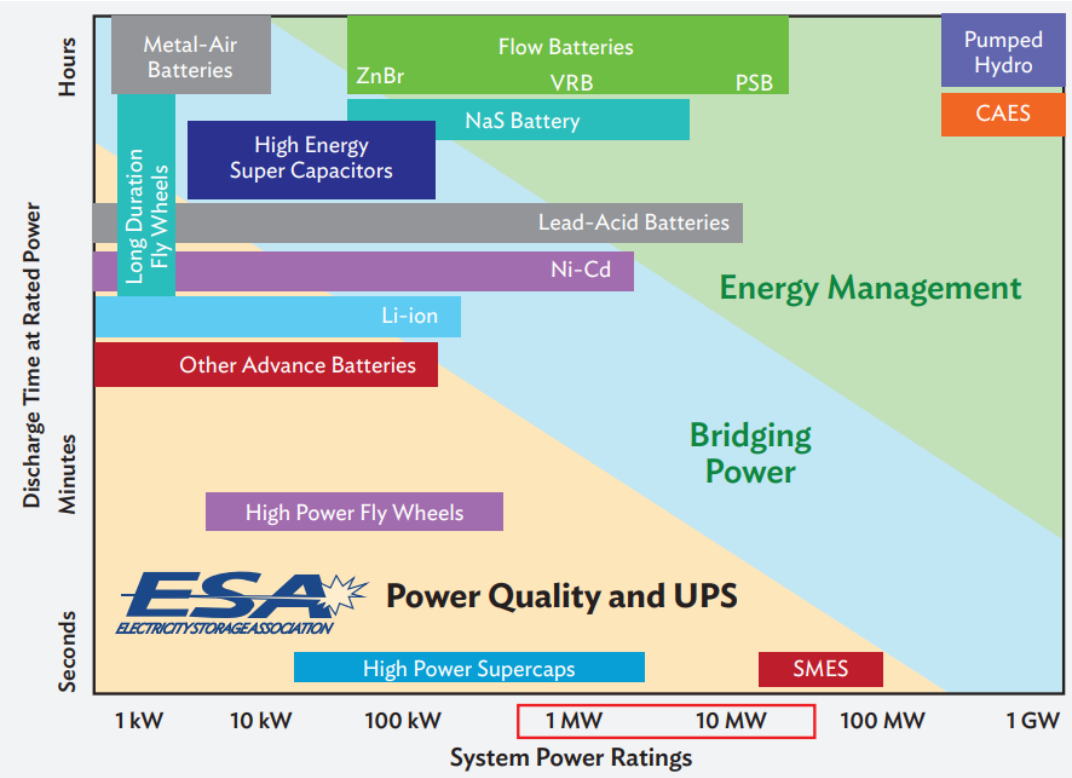

Figure 1.5 Comparison of energy storages used in microgrids [19]

Battery energy storage

Batteries consist of three parts: a cathode, an electrolyte, and an anode. Depending on the type of the battery these can be various chemicals. Repetitive cycling of the battery damages the chemicals, thus reducing its lifetime. In essence all batteries are similar, as they operate for a while, need recharging, and require an eventual replacement as the battery's capacity fades. [22]

Table 1.1 compares the two selected battery chemistries for microgrid energy storage system. Li-Ion batteries have great specific energy and energy density. Additionally, they allow high Depth-of-Discharge at high C-rates (typically 0.5-2 C). Their main disadvantages are their limited cyclic lifetime and high cost. Lead-acid batteries have been around for a long time, and they are reliable and cheap. Their disadvantages are low specific energy and power, which translates to much larger and heavier battery packs compared to Li-Ion batteries. They also have quite low cyclic lifetime and charge/discharge quite slowly. While lead-acid batteries are still popular, the future looks more promising for Li-Ion batteries for microgrid and residential energy storage systems. This is because Li-Ion batteries have a longer cyclic lifetime, and they have higher charging and discharging C-rates, which is especially useful for offering ancillary services to the main grid or for storing the energy during the cheapest hours of the day

for later use. As Li-Ion batteries were found to be better for microgrid applications, they will be researched in more detail.

Table 1.1 Comparison of Li-Ion and lead-acid batteries [23, 24]

Metric	**Li-Ion**	**Lead Acid**
Specific energy (kW/kg)	90-250	30-50
Energy density (kWh/vol)	94-500	25-415
Specific power (W/kg)	8-2000	25-415
Cycle life	500-10000	200-2000
Advantages	• Very fast response • High specific power • High DOD • Good C-rates	• Mature technology • Cheaper
Disadvantages	• Safety concerns (based on used chemistry) • High cost	• Low cyclic life • Low DoD • Low C-rates

Lithium-Ion batteries have high energy density, are considered safe and they are commercially available batteries. These batteries do not require scheduled cycling and they do not have memory. Historically Li-Ion batteries were used in mobile phones, laptop computers etc. Nowadays they are increasingly being used in the electric mobility sector, grid-tied energy storages and microgrids. Although Lithium-Ion batteries have drawbacks, such as the need for protection circuits, performance drops with either too low or high temperatures, there is no doubt that their advantages outweigh the disadvantages. The main advantages of Lithium-Ion batteries are their high energy density and capability to handle high loads with power cells, long cycle-life, lack of maintenance, high capacity and high charging/discharging rate which allows the battery to be quickly charged and discharged. One of the most important advantages of Lithium-Ion batteries is their safety. The advantages and disadvantages of Lithium-Ion batteries are summarized in Table 1.2. The main characteristics of Lithium-Ion battery cells are: [23, 24]

1. Specific energy (Maximum storable energy per mass unit, Wh/kg)
2. Specific power (Maximum power per mass unit, W/kg)
3. Cost (Availability, processing complexity, cost of raw materials)
4. Safety (Temperature threshold for thermal runaway, other risk factors)
5. Lifespan (Maximum Cycle-life, calendrical age)
6. Performance (Voltage, capacity, resistance)

Table 1.2 Advantages and disadvantages of Lithium-Ion batteries [23, 24]

Advantages	**Disadvantages**
High energy density and can handle high loads	Need protection circuits to prevent thermal runaway if stressed
Long cycle-life and maintenance-free	High temperature causes degradation
High capacity and good coulombic efficiency	Charging power limitations at freezing temperatures
High rate of charging/discharging, high depth of discharge (DOD)	Relatively expensive
Considered safe	

The most attractive and commercially mature Lithium-Ion cell chemistries are currently considered to be Lithium Ferrophosphate (LFP), Lithium Nickel Manganese Cobalt Oxide (NMC), Lithium Nickel Cobalt Aluminium Oxide (NCA) [23, 22]. Table 1.3 and Figure 1.6 summarize the comparison of different Lithium-Ion cell chemistries [24, 25].

Table 1.3 Comparison of different Lithium-Ion batteries [24, 25]

Chemistry	**Lithium Iron Phosphate**	**Lithium Nickel Manganese Oxide**	**Lithium Nickel Cobalt Aluminium Oxide**
Abbreviation	$LiFePO_4$ (LFP)	$LiCoO_2$ (NMC)	$LiNiCoAlO_2$ (NCA)
Nominal voltage	3.3V	3.7V	3.6V
Voltage range	2.5-3.65V/cell	3.0-4.2V/cell	3.0-4.2V/cell
Specific Energy (Wh/kg)	90-120	150-220	200-300
Charge rate (C-rate)	1.0C	0.7-1C	0.7C
Discharge rate (C-rate)	1.0C	1C	1.0C
Lifespan (Cycle-life)	2000+	1000-2000	500
Thermal runaway	270°C	210°C	150°C
Price	~370 €/kWh	~580 €/kWh	~350 €/kWh

In conclusion, Lithium Iron Phosphate (LFP) chemistry provides greater safety, specific power, and longer lifespan compared to other studied chemistries. This makes LFP the best option for a relatively low-power system that requires high safety such as a small microgrid.

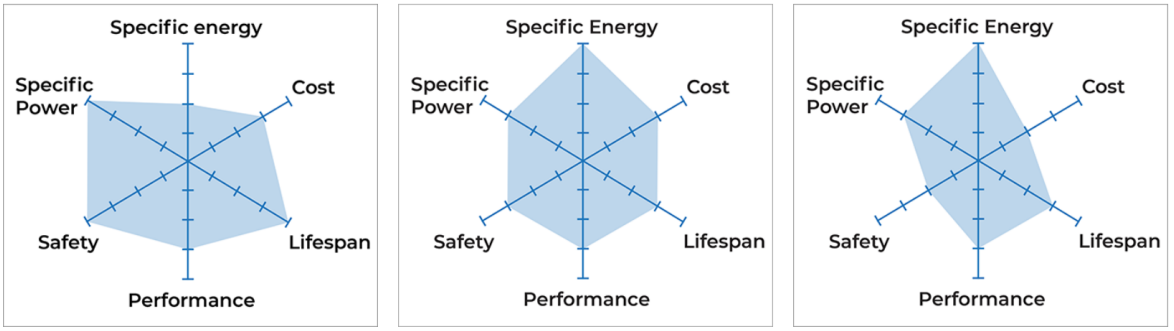

Lithium Ferrophosphate (LFP) **Lithium Nickel Manganese Cobalt Oxide (NMC)** **Lithium Nickel Cobalt Aluminum Oxide (NCA)**

Figure 1.6 Comparison of the main characteristics of various Lithium-Ion batteries [25]

BESS lifetime influence overview

The economic viability of BESS is directly related to its operational lifetime. The lifetime of BESS depends on different factors, such as charge and discharge cycles, depth of discharge, time, and environmental conditions such as temperature.

The useful life (in cycles) of the battery depends on two factors: cell chemistry and aging. Cell chemistry includes, anode and cathode materials, cell capacity, energy density, and energy-to-power ratio. Aging includes calendar aging and cycling aging. Calendar aging is caused by the reactions at the electrodes that occur when the battery is not being cycled. Cycling aging is caused by the stress put on battery by charging and discharging.

Batteries that are discharged very deeply (to below 20% SOC) tend to age faster. It is recommended to keep battery maximum DOD to 90% to prolong battery life. Figure 1.7 shows how cycling depth affects the cyclic lifetime of the LFP battery. By lowering the maximum permissible depth-of-discharge, the battery yields greater lifetime energy throughput. Some sources claim that the total lifetime energy throughput of a Li-Ion battery can increase by 10 times by lowering the maximum DOD from 100% to 10%. [23]

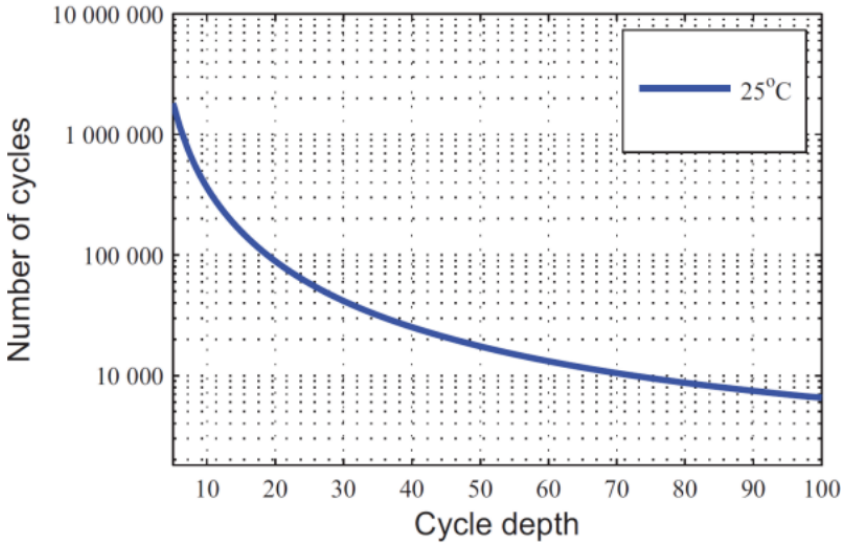

Figure 1.7 LFP battery lifetime curve [23]

Current generation batteries are considered useful while their capacity remains above 80% of their nominal capacity. Reaching 80% nominal capacity is called battery's end-of-life (EOL) [26]. This means that once a 10 kWh BESS maximum storage capacity has dropped to 8 kWh, it should be replaced with a new equivalent battery. However, this does not mean that the batteries cannot be used at all and, depending on their usage, they could be used for years after reaching EOL. Extending the lifetime

of batteries can be very difficult depending on the purpose of the BESS. Batteries that provide critical services or power systems operating in islanded mode are usually load-following and have very minimal to no flexibility of their own.

Flywheel Energy Storage

The flywheel is a mechanical device that is specifically designed energy storage system that stores kinetic energy in a spinning mass, called a rotor. Kinetic energy is charged to and discharged from the flywheel via an electric drive capable of operating as both a motor and a generator. The kinetic energy is stored by applying torque to the flywheel, which increases the speed of the flywheel (and thus the energy stored). During discharging, the motor acts as a generator that decelerates the rotor and discharges power as a result.

Modern flywheels typically consist of a flywheel (rotor), electrical drive, power conversion system, protective containment, and bearings. A schematic of a simple FESS is shown in Figure 1.8. The AC/DC/AC Power conversion system, visible on top of the figure is responsible for integrating the flywheel energy storage with grid and it must support bidirectional power flow. The electrical drive acts as either a motor or a generator and is tasked with accelerating, maintaining, or decelerating the flywheel (rotor). The main shaft acts as a connector between the electrical drive and the rotational mass (flywheel). The primary objective of the chamber is to protect the surrounding environment from malfunctions. Flywheels can be both very heavy and operate with high velocity meaning that they have great destructive power. Additionally, the chamber can be used to improve the efficiency of flywheel energy storage by applying vacuum in the chamber. This helps to reduce the air friction. High quality bearings and their maintenance is important to minimize the friction losses.

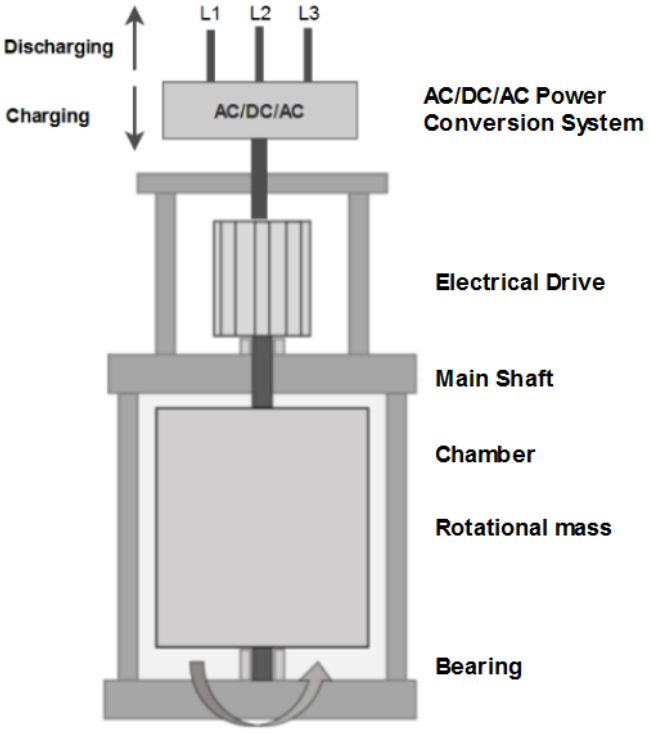

Figure 1.8 Schematic of a FESS based on [27, 28]

One of the most important aspects of using flywheels as energy storage is considering their energy losses due to friction. Old flywheels operating without vacuum chamber and magnetic bearings cannot be taken seriously when considering high efficiency solutions. New generation flywheel energy storages use the previously mentioned and additional methods to increase the overall efficiency of the flywheel energy storage. According to equation 1.1 the energy stored in flywheel scales linearly with the inertia of the flywheel and by the square of the rotational speed hence lightweight high-speed flywheel systems can store more energy than heavier and slower ones.

$$E_k = \frac{1}{2} I \omega^2 \tag{1.1}$$

The moment of inertia of a solid cylindrical flywheel can be expressed with equation 1.2. According to the equation the moment of inertia scales linearly with the mass of the flywheel and by the square of the radius of the flywheel. Therefore, flywheels with a larger radius can store more energy.

$$I = \frac{1}{2} m r^2 \tag{1.2}$$

FESS-BESS comparison

Table 1.4 showcases the differences between FESS and Li-Ion based battery energy storage systems. FESS stores relatively little energy and discharges quickly but can operate for very many cycles with regular maintenance. BESS can store a lot of energy and is capable of discharging at rated power for an extended period. BESS, however, has limited cyclic lifetime. Based on this, the combination of BESS and FESS could be used to help mitigate the weaknesses of each other. FESS could be used to supply the short, high peak loads while the BESS could be used as the microgrids main power supply for long term. FESS typically has a faster response time compared to BESS, which is especially useful for smoothing load peaks and helping with frequency balancing [29, 30].

Table 1.4 Comparison of potential storage systems [23]

Metric	**FESS**	**Li-Ion**
Specific energy (kW/kg)	5-200	90-250
Energy density (kWh/vol)	0.25-424	94-500
Specific power (W/kg)	400-30000	8-2000
Cycle life	Indefinite	500-10000
Advantages	Very fast response High specific power Low cost Long life	Very fast response High specific power High DOD Good C-rates
Disadvantages	Low energy density High self-discharge Requires more maintenance	Safety concerns (based on used chemistry) High cost

Conclusion: hybrid energy storage

It can be concluded that the battery energy storage systems and flywheel storage systems are not competitors, but they can instead effectively complement each other. BESS can store energy for longer periods of time but has limited lifetime due to cycling degradation. FESS can operate up to millions of charge cycles with regular maintenance, but it cannot store energy for long term as its self-discharge is higher. FESS can be more beneficial in storing the energy for short durations while BESS is more efficient for storing energy for longer periods. FESS could also be used to smooth the load peaks while BESS, could supply the constant load at reduced peak currents. The reduction of peak currents should help prolong the lifetime of battery storage system as well as reducing the cycles performed by the BESS. [31]

1.1.4 Microgrid technical challenges

Microgrids and their implementation have many challenges such as lack of scalable prototype installations, lack of unified microgrid performance metrics, various country or region-based regulations, cybersecurity concerns etc. The most important microgrid challenges in the view of this thesis are the technical challenges. The main technical challenges regarding microgrids are [19, 32]:

- Maintain high power quality
- Control strategies
- Energy management
- Stability and reliability
- Protection

Power quality is one the most important issues in a microgrid due to intermittent nature of renewable energy sources, transition between grid-connected and islanded mode, high reactive power, and nonlinear loads. Power quality disturbances in AC microgrids adversely affect the frequency and voltage of the system via voltage fluctuations, transients, and voltage flickers. It is possible to utilize batteries, flywheel energy storages, and filters to increase the system power quality [19, 32].

Control strategies are necessary to maintain required microgrid parameters such as frequency and voltage within certain limits and perform demand-side management etc. Microgrids can use various control strategies to maintain the required power quality (e.g., active/reactive power (PQ), voltage/reactive power (V-Q), frequency/active power (f-P), voltage/frequency (V/f)) [19] [33].

Energy management system must ensure the efficiency and stability of the microgrid. This is achieved by combining different energy storages and managing power flows between different energy sources and storage systems within the microgrid based on generation and load forecasting [19, 34].

Stability and reliability are key issues for microgrids due to grid synchronization and transition from grid-connected to islanded mode, lack of inertia, supply-demand randomness, reverse power flows of renewable generation units, unpredictable frequency deviations in islanded mode [19] [32].

Protection in microgrids is of critical importance as it is in all electrical power systems. There are certain technical requirements to ensure that the required response to microgrid and main grid faults is as fast as possible to isolate the microgrid from the main grid. One of the bigger issues in microgrids is that the short circuit capacity is

different in grid-connected and islanded mode and traditional overcurrent protective devices may not actuate when necessary. There are various methods to deal with this issue such as using adaptive protection system to change relay settings in real time or using digital relays that can be remotely controlled to ensure the protection of the microgrid [19] [32].

There are several standards regarding AC microgrids should be used to aid in the planning and design of a new microgrid as they describe various technical specifications, general conditions, and rules for interconnected microgrids. These standards are [19]:

- IEEE 1547 – Criteria and requirements for interconnection of DERs with the main grid
- EN 50160 – Voltage characteristics of electricity supplied by public electricity networks
- IEC 61000 – General conditions or rules necessary for achieving electromagnetic compatibility
- IEEE C37.95 – Protective relaying of utility-consumer interconnections

IEEE 1547 is a set of technical specifications that defines the performance and functionalities of DER connected to the distribution grid – the part of the electric grid that delivers power to homes and buildings. This standard provides uniform requirements for the safe interconnection of DER to the grid and details the associated tests needed for the interconnection.

EN 50160 describes the voltage characteristics of the electricity supplied by public distribution networks. This is an important standard for voltage characteristics as it provides information on power quality, frequency, and voltage variations such as voltage sag and swell, unbalanced voltage, current flows, and harmonics in microgrids.

IEC 61000 describes general conditions or rules necessary for achieving safety functions and integrity of requirements related to electromagnetic compatibility.

IEEE C37.95 describes the protective relaying of main grid-consumer interconnections.

1.2 Power hardware-in-the-loop (PHIL)

As contemporary power system devices and solutions are becoming increasingly complex, the planning and designing of these systems can become time intensive and expensive. This has led to the increased demand for laboratory testing facilities to reduce product development time and to validate their performance. The practise of hardware-in-the-loop (HIL) and software-in-the-loop (SIL) testing has become common in validating the safety and performance of power systems. [35]

Traditionally, new devices and control systems were tested directly on the proposed system or on the device. Although such an approach provides the highest testing fidelity, such a practise can be very time-consuming and expensive. Also, such a method has reduced test coverage.

Hardware-in-the-loop (HIL) is the current household standard for developing and testing new complex control, protection, and monitoring systems. The main difference between traditional development is that the physical device(s) are replaced by an equivalent computer model that is running in real-time on a simulator that interfaces with testable equipment. This provides the system with the capability to exchange control and measurement signals. [36]

Software-in-the-loop (SIL) simulation represents the integration of compiled production source code into a mathematical model simulation. SIL provides a virtual simulation environment for the development and testing of different control strategies for complex systems. SIL accelerates the production time for development by allowing the user to test the developed programs before hardware prototyping. [36]

Power hardware-in-the loop (PHIL) simulations represent a natural extension of HIL, in which the real-time simulation environment is capable of exchanging control and measurement signals, and the power required by the Hardware Under Test (HUT) [36]. The inclusion of real power improves the test fidelity as testing can be performed under more realistic conditions. PHIL setups typically consist of three main parts: the HUT, the PI, and the Simulation Module [37].

- *Hardware-under-Test (HUT)*: In the domain of microgrids, it is usually either the microgrid as a whole or a specific device(s). The device(s) could be a generation source, consumer or even the microgrids controller. This is the basis for the PHIL system, as it defines the element that is examined.

- *Power Interface (PI)*: It provides the ability to set the operating points of the real electrical system. The PI set output variable can be either the voltage or current.

- *Simulation Module*: It is usually a Digital Real-Time Simulator (DRTS) that calculates new reference values based on the measured values received and the mathematical model. The calculated values are sent to the power interface as analog signals or digital values. The specifics depend on the used real-time simulator and the power interface.

The basic structure of a PHIL setup is shown in Figure 1.9 [5, 38]. Furthermore, the figure showcases how the software and hardware are conjoined in the PHIL setup.

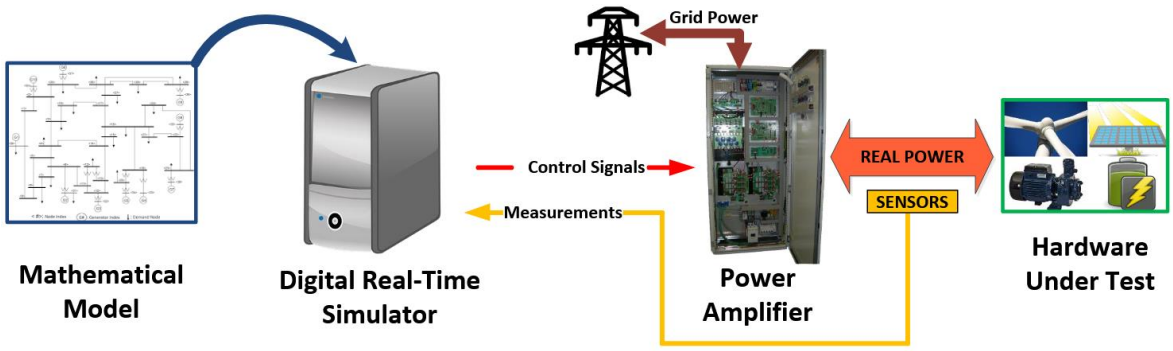

Figure 1.9 Basic structure of a PHIL setup [5]

There are four main benefits of implementing PHIL technologies:

- Faster and cheaper development
- High fidelity simulation results
- Easy to add or modify simulated devices
- Ability to simulate scenarios that are hard-to-achieve in the real world

PHIL development is faster and cheaper compared to traditional development as it's possible to use digital twins instead of real devices. This is achieved through modelling of the real devices based on their datasheet parameters. Planning, designing, and building a real system for testing purposes would usually result in the highest fidelity for measurements. However, this is usually the most time-consuming and expensive option. Modelling everything should be the cheapest and fastest method, but the models have to be validated to get reliable and accurate simulation results. PHIL-Simulations attempt to combine the best of pure simulations and real hardware tests. As shown in Figure 1.10, the PHIL setup has a good mix of test fidelity and test coverage at a moderate cost [5]. It is also easier to make changes and to quickly test various scenarios with PHIL setups compared with full built systems. For example, it is possible to repeatedly simulate the discharging of a battery without recharging a physical battery.

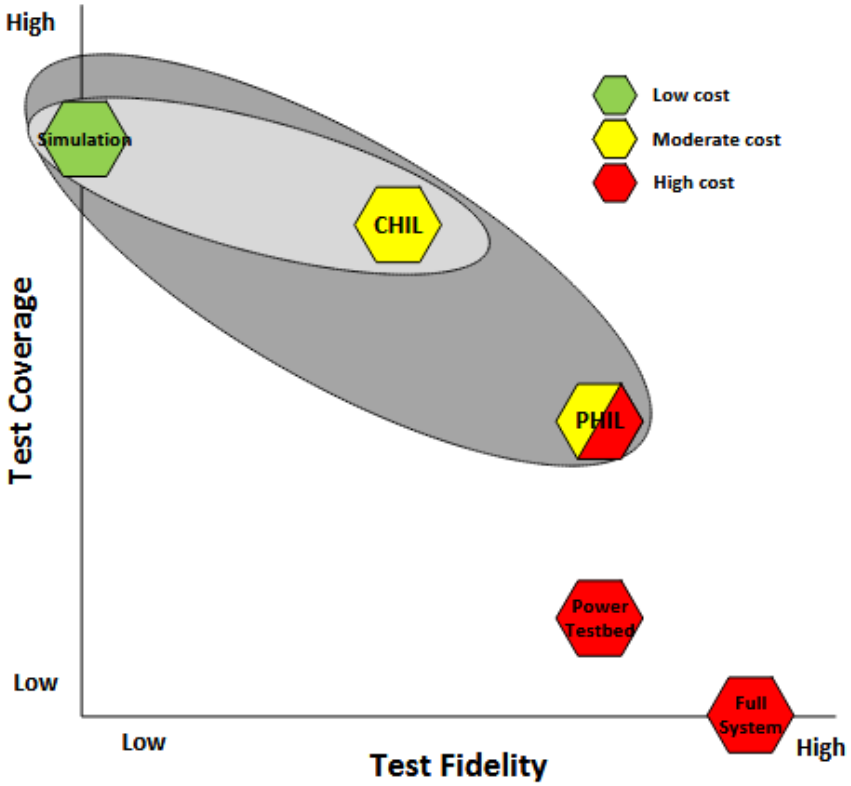

Figure 1.10 Smart Grid test beds and their comparison [5]

The main problem with implementing PHIL technologies is that the accuracy of the hardware/software interface must be proven and that can be challenging. The inaccuracy/distortions of measurement signals can negatively affect simulation results. As the potential benefits outweigh the problems, PHIL systems are becoming an increasingly popular choice to test both the new hardware and software. [39]

1.2.1 Review of existing PHIL setups in scientific literature

PHIL setups have been gaining popularity in the field of microgrids to test new smart solutions in a quicker and more cost-efficient way. This chapter reviews some of the developed PHIL setups.

FREA PHIL setup

The FREA PHIL setup was developed at the Fukushima Renewable Energy Institute, AIST (FREA) in Fukushima, Japan [40]. The goal of the developed setup was to investigate the performance of a microgrid controller. The developed system consists of a diesel generator, PV-system, BESS, load, microgrid controller, and measurement devices (DAS 1-2). The diesel generator was responsible for forming the power grid as PV and BESS inverters did not possess the capability to act as auxiliary grid supporting devices.

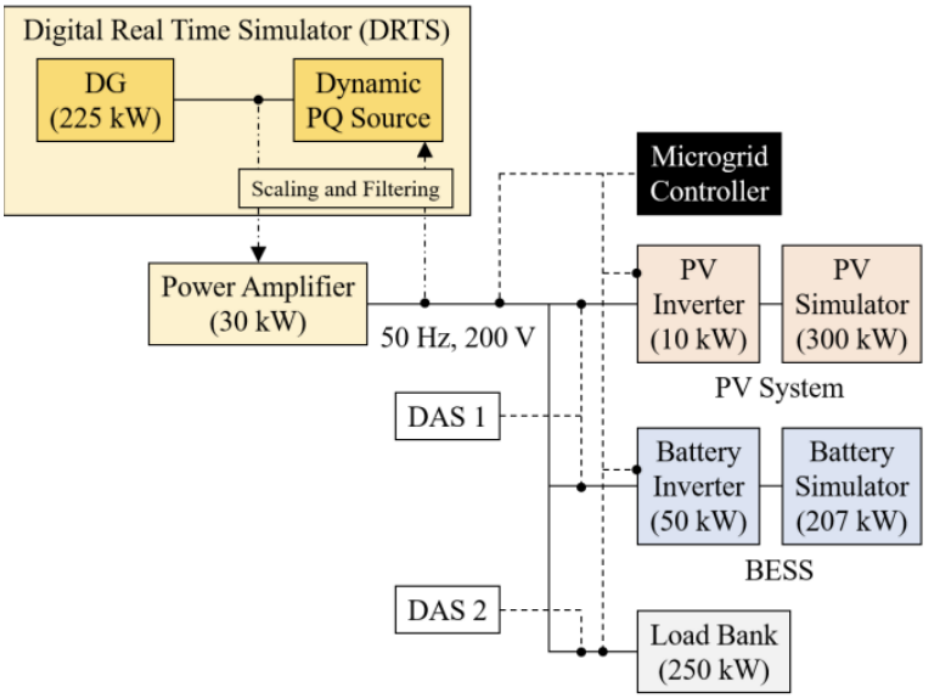

Figure 1.11 FREA PHIL-Setup for testing microgrid capabilities [40]

The integrated PHIL setup is shown in Figure 1.11. The PV-system is implemented with a PV-inverter connected to a PV simulator while BESS is implemented with a battery inverter-simulator pair. An electrical load bank is used as the aggregated load. The diesel generator is modelled in DRTS (Digital Real Time Simulator), and it was coupled via AMETEK MX30 power amplifier. Since existing devices had different power ratings, all the components were scaled to match. The actual and scaled power ratings of components are shown in Table 1.3.

Table 1.3 Actual and scaled ratings of components [40]

	Actual Rating	**Capacity**	**Scaled Rating**
DG	225 kW	30 kW	22.5 kW
PV-System	50 kW	10 kW	5 kW
BESS	100 kW	50 kW	10 kW
Load	250 kW	250 kW	25 kW

Microgrid controller monitored the power of the diesel generator, PV, BESS, and load. The controller would send operation signals to PV and BESS every 0.1 second to control the operation of the microgrid. It is important to note that it was necessary to synchronize DRTS (0.0032 s) and measurement devices (0.05 s) to ensure that all measurements were obtained at the same time. This was achieved by modifying the event start times.

There were 2 main tests simulated with the developed PHIL-setup: supply-demand control tests and frequency control tests. The PHIL-setup simulations were successful, as the microgrid controller was able to control devices as planned.

AIT PHIL-setup

The PHIL setup was developed at the Austrian Institute of Technology in Vienna, Austria [41]. The goal of the developed setup was to compare and validate the modelled battery in PHIL simulation and to compare the results with pure software simulation. The developed system consisted of RTDS, programmable load, power amplifier and BESS.

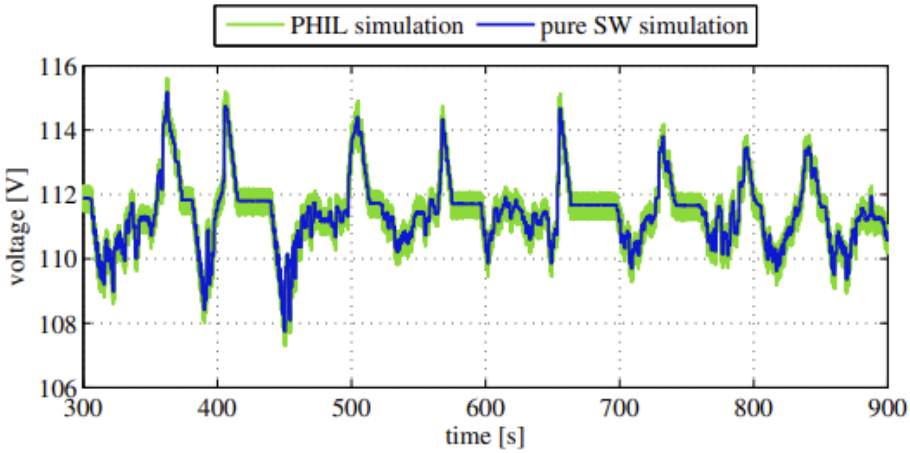

Figure 1.12 Comparison between PHIL simulation and pure software simulation [41]

The testing consisted of measuring the voltage of the battery model in both PHIL simulation and in pure software simulation. The developed setup was considered a success, as the PHIL-simulation showed very good results compared to the pure software simulation as shown in Figure 1.12. The simulations had a maximum error of 1.78% and an RMS error of 0.16%. The benefits of the developed PHIL setup are that there is no need to buy real batteries and that the tests are reproducible. Additionally, the tests should be less time-consuming, as charging/discharging before new experiments could be skipped.

Test bench for PHIL simulation of PowerCorner device

The goal of the developed PHIL test bench was to develop a PHIL simulation framework to test the PowerCorner device [42]. The PHIL simulation of PowerCorner integrated the physical hardware and the software model of an AC microgrid in a single closed-loop simulation. The PowerCorner device embeds a PV-System and an energy storage system and is designed to be used in Africa as the backbone for islanded microgrid. The developed PHIL test bench consisted of DRTS, power amplifier, A/D and D/A Converters, and power device under Test (DUT). Three single-phase Victron inverters were used to form the grid in the developed setup. The simplified setup of the experimental test bench is shown in Figure 1.13.

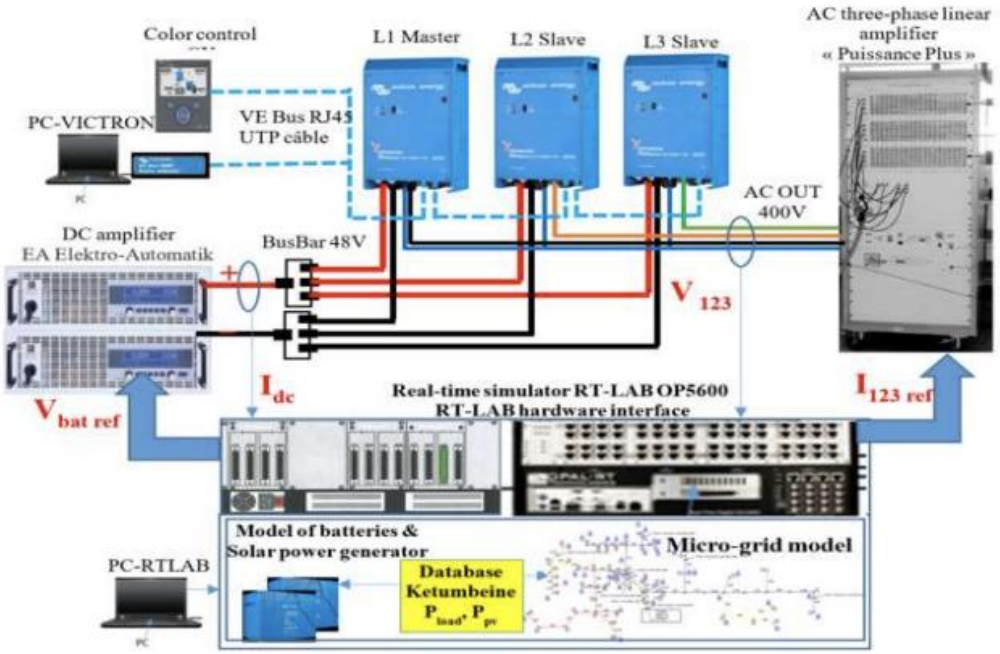

Figure 1.13 Real-time PHIL experimental bench [42]

The AC power system and the battery storage system were modelled in Matlab/Simulink. The developed models were conjoined with the real physical system and validated on load profiles.

First, a PHIL simulation was carried out with a linear load. The output voltages of the inverter were measured and used in the real-time simulation. The results of the PHIL simulation were good because of the phase-locked loop (PLL) which ensured the synchronization of loads and the PHIL simulation remained stable. Second PHIL simulation was done with a given daily load and PV-generation profiles, whose results were also as expected.

System developers emphasized the importance of developing a simplified AC load model as three-phase AC load simulation is very computationally demanding.

1.2.2 Review of existing PHIL testbench at TalTech

The goal of the developed TalTech flywheel PHIL setup was to analyze different FESS control scenarios [27]. The control scenarios researched included:

- Load levelling of building with moving average controller
- PV output levelling
- FESS as power buffer in microgrid applications
- FESS as buffer for fast charging of electric vehicles

The developed PHIL setup consisted of a FESS (flywheel, asynchronous motor, and two bidirectional converters) and a Siemens PLC as the main controller as shown in Figure 1.14. The control algorithms and additional models were created in Matlab/Simulink.

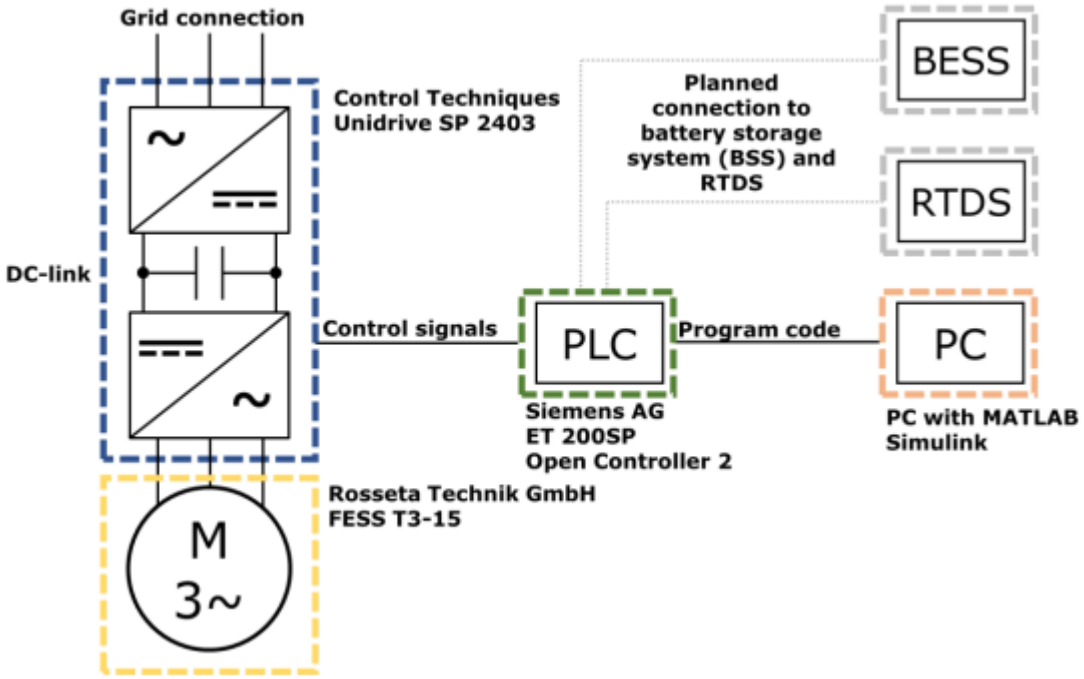

Figure 1.14 Schematic of TalTech PHIL setup [27]

The performance of the developed setup was studied: characterization of the FESS's self-discharge, the necessary power to keep the level of charge, the repeatability of the control, and the round-trip efficiency.

The most important technical founding's of the developed PHIL setup:

- If the flywheel is controlled to a power of zero watts from full charge, it is completely discharged in less than 500 s.
- The power which the flywheel needs to keep its current state of charge depends on the state of charge. At 65% SOC, 1.2 kW is necessary.
- Controllers ramp signal RMS error: 97.74 W
- FESS Round trip efficiency: ~71.8 %
- FESS maximum rpm: 5030 rpm
- 'Ringing' of measurement signals (analog inputs)

It was concluded that the developed PHIL setup was capable of simulating developed control scenarios. On the negative side, it was found that the flywheel has limited potential for research and development as it has a high self-discharge rate.

2. DEVELOPMENT OF THE PHIL SETUP

The first step to PHIL development is to have a clear vision of what scenarios will be simulated and what hardware (HUT) will be tested. The design and selection of PHIL setup components can be quite challenging. This is because components of PHIL setups must be selected based on their technical capabilities while keeping inter-compatibility in mind. An additional important aspect of PHIL setup is the testing capabilities of the setup. Different Digital Real-Time Simulators (DRTS) have different calculational capabilities, and it must be ensured that the DRTS is able to perform simulations within the defined time step. The use of DRTS with insufficient calculation power can lead to distorted results and simulation instability [36]. The desired scenarios can set limitations for the devices in PHIL setup. Properly designed PHIL setup provides an effective environment for testing various microgrid power devices. Different testing scenarios, including testing control strategies, can be simulated with PHIL setups. [39, 43]

In this thesis the existing TalTech PHIL setup is further developed to research the effects of flywheel energy storage, PV-system, and different loads on the islanded mode time duration and battery's lifetime in a microgrid. The first subchapter introduces the existing PHIL setup while the second subchapter focuses on the development of the upgraded PHIL setup.

2.1 Existing setup

The existing PHIL setup was developed and built as part of a previous thesis [27]. Currently the PHIL setup consists primarily of a Rosetta Technik GmbH T3-15 flywheel, two EPA Unidrive SP 2403 frequency inverters with a 700V DC-link and Siemens ET 200SP Open Controller 2. One of the SP 2403 frequency inverters is connected to the microgrid bus while the second frequency inverter controls the induction motor. The induction motor is controlled with the analog output signal from the PLC. Differential $\pm$10V 16bit analog signal is used for communication. It is possible to set either the rotational speed or the motoring torque value via the PLC analog output signal. The inverters also have analog outputs that can be configured to send various data to the PLC such as active current, active power, or the rotational speed. A schematic of the existing FESS Setup was shown in Figure 1.14. [27]

The most relevant aspects from previous research for this work are: The PLC already has a basic configuration, the PLC is installed and connected with the FESS, and there

are control algorithms developed for the FESS. The FESS can be controlled by setting the desired power value in watts.

2.2 Upgraded setup

2.2.1 Requirements

The upgraded PHIL setup must meet the aim of the thesis which was to develop a power hardware-in-the-loop setup (PHIL) that enables to study the effects of flywheel energy storage, PV-system, and different loads on islanded mode duration and battery's lifetime in a microgrid. This means that the upgraded setup must include the following components:

- Controller capable of real-time simulations (Matlab/Simulink)
- Flywheel energy storage system
- PV-system
- Battery energy storage system
- Power metering devices
- Electrical load/consumer

Requirements for the components of the PHIL setup:

- Devices must be capable of real-time communications
- The devices must be intercompatible
- The voltage and power ratings of the devices should be similar
- Measurement devices should have a good accuracy class, such as 0.5S

All the main devices of the developed system must be manageable and controllable by the PLC. Such a setup allows for quicker research of different microgrid related scenarios. The simplified overview schematic of the microgrid represented with the upgraded PHIL setup can be seen in Figure 2.1.

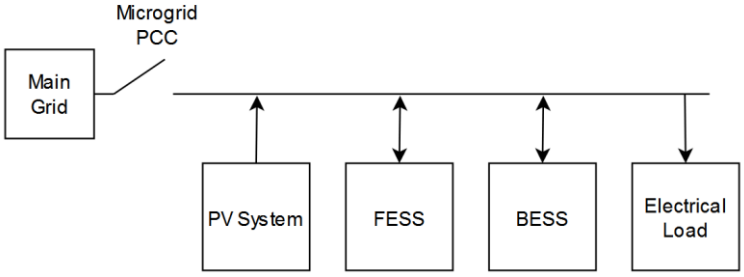

Figure 2.1 Represented microgrid with the upgraded PHIL setup

2.2.2 Overview of the devices

In this subchapter, the main devices/components of the upgraded PHIL setup are described. First, the real physical devices are described, and then the simulated devices. Specific information and examples of Ethernet/Modbus TCP communications are shown in chapter 4.1. All the Ethernet/Modbus TCP devices are connected via a MOXA EDS-208A unmanaged switch.

Real physical devices

PLC - The controller of the microgrid PHIL setup is the CPU 1515SP PC2, which is a PC-based automation device in the design of the ET 200SP [44]. It is capable of both real-time MATLAB Simulink simulations and for control of other devices. The components of the PHIL Setup can be connected via Industrial Ethernet using the integrated interface. This PLC was chosen and installed as part of a previous thesis in which only analog signals were used for the control of FESS [18]. This controller is used as the basis for the new developed PHIL setup.

FESS - The flywheel energy storage system is based on a Rosetta Technik GmbH T3-15 flywheel, VEM WE1R 160 MX2 S9 duty asynchronous motor, and two EPA Unidrive SP 2403 frequency inverters [45]. The PLC controls the frequency inverter that is connected to the motor via analog signals. Integration of FESS and PLC was done as part of the previous thesis [18] and more detailed information on the flywheel can be found in [46]. The main technical parameters of the flywheel energy storage system are:

- Device Model: Rosetta Technik GmbH T3-15
- Maximum power: 15 kW
- Maximum stored energy: 300 kWs / ~0.1 kWh
- Maximum rotational speed: 5000 rpm

PV-System - The developed PHIL setup's PV-system is controllable and consists of two devices - a solar inverter and a programmable DC power supply. This ensures that different scenarios can be simulated at any time without the need for an actual PV-system. These devices are VACON 8000 SOLAR [47] and MagnaPower TSD800-18/380 [48] respectively. The main parameters of the **VACON 8000 Solar inverter** regarding the thesis are:

- Nominal output power: 10 kW
- Maximum recommended PV-system size: 12 kW
- Range of input voltages: 340...800 Vdc
- Efficiency: ~ 95 %

- Communications: Modbus TCP

The main parameters of the **MagnaPower programmable DC power supply (TSD800-18/380+HS+LXI)**:

- Rated power: 15 kW
- Max voltage: 800 Vdc
- Max current: 18 A
- Programming accuracy: ±0.075% of max rated voltage or current
- Efficiency: 92 %
- Communications: LXI TCP/IP Ethernet or GPIB

The PV-generation profiles are modelled, and they are described in detail in chapter 3.3.

Power metering devices - The developed PHIL setup uses Siemens PAC3200 measuring devices. The PAC3200 is a powerful power monitoring device that is suitable for measuring the parameters of the designed microgrid and has the functionalities to research other microgrid related scenarios in the future [49] .The most important functionalities of the **PAC3200 power meter** regarding the thesis are:

- Instantaneous values for voltages, currents, power
- High power measurement accuracy (±0.5 %)
- Communications: Modbus TCP

Simulated devices

BESS - There is no real battery storage system as part of this thesis. The BESS is modelled after the datasheet of the SunGrow's SBR series LFP battery. SunGrow BESS was chosen after researching commercial BESS solutions that could be suitable for microgrid use. The main benefit of the SunGrow BESS system is that the pricing is good, battery/hybrid inverter parameters are flexible, the BESS has grid-forming functionality and can be controlled via Modbus TCP.

The battery storage system is modelled after SunGrow SBR096 Lithium-Ion (LFP) battery datasheet. The 9.6 kWh battery storage system consists of three 3.2 kWh battery modules. Key features of the SunGrow battery storage system are:

- Battery Type: LiFePO4 Prismatic Cell
- Nominal Capacity: 9.6 kWh
- Nominal/Operating voltage: 192 V / 150-219 V

- Rated DC power: 5.76 kW
- Max charge/discharge power: 6.57 kW
- Max charging/discharging current: continuous - 30A
- Maximum DOD: 100% (configurable)

Details about the modelling of the BESS are described in chapter 3.1.

Electrical load - There are no real loads/consumers as part of this thesis. The load profile is modelled after a residential household. The developed PHIL setup's load profile represents the measured power flow of the microgrids PCC. This means that the main grid acts as the load by absorbing the real power output of real devices. Details about the modelling of the electrical load is shown in chapter 3.2.

2.2.3 Proposed PHIL setup

The proposed PHIL setup primarily consists of the devices described in previous chapters. Pictures of the main devices can be found in Appendix 2 Pictures of devices. The simplified schematic of the proposed PHIL setup is shown in Figure 2.2. The communication centre of the proposed PHIL setup is the PLC of the existing PHIL setup located in the FESS electrical cabinet. The existing PHIL setup is improved by adding additional intelligent power metering devices, controllable PV-system, new models of battery storage system and loads. The proposed new setup attempts to maximize the usage of compatible existing devices. The proposed system can be easily upgraded with additional and more complex models or new devices (real battery storage system, hydrogen storage etc).

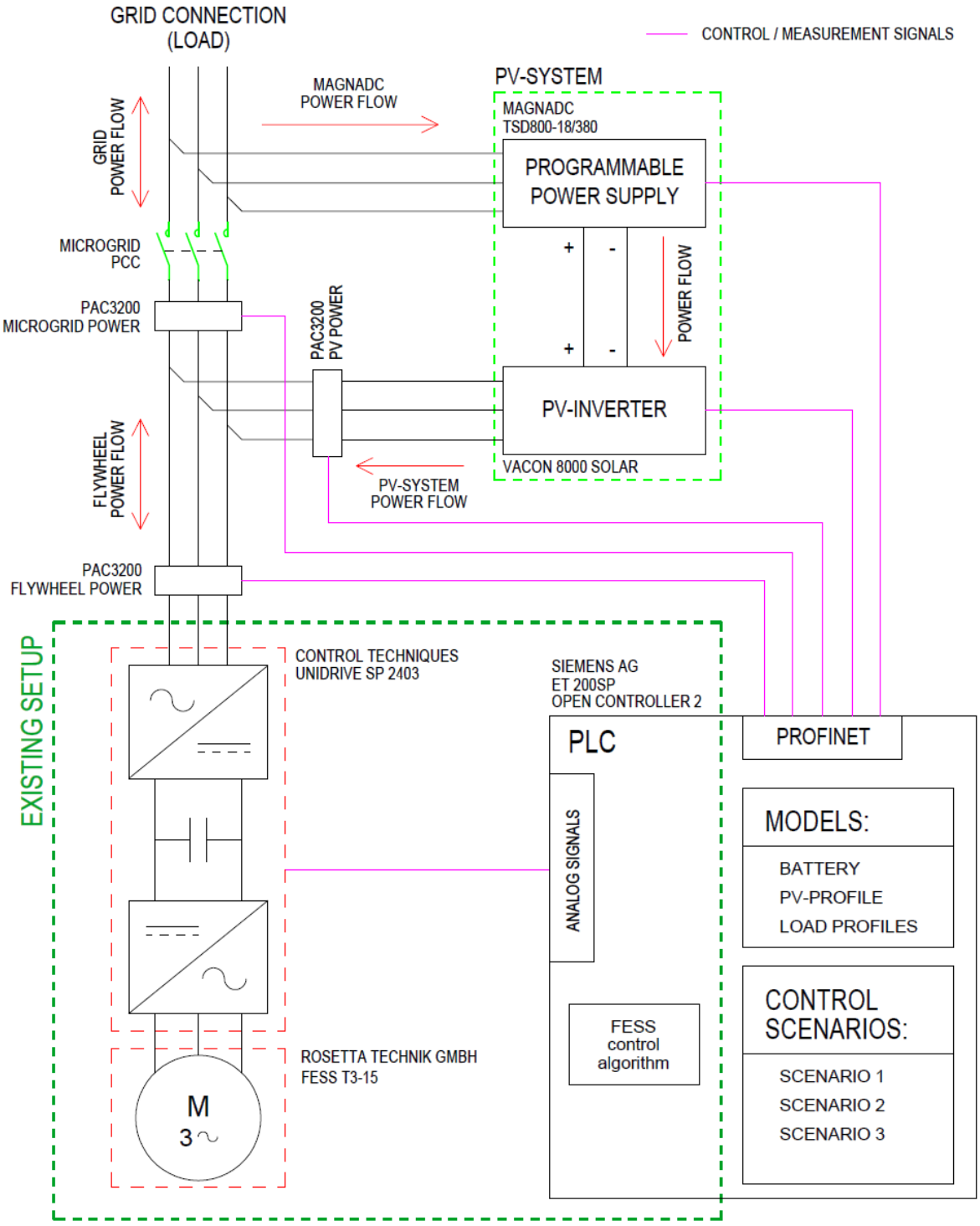

Figure 2.2 Simplified schematic of the proposed PHIL setup

The developed PHIL setup consists of the FESS, programmable PV-system, power metering devices, PLC, and various Matlab/Simulink models such as the BESS model. At the top of Figure 2.2, the connection with the main grid is shown, and that the main grid acts as the load for the PHIL setup. This means that the power generated in the Microgrid PHIL setup is sent back to the grid. The PAC3200 marked as "Microgrid power" measures the proposed microgrid's power flow with the main grid. This point can be

considered the Microgrid's PCC. Additional power metering devices measure the power flows of the FESS and PV-system.

To simulate islanded mode scenarios, the proposed system will attempt to maintain virtually zero power flow with the main grid. This is achieved through multiple steps. First, a load profile of a consumer is loaded into the PLC. Next, according to the chosen test scenario, the modelled BESS and the real PV-system and the FESS will attempt to match the load profile. The PV-system only generates power and generated/discharged power is marked as positive. BESS and FESS can be either charging or discharging, thus their output power reference value can be either positive or negative. While it is possible to match the consumption (load profile), the developed setup is considered to be successfully operating in islanded mode. The exact prioritization of charging and discharging of storage systems will be based on the specific scenario. If the available power from the combination of PV-system and storage systems is not sufficient to match the load profile, then the islanded mode of the microgrid is considered over and the system has experienced a power outage. This represents the end for current simulation.

2.2.4 Development of electrical schematics

This chapter focuses on the development of the electrical schematics of the proposed PHIL setup, see Figure 2.2. The new PHIL setup was developed in accordance with the previous chapters, the manuals of the devices, and various electrical installation standards. The first part of the chapter focuses on the technical details such as how the devices are connected and how to ensure the proposed PHIL setups safety. The subchapter concludes with the creation of the electrical schematics of the proposed PHIL setup.

Technical description

To ensure electrical safety, the developed system is planned in accordance with IEC 60364-4-4 which specifies essential requirements regarding protection against electric shock, including basic protection and fault protection of persons. In electrical installations, the minimum short-circuit current is the single-phase short-circuit current. The minimum short-circuit current occurs at the furthest point in the circuit (i.e., at the consumer/load). The maximum short-circuit current is the three-phase short-circuit current. It occurs along the shortest path (i.e., at the terminals of the circuit breaker). The circuit breaker must be able to trip at the minimum short-circuit current in required time and the breaking capacity of the circuit breaker must be higher than the maximum

short-circuit current of the circuit. Additionally, the selectivity of the circuit breakers must be achieved.

Overcurrent protection

Miniature circuit breakers (MCBs) are used to protect the wires and cables of electrical installations from both overloading and short circuiting. The bimetallic strip of MCB's is responsible for protection against small and longer-term overcurrent using thermal operation, while electromagnet is used to protect against high overcurrent/short-circuit by tripping a coil. MCBs will trip and interrupt current flow after their internal protective relay(s) detects excess current. MCBs can have different tripping characteristics, and the main versions are type B and C.

Type B MCBs are used for devices/lines with small inrush currents such as typical household loads: electrical heaters, lights, home entertainment systems etc. These MCBs are designed to trip instantly if the current flowing through them is 3-5 times higher than the MCBs rated current.

Type C MCBs are used for devices/lines with higher inrush currents, such as AC-motors. These MCBs are designed to trip instantly if the current flowing through them is 5-10 times higher than the MCBs rated current.

The main parameters of MCBs are the number of poles, rated current, tripping characteristics, short-circuit breaking capacity. Number of poles is selected based on the protected line. The rated current of the MCB is chosen based on IEC 60898:

$$I_b \leq I_n \leq I_z \tag{2.1}$$

Where $I_b - Calculated\ circuit\ current$

$I_n - MCB\ rated\ current$

$I_z - Maximum\ continuous\ current\ of\ cable$

The tripping characteristics of MCBs are chosen based on the type of load. Short-circuit breaking capacity of the MCB must be greater than the maximum possible short-circuit current in the protected line.

Selectivity

Selectivity is the coordination of overcurrent protection devices so that the fault is cleared by the protection device located immediately upstream of the fault. It is important to localize the fault and to avoid triggering of protective devices further

upstream of the fault. This can cause unnecessary power outages to other, properly working lines.

Selection of cables/wires

FESS - As the nominal input/output parameters of the FESS are 15 kW 400 V, a cable with an insulation rating of 300/500V or greater must be used. Additionally, the cable must withstand continuous current of up to 30A. Therefore, a suitable cable would be a copper cable with a wire cross section of at least 4 mm² for surface mounting, but a 6 mm² cross section with maximum permissible continuous current of 44A is recommended to reduce the voltage drop of the cable. The FESS has bidirectional power flow, thus it is necessary to protect the power cable from both the flywheel and the microgrid side. The flywheel energy storage cabinet already has a main 3P C32A protective switch that is suitable for the new developed setup. Additional 3P C32A protective switch was installed in the grid side.

PV-System – VACON 8000 Solar and MagnaPower programmable DC power supply were already connected via DC bus, and it was determined that no changes were necessary to the PV-system's protection and measurement circuits.

Connection with the main grid

The Microgrid PHIL setup is connected with the main grid through existing 5P 63A industrial socket. 63A protective device is used to protect the incoming 5G16 power cable. It was determined that the current connection with the main grid is sufficient to tolerate the maximum power flows of the PV-system (~10 kW) and FESS (~17 kW).

A Siemens 3RT2037-1AP00 contactor was chosen as the microgrids PCC. Since on both sides of the PCC there are separate voltage sources, extra safety measures must be implemented. If different voltage sources (grid/microgrid DER-s) are not synchronized and if there are phase offsets, then the switching currents could be dangerous if connecting the microgrid setup with the main grid. To avoid this, it is only possible to connect the developed microgrid PHIL setup with the main grid if the microgrid is de-energized. This is achieved by providing the power supply to the microgrid's main contactor coil via the voltage monitoring relay's auxiliary contact.

The developed schematics can be found in Appendix 1. As there were no accessible drawings of the old microgrid electrical cabinet, new schematics were drawn from existing setups .PDF and the changes were implemented in the new drawings. The schematics presented in the appendix of the thesis are partial as additional external connections are not shown.

3. RESEARCH AND DEVELOPMENT OF SIMULATED OBJECT MODELS FOR THE PHIL SETUP

3.1 Battery

This chapter focuses on the modelling of the battery energy storage system. BESS and its model are one of the key parts of the thesis as they are directly correlated with the aim of the thesis. The battery model is based on [50, 51] and changed to fit the needs of this thesis. Various simplifications were made in the modelling of the battery. Based on the datasheet it is possible to develop the basis for the battery model.

Description of the battery model

The battery is modelled to be easily configurable in case it is determined that a battery with a different capacity, parameters or initial settings would be necessary. The main block of the modelled battery is shown in Figure 3.1. The battery model has one input that sets the charging or discharging reference power value for the BESS. The model has 5 outputs: the current SOC of the battery, number of full cycles performed, current charging/discharging power, and the current maximum charging/discharging power of the battery.

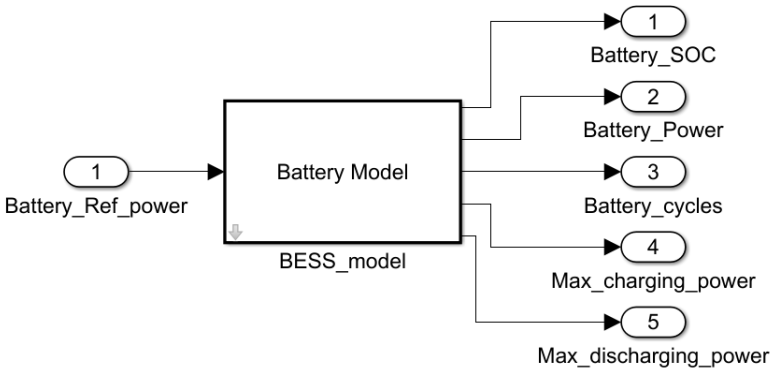

Figure 3.1 Modelled Matlab/Simulink battery

The main configurable parameters of the modelled SunGrow SBR096 LFP battery are shown in Table 3.1. The shown parameter values are used for the modelled battery.

Table 3.1 General parameters of the modelled battery

Parameter	**Value**
Number of LFP cells	60 cells
Rated Capacity	50 Ah
Initial SOC	50%
Maximum SOC	90%
Minimum SOC	20%
Maximum charging current	0.6 C
Maximum discharging current	0.6 C
BESS efficiency	97%

It is possible to change the initial parameters of the battery model to allow testing different sized LFP battery storage systems. The main input parameters of the BESS model are the number of 3.2V LFP cells, rated capacity of the battery storage in Ah, initial state-of-charge, maximum battery state-of-charge, maximum depth-of-discharge, maximum charging and discharging current in C rate.

Number of 3.2 V battery cells and their voltage range was calculated based on datasheet given Nominal/Operating voltage:

$$n_{cells} = \frac{V_{nom}}{3.2} = 60\ cells \tag{3.1}$$

$$V_{cell.max} = \frac{V_{max}}{n_{cells}} = 3.65\ V \tag{3.2}$$

$$V_{cell.min} = \frac{V_{min}}{n_{cells}} = 2.5\ V \tag{3.3}$$

Rated capacity of the battery in Ah was calculated according to equation 3.4:

$$C_{bat} = \frac{Nominal\ capacity}{Nominal\ voltage} = 50\ Ah \tag{3.4}$$

The initial state-of-charge (SOC), maximum/minimum battery SOC are not calculated but are configured as base constant values. Maximum Depth-of-Discharge (DOD) is calculated according to equation 3.5:

$$DOD_{max} = SOC_{max} - SOC_{min} \tag{3.5}$$

The maximum charging and discharging currents are calculated using the batteries C-rate and the nominal capacity of the battery as shown in equation 3.7:

$$C_{rate} = \frac{Rated\ DC\ power}{Nominal\ Capacity} = 0.6 \tag{3.6}$$

$$I_{max.charge/discharge} = C_{bat} * C_{rate} = 30\ A \tag{3.7}$$

The charging voltage of the battery is simplified to be a constant value of:

$$V_{charge} = n_{cells} * V_{cell.max} = 219\ V \tag{3.8}$$

The general maximum charge and discharge power of the battery is calculated with equations 3.9 and 3.10. Charging and discharging power depends on the current, capacity, and voltage of the battery.

$$P_{max.c} = C_{bat} * I_{max.c} * V_{charge} \tag{3.9}$$

$$P_{max.d} = C_{bat} * I_{max.d} * V_{bat} \tag{3.10}$$

The battery current is calculated based on the power flows and the voltage. In case of zero power flow, the battery self-discharges at the rate of 3% a month. The charging and discharging process is limited by the minimum and maximum SOC values defined. Self-discharge power is considered a waste and the power value will not go to the output of the model.

$$if\ P_i > 0\colon\ I_{charge} = \frac{P_i}{V_{charge}} \tag{3.11}$$

$$if\ P_i < 0\colon\ I_{discharge} = \frac{P_i}{V_{bat}}$$

$$else\colon I = 0$$

$$P_{self.discharge} = -\frac{C_{bat} * 0.03}{24 * 30} * V_{bat}$$

The Voltage-SoC discharge curve of the modelled battery is shown in Figure 3.2. The difference between 90% SOC and 20% SOC is only 9 V for the modelled battery.

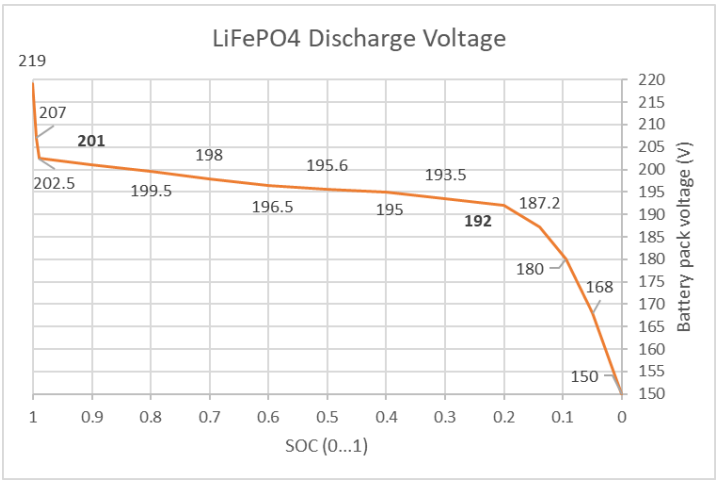

Figure 3.2 Modelled battery discharge voltage curve

The SOC of the battery is calculated based on the charging or discharging operation.

$$if\ P_i > 0\colon\ SOC_{new} = \frac{(SOC * C_{bat.new} * V_{bat}) + \left(I * V_{charge}\right) * dt * \eta_{bat}}{C_{bat.new} * V_{bat}} \tag{3.12}$$

$$if\ P_i < 0\colon\ SOC_{new} = \frac{(SOC * C_{bat.new} * V_{bat}) + (I * V_{bat}) * dt * \eta_{bat}}{C_{bat.new} * V_{bat}} \tag{3.13}$$

To calculate how the PV-system and FESS affect the cyclic lifetime of the battery, the battery model sums up all the energy charged and discharged by the BESS. It is then possible to divide this energy sum with the maximum initial battery capacity to calculate the number of 100% charge-discharge cycles for the battery. This is implemented in Simulink as shown in Figure 3.3.

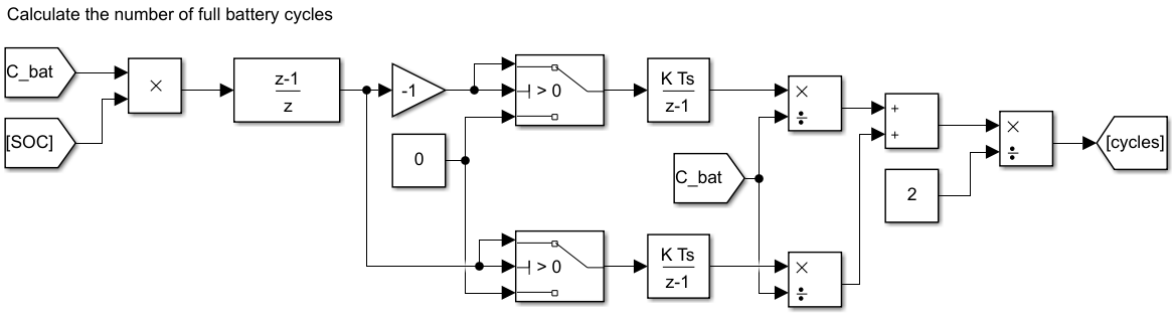

Figure 3.3 Battery cycles calculation

Verification of the battery model

The modelled battery was tested by running a few basic simulations. First, the battery was set to 0% SOC, maximum SOC was set to 100%, and minimum SOC was set to 0%. The battery was charged with constant power of 5 kW and then discharged with a constant power of 2.5 kW. Since the BESS has a nominal capacity of 9.6 kWh, the battery should be fully charged in approximately 1 hour and 55 minutes with constant charging power of 5 kW, when we divide the capacity of the battery with the charging power. Total time to fully discharge the battery with 2.5 kW should take approximately 3 hours and 50 minutes.

Based on simulations and results shown in Figure 3.4, the battery model works as intended. The graph is scaled in seconds, and the battery was fully charged in just under 2 hours (~7170 seconds). The full discharge of the battery took just under 4 hours (~14350 seconds). The slight differences occur mainly because the model includes the efficiency of BESS.

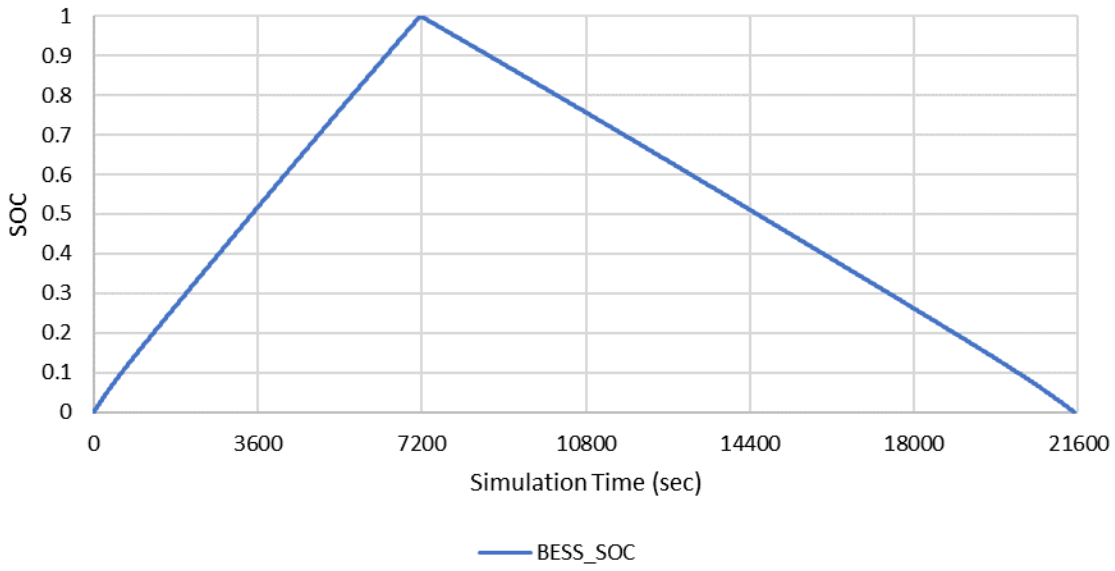

Figure 3.4 Battery model basic charging-discharging test

Figure 3.5 showcases the modelled battery's self-discharging. The battery was set to a 100% SOC. It was modelled, that the BESS has a self-discharge of around 3 % a month or 1.5 Ah. Based on the 1-hour simulation, it was found that the battery discharged 0.002021 Ah. This means that it discharges ~1.46 Ah or 2.92 % a month, which is around the set goal of 3 %.

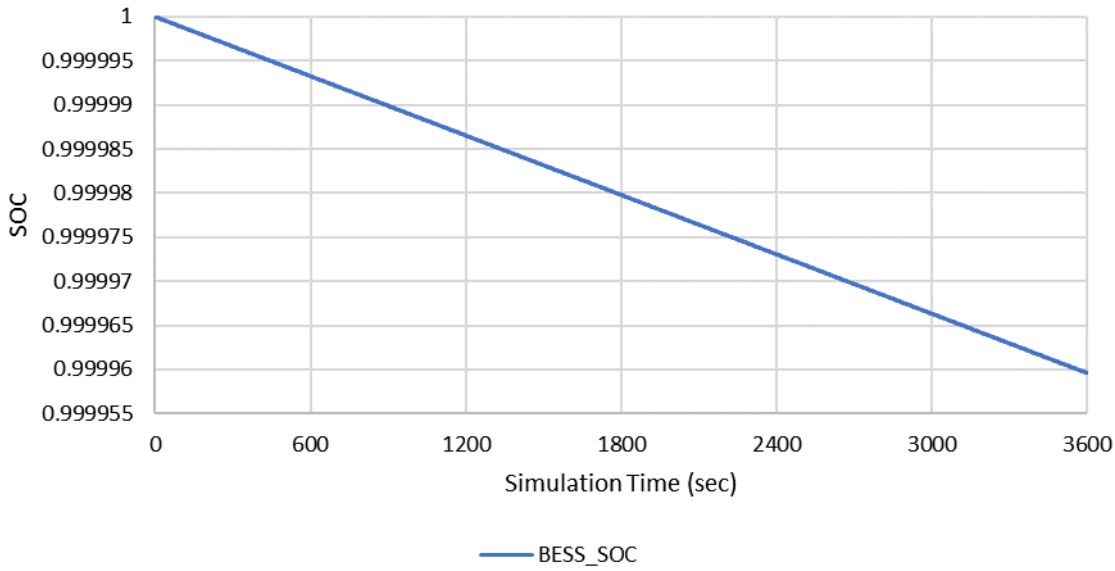

Figure 3.5 Battery model self-discharge test

The battery cycle counting algorithm is verified by setting the initial battery SOC to 100% and discharging it until it has SOC of 0%. The battery is discharged with variable power under 2.5 kW. The battery cycle counting algorithm test was a success as the 50 Ah nominal capacity battery was fully discharged, and the calculations based on Figure

3.3 show that the battery performed ~0.5 full cycles (charging the battery back to 100% SoC would result in 1 full battery cycle).

3.2 Load

An electrical load is necessary to study how FESS and PV-System affect the lifetime of BESS and the islanded mode duration of the microgrid. The developed PHIL setup does not have a real load, as the load is modelled to reduce the cost of the developed system. The main grid acts as the load instead. Microgrid islanded mode is emulated by mathematically maintaining zero power flow with the main grid. The BESS model acts as the final power generation-consumption balancer.

Conditions

The main desired conditions and requirements for the modelled load:

- The modelled load profile represents a residential household.
- The household should represent a family of at least 3 people.
- Electricity should not be the main heating source of the household.
- The peak load should not exceed 5 kW.
- Time-step of measured consumption data: 1 second.

A small time-step is necessary to research the effect of FESS on the BESS lifetime and microgrid islanded time duration as the existing flywheel has low energy storage capacity and high self-discharge as proven in [27]. Power metering of residential household with the required small time-step is not common. As a result, it was decided that the load profile should be obtained in another way.

Outcome

The load profile was generated by using LoadProfile Generator [52]. The software includes many different pre-defined options that were used in the generation of a suitable load profile. The generated load profile belongs to a modern family's household, where one parent goes to work, one works at home and there are 3 children around the age of 10. The generated household has monthly electricity consumption between 250 to 450 kWh. The load profiles of two different days in October were chosen as the 24-hour test periods for this thesis. The generated household does not use electricity for primary heating. The main consumers during the selected 24-hour periods are cooking (meals), TV/Audio (entertainment) and drying (laundry). The distribution of power

consumption for the first day of the household is shown in Figure 3.6. The second day's consumption data is similar and not described in such detail.

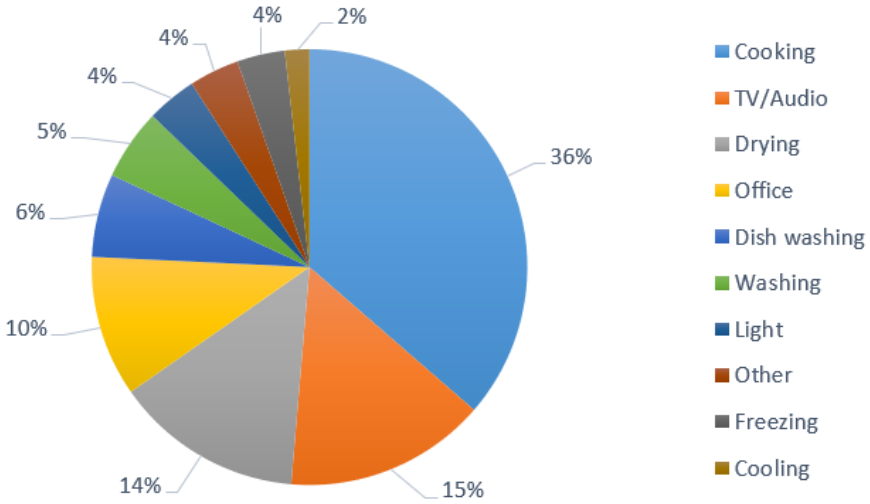

Figure 3.6 Household electricity consumption

Most important parameters of the first selected 24-hour load profile:

- 1 second measurement data
- Total electricity consumption: 13.5 kWh
- Peak load: 2.6 kW

The second selected 24-hour load profile is similar to the first one, but there are higher peak loads at ~3.5 kW. The generated 24-hour load profiles can be seen in Figure 3.7. It can be noted that a large portion of the consumption for these two load profiles occurs at different times.

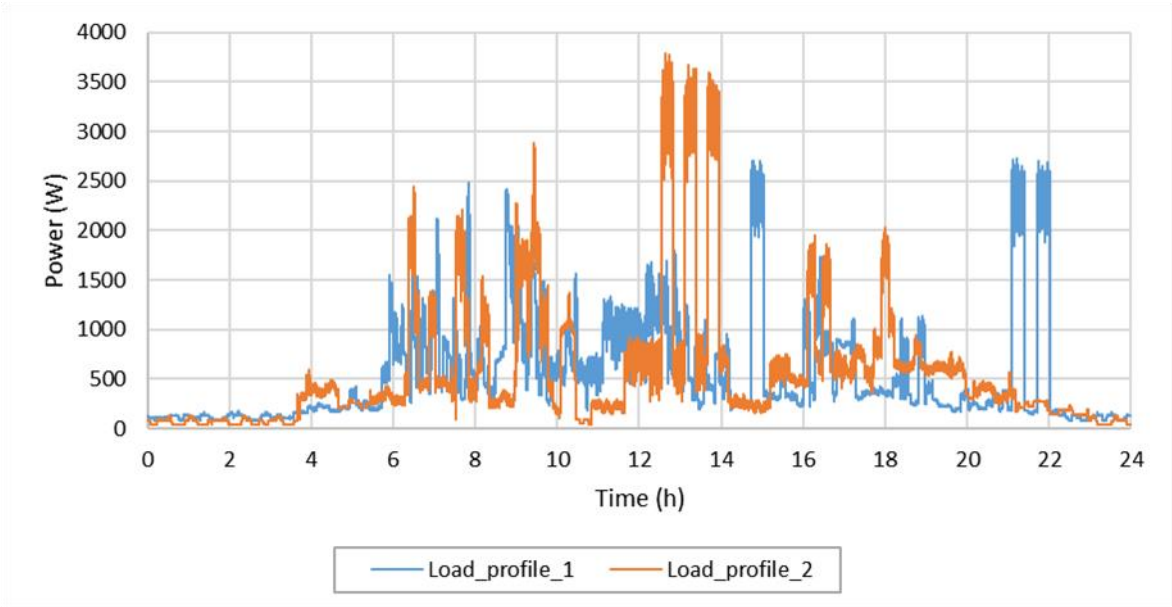

Figure 3.7 24-hour generated load profiles

Matlab/Simulink model

The Matlab/Simulink model of the simulated load profile is very simple as the generated dataset is loaded into Matlab from Microsoft Excel. Figure 3.8 showcases the main block of the modelled load profiles and the sub-block which contains the generated load profiles data. The model outputs a power value in Watts based on the input variable (time). Power values of the load profile are loaded into "Lookup Table Dynamic" that creates a XY-graph and allows to retrieve power (y-axis) value based on current time (x-axis). The model outputs the raw base power data in 1-second steps totalling 86400 values (24 hours).

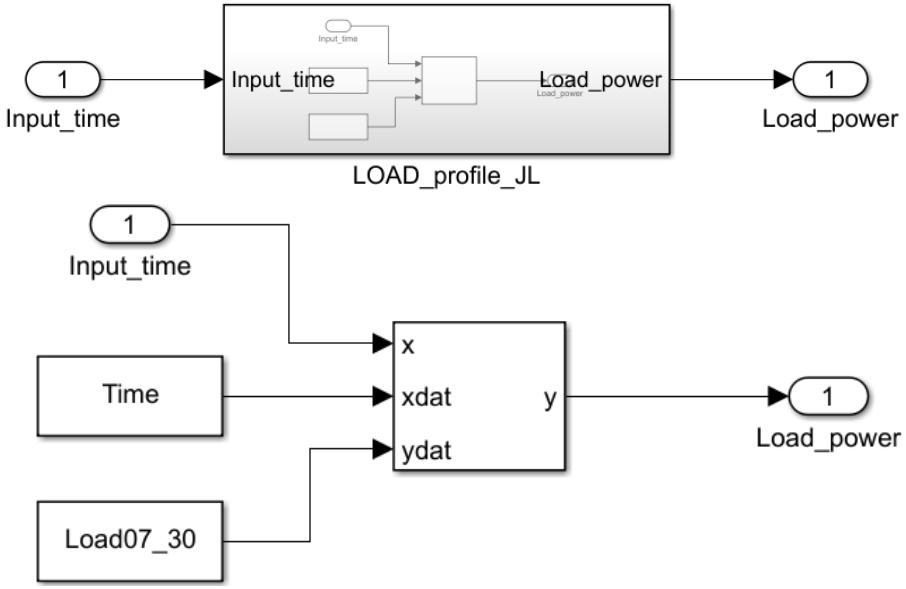

Figure 3.8 Load-profile model's main block and corresponding sub-block

3.3 PV-System

The PV-System is necessary to research the effect it has on BESS lifetime and microgrids islanded mode time duration. The PV-system was chosen based on the geographical location and the consumption of the household. Figure 3.9 shows the energy generation of the PV-system per installed 1 kW solar panels with 15% losses. This is with a PV-system installed at the optimal slope and azimuth angle, 42° and 3° respectively.

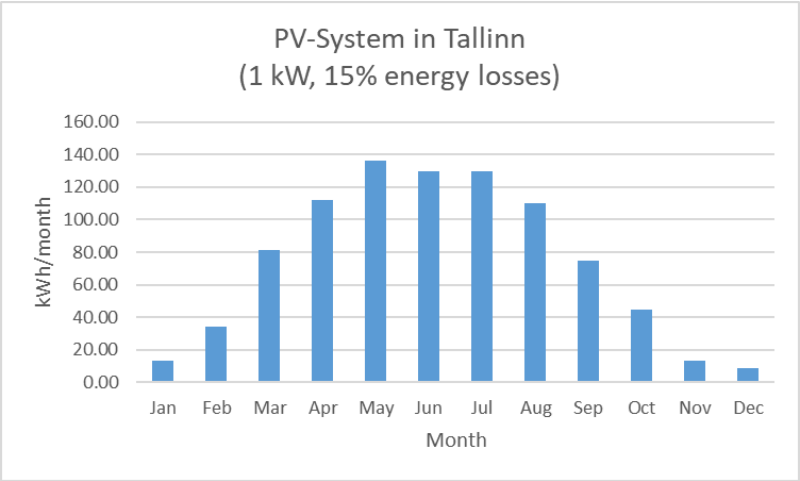

Figure 3.9 Monthly energy generation of the 1 kW PV-system in Tallinn

Conditions

The main desired conditions and requirements for the modelled PV-system:

- PV-System must cover the monthly net consumption of the household during March-September (In relation to average consumption / PV-generation).
- PV-system must cover 100% of annual net electricity consumption.
- Time-step of measured PV-generation data: 1 second (must match the time-step of the load profile).

A small time-step is necessary to research the effect of PV-System on the BESS lifetime and microgrid islanded time duration. The time-steps of the load profiles, PV-generation profiles and BESS must be identical.

Outcome

There were no existing 24-hour PV-system measurement data available for Estonia with 1 second time-steps, so existing measured 1-minute PV-generation data was converted into 1 second data and scaled appropriately. The minutely PV-data was converted into seconds (24*60*60 values) to enable synchronous simulations and experiments. Converting the 1-minute PV-data into seconds was done via MATLAB. Interpolation was found to be the most efficient and suitable method. Example of the MATLAB code for PV-data interpolation (from 1-minute into 1-second data):

```
Input.Data = [array of known values];  % Import known values (24-hour in minutes)
t = 1 : 60 : 24*60*60;              % Current data: start 1, step 60, end 24*60*60
ti = 1 : 1 : 24*60*60;               % Desired data: start 1, step 1, end 24*60*60
Output.Data = interp1(t,Input.Data,ti);          % Interpolation and output data
```

After the PV-data was converted into suitable time-step, it was necessary to scale it according to the required conditions.

Based on Table 3.2, it can be noted that during the months of March-September, September would require the largest PV-System at 5.17 kW to have net positive energy balance. Thus, a 6 kW PV-system was chosen as suitable for the developed PHIL setup. Column 2 shows the monthly consumption, and column 3 presents the required minimum PV-system kW size to generate the required net positive energy in the given month. Average PV generation in a month per chosen 6 kW PV-system with 15% losses is shown in column 4 (based on Figure 3.9). Column 5 shows the net balance of monthly generated and consumed energy with the chosen PV-system. The chosen PV-system covers the monthly net consumption of the household during required period of March-September, and it also generates net positive ~0.8 MWh in the year under review.

Table 3.2 Sizing of the PV-system

Month	**Monthly consumption (kWh)**	**PV-System size (kW)**	**6 kW PV-System generation (kWh)**	**Net power (kWh)**
Jan	442.13	32.80	80.89	-361.24
Feb	351.82	10.33	204.31	-147.51
Mar	395.79	4.85	489.65	93.86
Apr	380.53	3.40	671.87	291.34
May	379.54	2.78	819.16	439.62
Jun	247.92	1.91	777.80	529.88
Jul	374.78	2.89	779.43	404.65
Aug	393.29	3.58	659.12	265.83
Sep	387.57	5.17	449.62	62.04
Oct	405.07	9.07	268.01	-137.07
Nov	372.10	27.62	80.84	-291.26
Dec	404.98	45.59	53.30	-351.69
Total yearly net energy generated:				**798.45**

Similarly, to the load model, October was chosen as the base month for the PV-System performance. The generation profile of the PV-system was modelled to generate the average amount of energy per day during a day in October. The generation data was modelled after October because it was necessary that the PV-systems daily generation would be lower than the consumption. This was necessary to meet the aim of the thesis as the microgrid must be moving towards power outage to study how the microgrids islanded time duration changes. Therefore, the chosen 6 kW PV-System generates on average ~8.93 kWh per day. The PV-data after scaling and conversion to 1-second data is shown in Figure 3.10.

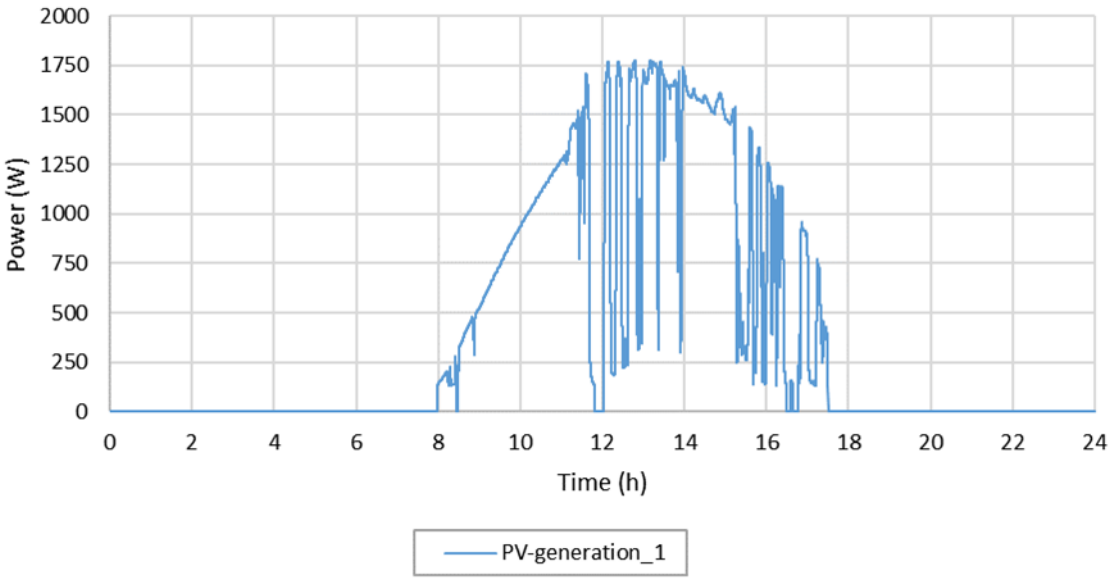

Figure 3.10 PV-generation profile generated from real measured PV-data

Matlab/Simulink model

The modelled PV-generation profile is shown in Figure 3.10. The model works identically to the load profile model as shown in Figure 3.8. The "ydat" array contains the PV-data instead of load data.

4. RESEARCH AND DEVELOPMENT OF CONTROL STRATEGIES AND SCENARIOS

4.1 Basic device control

This chapter focuses on the developed PLC programs to send, receive, and store the data. The PLC programs are created in TIA Portal V16. This chapter also describes the control and control accuracy of the devices. The main communication parameters of the devices are shown in Table 4.1. All TCP/IP devices in Table 4.1 have an Ethernet interface and are connected through the Moxa EDS-208A switch.

Table 4.1 Communication parameters

Device	Communication	IP address	Subnet	Port
Siemens ET 200SP OC 2	PROFINET	169.254.167.94	255.255.0.0	
MagnaPower power supply	LXI TCP/IP	169.254.167.90	255.255.0.0	49151
Vacon 8000 SOLAR	Modbus TCP/IP	169.254.167.100	255.255.0.0	502
PAC3200-1	Modbus TCP/IP	169.254.167.101	255.255.0.0	502
PAC3200-2	Modbus TCP/IP	169.254.167.102	255.255.0.0	502
PAC3200-3	Modbus TCP/IP	169.254.167.103	255.255.0.0	502
SP 2403 (FESS)	Analog signals			

To initiate communication with the devices, they need to be configured in TIA Portal. For this, they need the TCON_IP_v4 system data. This was made for all the devices, and Vacon 8000 Solar TCON_IP_v4 setup is shown in Figure 4.1. Every device must have unique CONN_OUC ID in TCON_IP_v4 and that the Connection_ID and MB_Unit_ID need to be correctly set in the generated Tsend_C/MB_Client global databases.

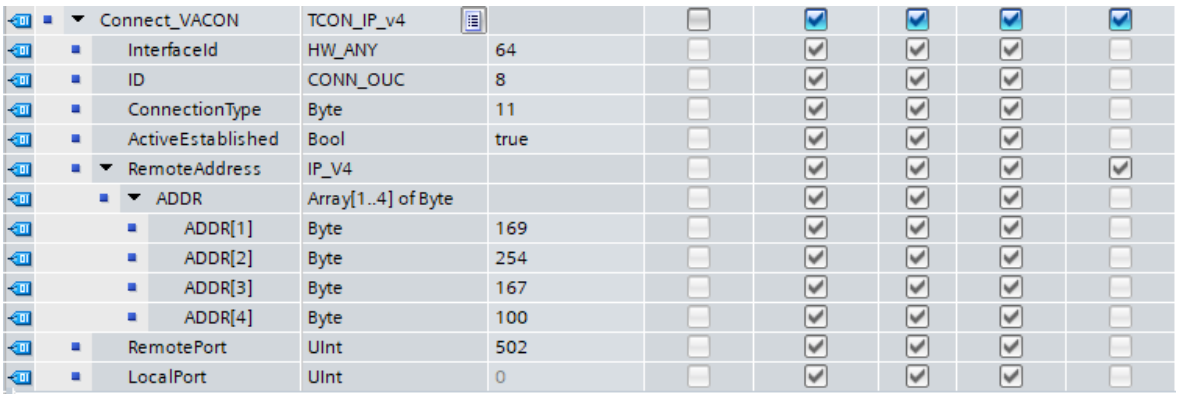

Figure 4.1 TCON_IP_v4 connection configuration

4.1.1 MagnaPower TSD800-18/380

MagnaPower TSD800-18/380 has an LXI TCP/IP ethernet interface that allows the user to make ethernet connections with the device and control it via terminal emulation programs, user written software (e.g., PLC code, python). The LXI TCP/IP Ethernet interface has an embedded web server where it is possible to change the module's network settings such as hostname, description, IP Address, Subnet etc.

The device uses Standard Commands for Programmable Instrumentation (SCPI) commands. SCPI commands are ASCII textual strings, which are sent to the instrument over the physical layer. SCPI commands are a simple way to control the device as they are driver and programming environment independent. SCPI has two types of messages: program and response. A program message consists of one or more properly formatted SCPI commands sent to the MagnaPower power supply. A response message consists of data in a specific SCPI format sent from the MagnaPower power supply to the controller. MagnaPower TS Series online documentation contains all the possible SCPI commands.

As the MagnaPower power supply uses ASCII textual strings, the data must be processed into a suitable format before sending by the Siemens PLC. To send a simple start command (OUTP:START) to close the internal power switch to energize the output of the device, the following data processing has to be done in TIA Portal:

1. Create a new variable 'x' in a global database with type of data "String" and set the start value to 'OUTP:START'.
2. Convert the created variable string to chars and store it in 'Array[0...10] of Byte'. (It is important that the array has an extra byte compared to the intended data. This is because SCPI commands use a new line character (\n) for the termination of the SCPI command string.
3. In the 'Array[0...10] of Byte', the start value of the last byte is set to 16#0A to generate the new line character for SCPI command string termination. Now the command is ready to be sent to the MagnaPower power supply as an array of byte with string termination.

To send the command to the device, first the communication must be established. This is achieved via TIA Portal's TSEND_C block. This block is responsible for establishing the connection, maintaining connection, and sending data. The example of sending the MagnaPower "Start" command is shown in Figure 4.2. The TSEND_C block receives connection description via TCON_IP_v4 system data type, connection is established based on CONT value, and send job is executed when a rising edge is detected at the

REQ parameter. DATA points to the array of bytes previously described. Parameters on the right side are used for process indications and control logic.

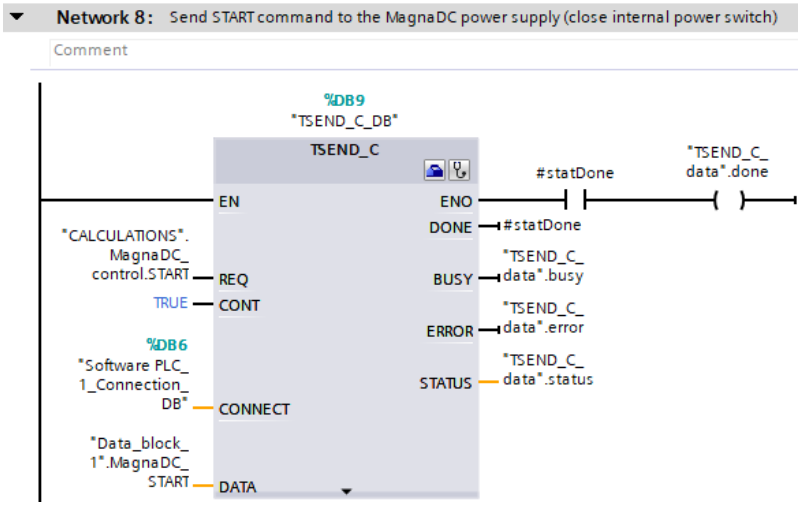

Figure 4.2 TSEND_C block – MagnaPower communications

The MagnaPower programmable power supply is controlled in real-time via reference set-points that are generated based on the modelled Simulink load profiles. The load profiles input data is in 1-second steps thus 1second OB Cyclic interrupt is used. A simple "Add" block is used to count the simulation time and to generate a suitable time signal for the developed models. The output of the profile is then loaded into a "real" variable (power value in watts). This value is divided with the voltage value to get the base reference current value for the power supply.

This initial setup of the PV-system was very inaccurate and was practically unusable for PHIL setup control. The accuracy of the PV-system is improved by adjusting the reference current value with developed corrective factor. This allows the system to achieve good accuracy for maintaining chosen reference output power. Additionally, basic error feedback is used to offer greater accuracy during power ramps and changes in the reference signal. The reference current value is then converted to a suitable SCPI format with specific size, length, and format. The result is the SCPI command "CURR x.xxxx", where x is the new current reference value to output the reference power value. The Siemens PLC sends new reference values to MagnaPower every 200ms. This was found to be the suitable value to get achieve good accuracy. The voltage is held at 470 V for the generated PV-profile as it was experimentally determined to be suitable (this was also the initial reference setpoint for the Vacon inverter). The voltage setpoint of DC-link 470 V is set via Vacon 8000 Solar general parameters.

All other possible SCPI commands are generated and sent in similar way. TRCV_C can be used to read program responses but that was deemed unnecessary for this thesis.

The final control system developed for the PV-system had an error of ~0.3% during the 24-hour simulation of generated PV-profile and an RMSE of ~8 W. The control system was validated with PV-generation profiles with peak generation of up to 5 kW, and the error remained below 1%. There are three short periods where the PHIL PV-system differs noticeably from Simulink model as shown in Figure 4.3. The moments that are responsible for generating the error are:

- Start-up of the inverter.
- External fan temporarily starting due to temperature increase.
- Shutdown of the inverter.

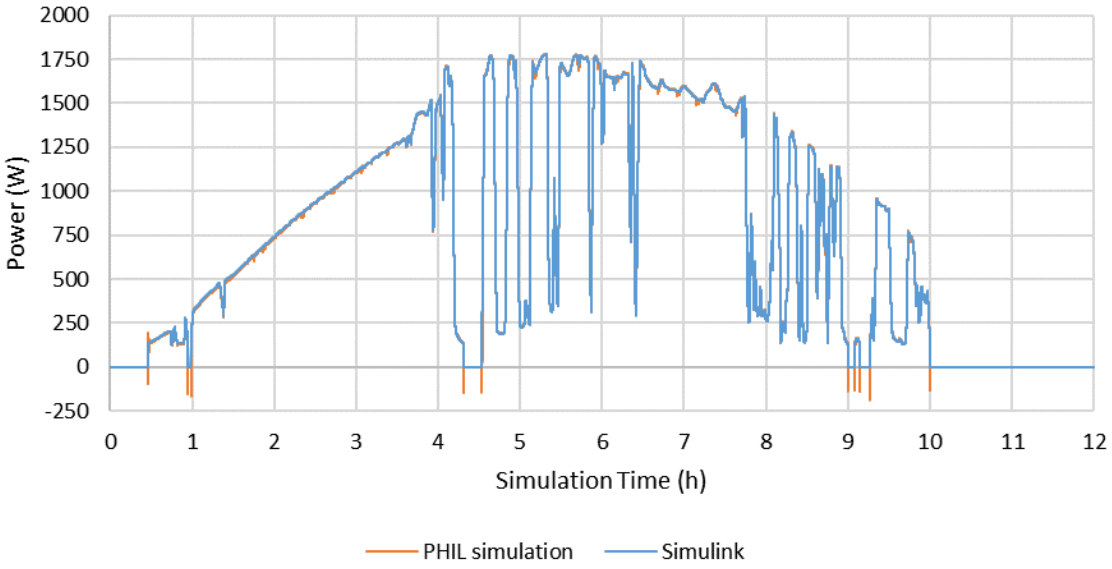

Figure 4.3 Comparison between Simulink and PHIL-simulation PV-output power

It is possible to see that during some moments the real PV-system (PHIL simulation) acts as a consumer (negative power). This happens during the start-up and shutdown of the inverter.

4.1.2 Vacon 8000 SOLAR

Vacon 8000 SOLAR has an OPTC-I Modbus TCP interface that allows the user to monitor the device. NCIPConfig can be used to modify the OPTC-I board parameters such as unit identifier, IP-address, subnet etc. NCDrive can be used to download and upload the configuration/parameters of the drive (RS232/Modbus TCP). The OPTC-I board manual has the base ModBus addresses defined. In this thesis, Modbus TCP is used to monitor the Control Word with address 10002 (RUN). The input status is used in the control logic of the developed PHIL-Setup. For future reference, the OPTC-I register bytes were found to be shifted by 8. [53, 54]

MB_CLIENT is used to initiate communication and receive the data. Configured MB_CLIENT block for reading Vacon 8000 Solar coil address is shown in Figure 4.4. The MB_MODE, MB_DATA_ADDR and MB_DATA_LEN values define that the PLC reads 1 input bit in address 10002.

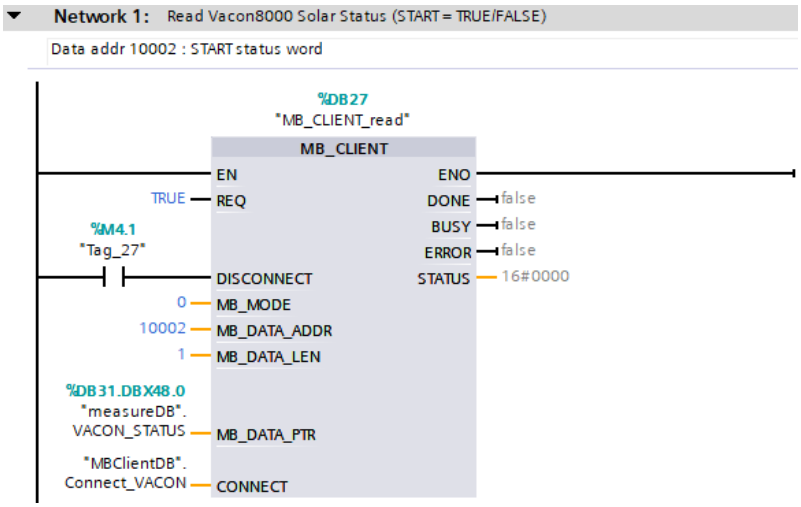

Figure 4.4 MB_CLIENT block – Vacon8000

The input address data is stored in bool called VACON_STATUS. The status of the device is monitored in 100ms intervals. The status of the Vacon is used to control the scenario(s).

As the PV-Inverter has a minimum start-up voltage of 340 V, the PV-generation profile is modified to start from 130W due to limitations of the Vacon 8000 Solar inverter. This power value was experimentally found to be optimal, as lower values would cause unnecessary ON-OFF switching of the device. In addition, several parameters of the Vacon inverter were changed for this thesis to improve the speed and accuracy of the PV-system:

- Startup wizard: OFF
- PwrStandbyLevel: 0.3%
- PwrStandbyDelay: 5sec

4.1.3 PAC3200

PAC3200 power metering devices have the capability to send measured values and/or receive commands via Modbus TCP. As part of this thesis, there is no need to send Modbus commands to these device(s). The communication parameters of the PAC3200 devices can be configured from the front panel. The value of total instantaneous active power value is read from the register. The value for instantaneous active power has an Offset 65 (from 400001) and a length of 2.

MB_CLIENT is used to initiate communication and receive data as shown in Figure 4.5. The configuration of the communication block is done similarly to previously described Vacon 8000 Solar. The input data (1 Real type value) is stored in an Array of Real. The measured values are read with 100ms intervals. All three PAC3200 devices are programmed similarly.

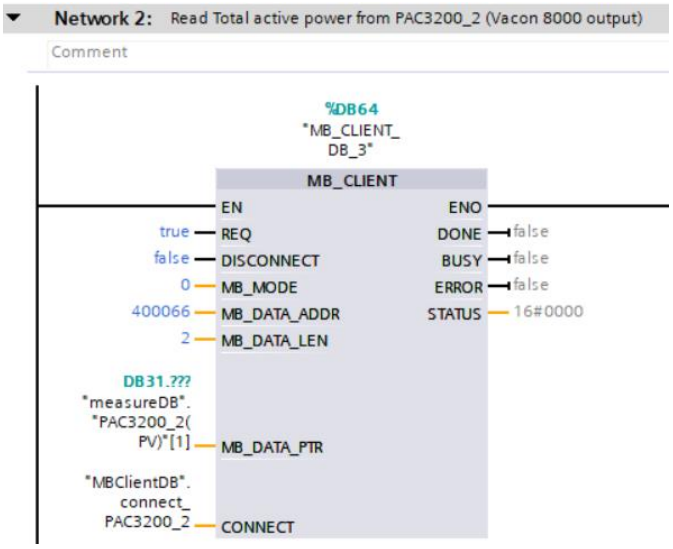

Figure 4.5 MB_CLIENT block – PAC3200

4.1.4 EPA Unidrive SP 2403

The communication-control of the flywheel energy storage is based on the existing solution. Safety and calculation methods were unchanged, but the reference power control was slightly modified to match the demands of this thesis. The power reference value is given to the control algorithm based on which the 'SetTorque' value is calculated. This value is then sent to the device through the analog output (%QW0) of the PLC. The PLC code created by previous student is modified to have free access to send new power reference values. Moving average (MA) filter with a window of 1000 was added as part of this thesis to reduce the ringing of the 1ms measurement signal for the 1-second based PHIL-simulations.

4.1.5 Simulink object models

The battery model is controlled via its input power port. The generated load and PV-generation profiles are controlled via their time input (time in 1 second intervals). Additionally, the Simulink model for the PV-systems corrective factor is also controlled by power reference.

Figure 4.6 shows the generated PV-profile model in TIA Portal. Simulink models are imported into the PLC by the following steps:

- Upload shared library files to the PLC web server (.so)
- Load external source files in TIA Portal (.scl)
- Generating TIA Portal blocks from loaded external source files
- Initialize the generated blocks by calling them in Unload-Load order
- Call the generated ...OneStep block in PLC code

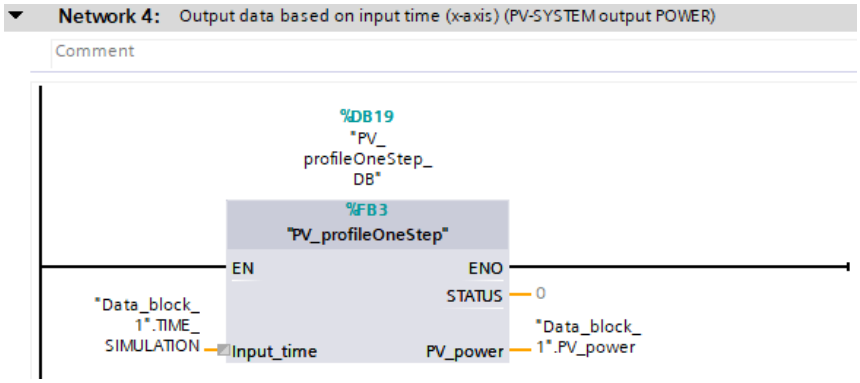

Figure 4.6 PV-generation model block in TIA Portal

4.2 Scenarios

All the scenarios consist of two sub-scenarios with different load profiles. The previous chapter has described the basic control of devices that will follow certain control scenarios described in the upcoming subchapters. The time duration of the simulations is 24-hours, and the start time of the simulations is set to be 07:30 in the morning, briefly before the sunrise (startup of the PV-system). To obtain PHIL simulation results, Traces are used in TIA Portal. A trace can store a specific amount of datapoints based on the number of tracked variables and their types. Traces are configured to start at specific simulation time automatically. The final extraction of data to .csv files and data handling is done manually.

The initial conditions for the 9.6 kWh BESS are shown in Table 4.2. Maximum and minimum SOC are limited to 90/20%, respectively, as it is not recommended to fully charge/discharge Li-Ion batteries to extend their lifetime. The maximum C-rate 0.6 of the BESS is given in the products datasheet. This means that the battery has discharging power in the range of 4,5...6,57 kW based on battery voltage. The lowest maximum output power occurs at the lowest SOC%/battery voltage. The BESS has an initial SOC of 50%. This value was chosen for two reasons: battery storage systems are usually

stored and delivered at such SOC, and it is important that the BESS does not reach minimum SOC value before the PV-system is able to start generating power. The load profiles of the scenarios can be seen in Figure 3.7. These BESS initial parameters and conditions will be used in every scenario.

Table 4.2 BESS parameters and initial conditions

BESS	C-rate	Initial SOC	Maximum SOC	Minimum SOC
	0.6	50%	90%	20%

4.2.1 Scenario 1: Base scenario

The PHIL system in Scenario 1 consists of the electrical load and battery storage system. There are no additional energy sources. The representative microgrid schematic of Scenario 1 is shown in Figure 4.7. The goal of Scenario 1 is to determine the microgrids base islanded time duration if the system consists of only the load and BESS with a specific initial SOC. Scenario 1 will be the base-comparison point for all the upcoming different scenarios.

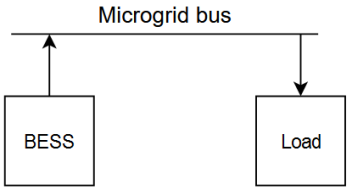

Figure 4.7 Representative microgrid schematic for Scenario 1

Scenario 1 Overview

In this scenario, the simulated microgrid will operate until the BESS reaches setpoint minimum SOC value. The resulting time-duration is then used as the base-comparison with the following scenarios in respect to both the battery cyclic lifetime and microgrids islanded time duration. The control logic flowchart of the scenario is shown in Figure 4.8.

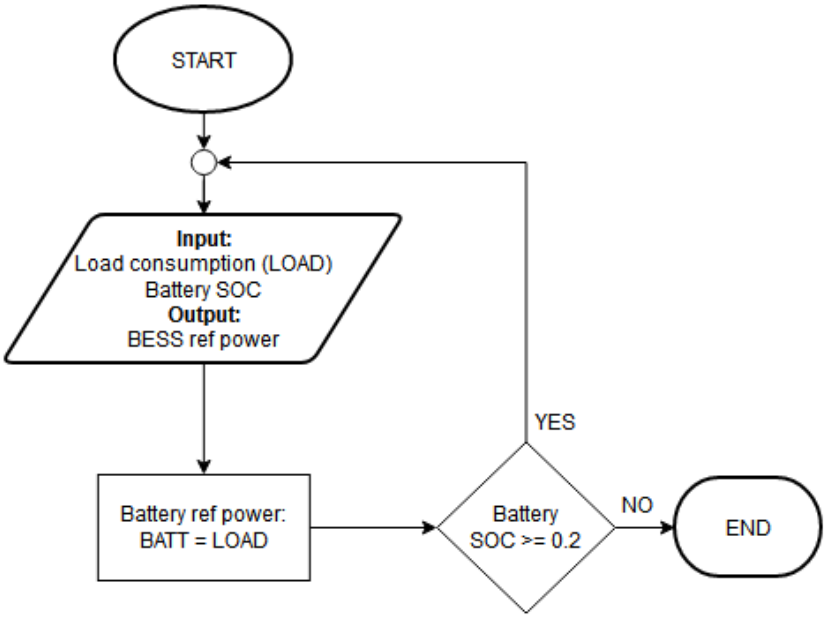

Figure 4.8 Scenario 1 control algorithm

Scenario 1 Matlab/Simulink simulation

The Matlab/Simulink model of Scenario 1: Base Scenario is shown in Figure 4.9. The model consists of the generated load profile and battery model.

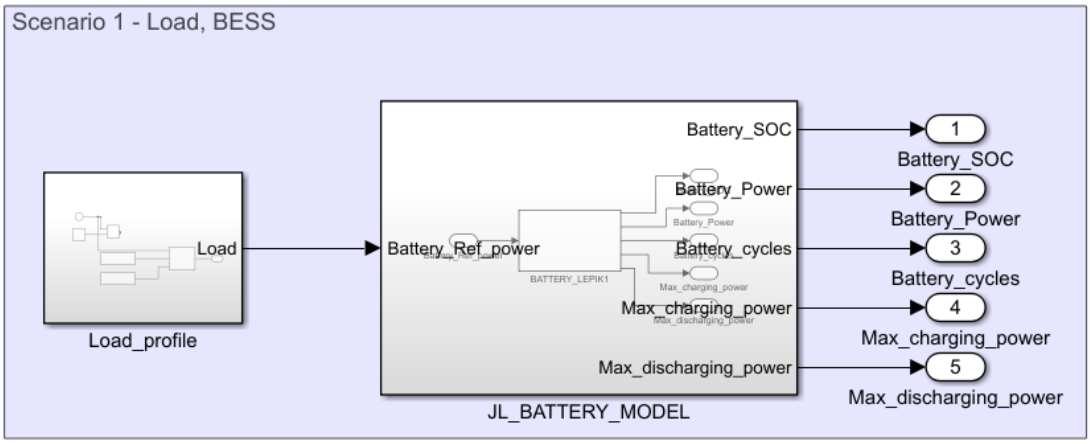

Figure 4.9 Matlab/Simulink model of Scenario 1

As this scenario does not include real physical devices, both the Simulink and the PHIL setup perform a 15-minute simulation to determine the capability of the Siemens PLC to run the models and accuracy of PHIL-simulations.

Scenario 1 PHIL real time simulation

PLC program, function block "Scenario 1", operating similarly to the Matlab/Simulink model was created for the PHIL-simulation. As there are no real devices as part of this scenario, pure software simulation was performed. The function block is called in 1

second cyclic OB once the scenario has been started from "Scenarios control" database. Based on developed Matlab/Simulink models, the power value of the load profile is sent as the power reference value of the BESS.

4.2.2 Scenario 2: Effect of PV-system

The PHIL system in Scenario 2 consists of the electrical load, battery storage system and PV-system. The schematic of the scenario's system is shown in Figure 4.10. The goal of Scenario 2 is to study how does the PV-system affect the cyclic lifetime of the BESS and islanded time duration of the microgrid.

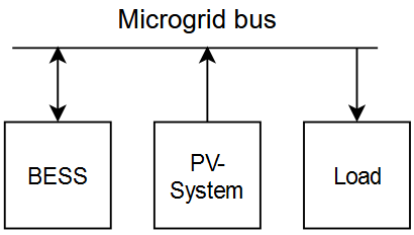

Figure 4.10 Representative microgrid schematic for Scenario 2

Scenario 2 Overview

In this scenario, the simulated microgrid will again operate until the BESS cannot provide sufficient power to match the load demand. The resulting time-duration of the microgrid islanded time and cycles performed by the BESS are the outputs of the simulation.

The power generated by the PV-system is prioritized to supply power to the electrical load and excess energy will be stored in the BESS, if possible. In case the BESS is fully charged to maximum allowed SoC value, and the PV-generated power is higher than the consumed power, the PV-system will limit its power generation to match the load to emulate capabilities of real modern PV-systems. The control logic flowchart of the scenario is shown in Figure 4.11.

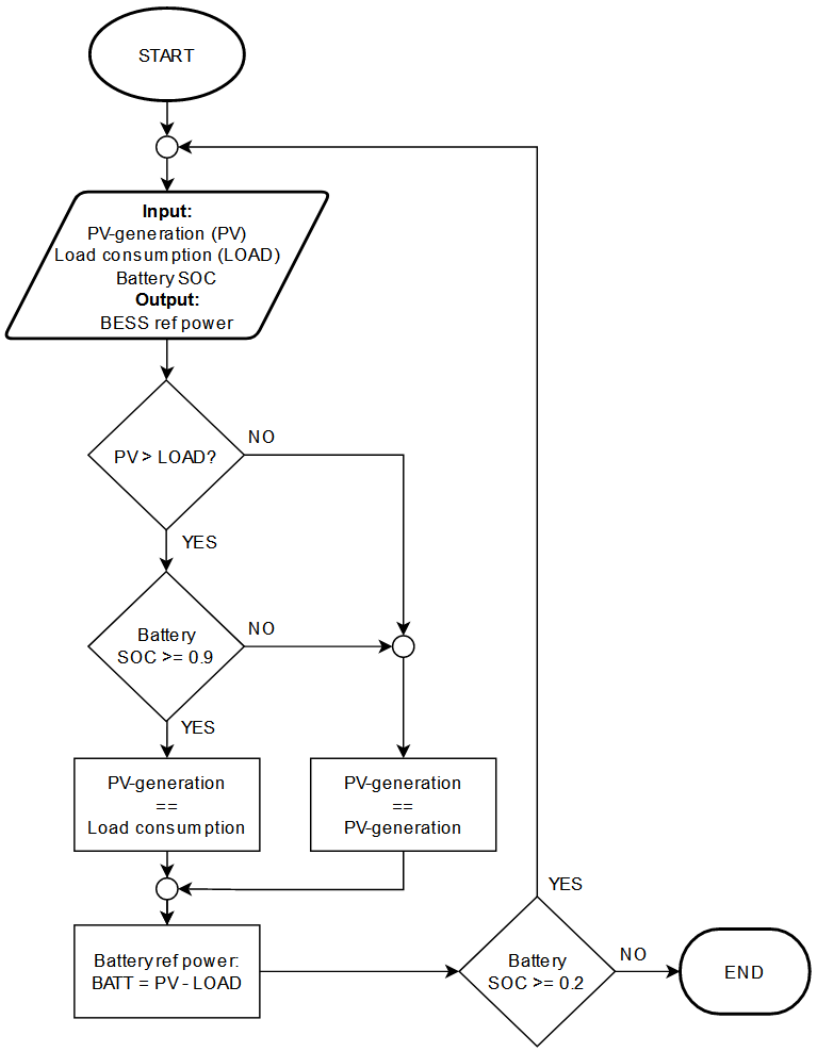

Figure 4.11 Scenario 2 control algorithm

Scenario 2 Matlab/Simulink simulation

The Matlab/Simulink model of Scenario 2: Base Scenario is shown in Figure 4.12. The model consists of the generated load profile, developed battery model and the control algorithm previously described for Scenario 2.

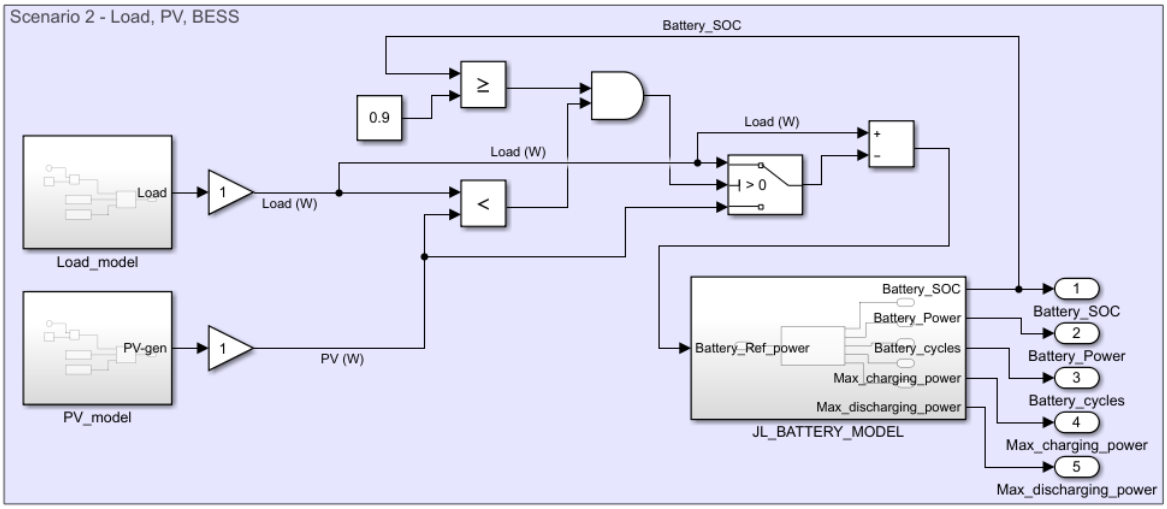

Figure 4.12 Matlab/Simulink model of Scenario 2

Scenario 2 PHIL real time simulation

PLC program was developed to simulate PHIL-simulations. Similarly, to Scenario 1, the primary function block is called in 1 second cyclic OB once the scenario has been started from "Scenarios control" database. In Scenario 2, the load and PV-generation profiles will output their respective reference values and BESS will either charge or discharge based on the generation-consumption mismatches of real power measurements.

4.2.3 Scenario 3: Effect of FESS

The PHIL system in scenario 3 consists of the electrical load, battery storage system, PV-system, and flywheel energy storage. The schematic of the scenario's system is shown in Figure 4.13.

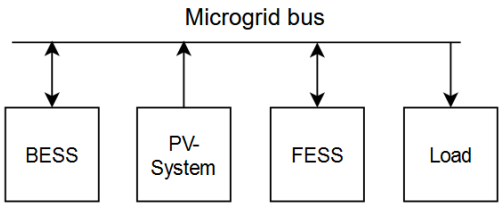

Figure 4.13 Representative microgrid schematic for Scenario 3

Scenario 3 overview

The goal of this scenario is to research how does using FESS as the prioritized energy storage affect BESS's cyclic lifetime and microgrid's islanded time duration. The FESS will be charged with any excess power generated by the PV-system until a specified setpoint SOC/rpm (4500 rpm of maximum 5000 rpm). 4500 rpm was chosen as a suitable value as trying to maintain the FESS's maximum 5000 rpm for extended period

is not preferred due to the measurement ringing and the potential for switching between valid rpm value (under 5030) and over 5030 (out of scope). 4500 rpm translates to roughly 77% FESS SOC.

Once the setpoint of 4500 rpm has been reached, the FESS will be charged with a power of up to 1055 W to keep the FESS at ~4500…4600 rpm. Any extra power generated by the PV-system will be stored in the BESS. Once the load consumption again exceeds the PV-generated power, the FESS will be prioritized to discharge the required power first. FESS will attempt to discharge reference power until 300 rpm, after which the FESS loses its capability to output any meaningful power.

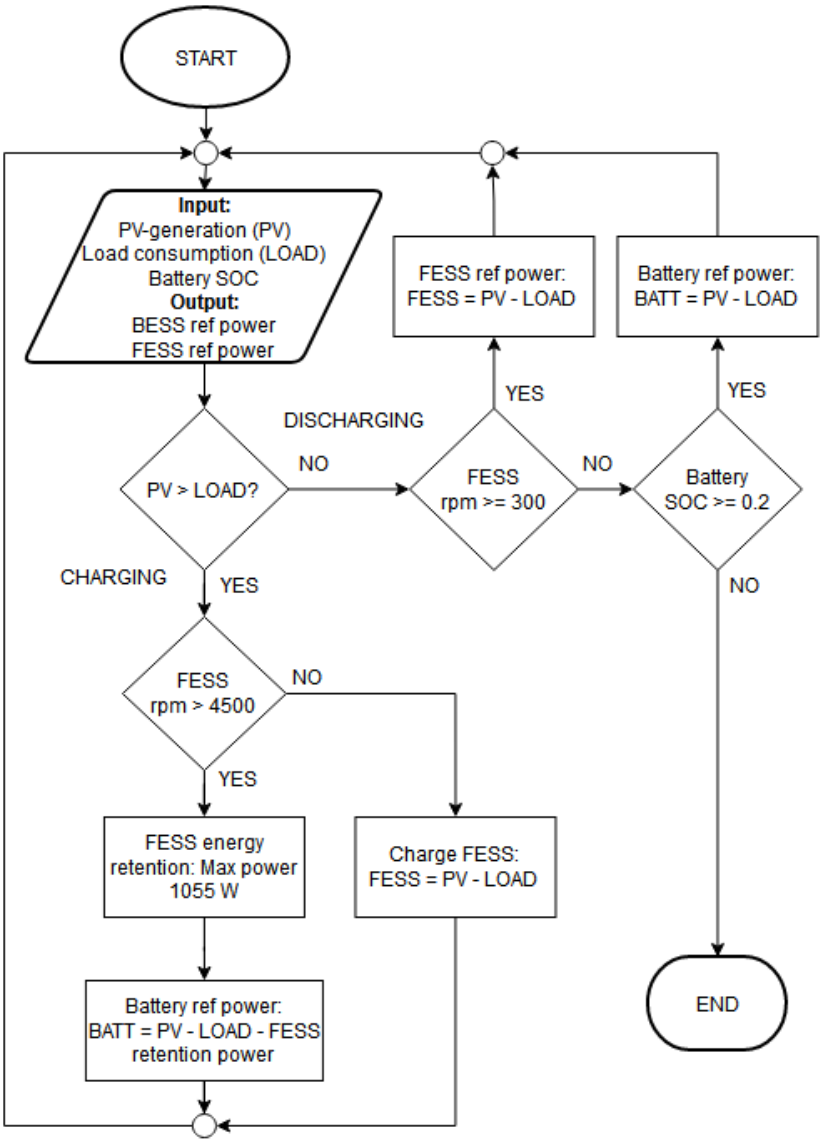

Figure 4.14 Scenario 3 control algorithm

Scenario 3 PHIL real time simulation

PLC program was developed based on the Scenario 3 control algorithm and description. The BESS will get reference power value based on the calculations of load model and real measurements from PV-system and FESS. The function block of scenario 3 is shown in Figure 4.15.

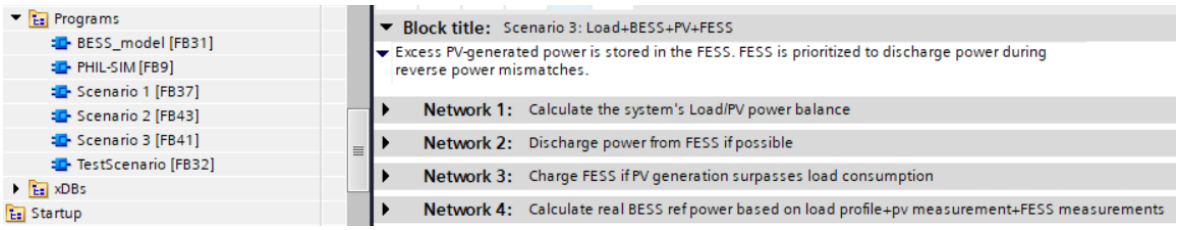

Figure 4.15 Scenario 3 function block

5. RESULTS AND VALIDATION OF CONTROL STRATEGIES AND SCENARIOS

5.1 Scenario results

This chapter presents the results of both Matlab/Simulink and PHIL-simulation results. Scenario 1 Matlab/Simulink and PHIL-simulation validation results are shown in Figure 5.1. The results of Matlab/Simulink and PHIL-simulation are identical (complete overlap of monitored parameters: BESS SOC and number of full cycles performed). As a result, the 24-hour simulation with the PHIL setup is not performed for Scenario 1, and the base comparison values are from Simulink simulation. Cycles represents the number of full discharge and charge cycles performed by the battery during the simulation. One full cycle is achieved by fully discharging the battery (9.6 kWh) to 0% SOC, and then recharging the battery to 100% SOC (9.6 kWh). Thus, one cycle is equivalent to ~19.2 kWh.

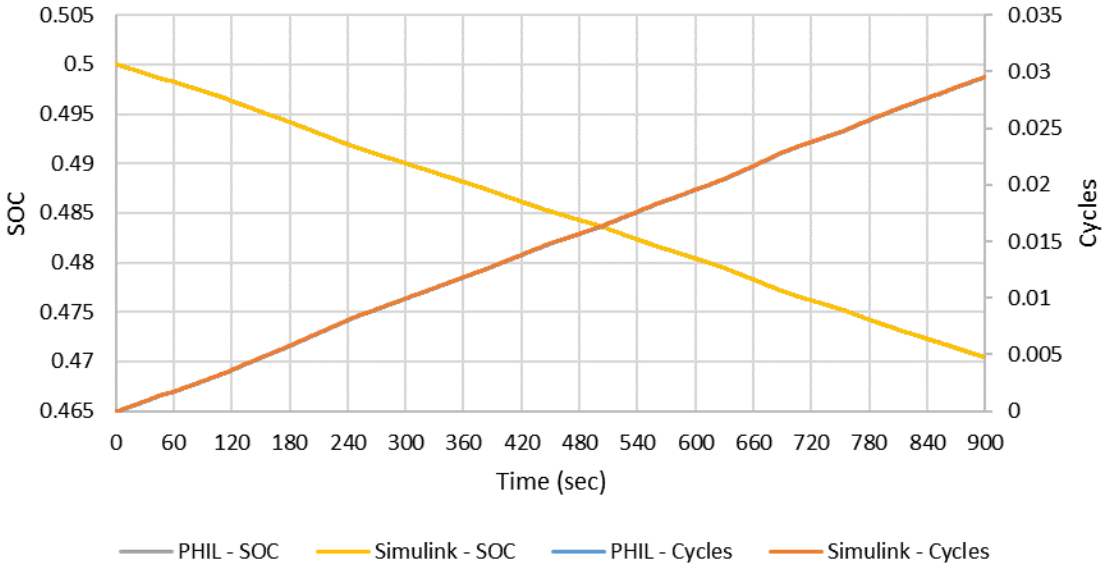

Figure 5.1 Results of 15-minute validation simulation results

In Scenario 1, the system consisted of only the BESS model and two different load consumption profiles. The battery is acting as load-following in this scenario, and there is no possibility for any additional control. In Scenario 2, the PV-system is added, and the power generated by the PV-system is prioritized to power the load and any excess power was stored in the BESS. In Scenario 3, the FESS was added to the system and prioritize to store of all excess energy from PV-generation. The FESS was prioritized to discharge the required power if power generation and consumption mismatches occurred.

Figure 5.2 presents the results of the 24-hour simulation of Scenario 1 with load profile 1. It was determined that the microgrid is capable of operating in islanded mode for 13 266 seconds or 3h 41min 6sec and the battery performs ~0.15 full cycles before BESS reaches the minimum setpoint of 20% SoC.

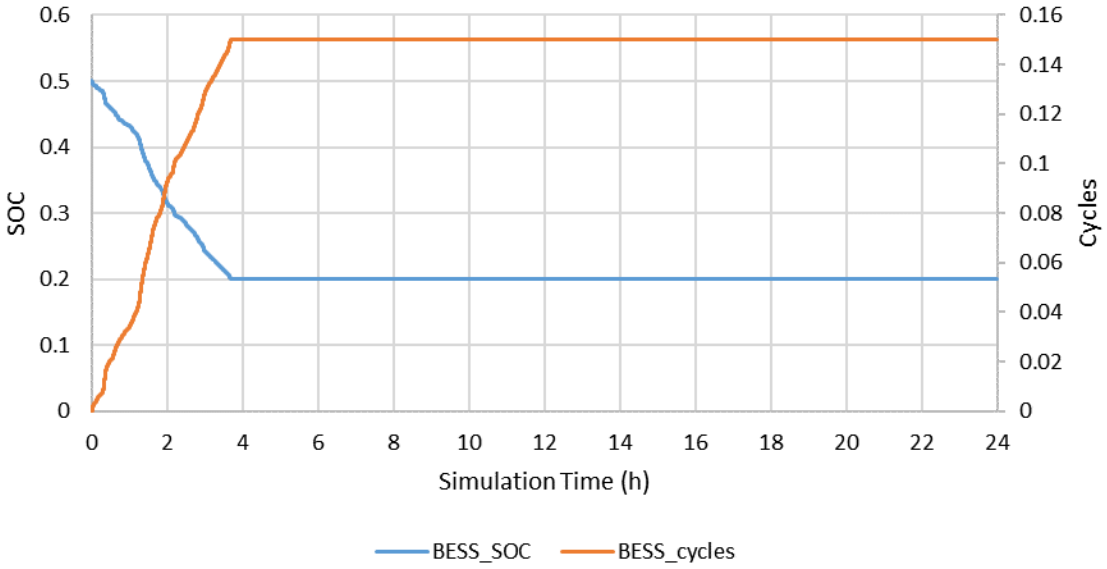

Figure 5.2 Simulation results for Scenario 1: Load profile 1

Figure 5.3 presents the results of the 24-hour simulation of Scenario 1 with load profile 2. The microgrid was found to be capable of operating in islanded mode for 13 183 seconds or 3h 39min 43sec and the battery performed ~0.15 full cycles before BESS reached the minimum setpoint of 20% SoC.

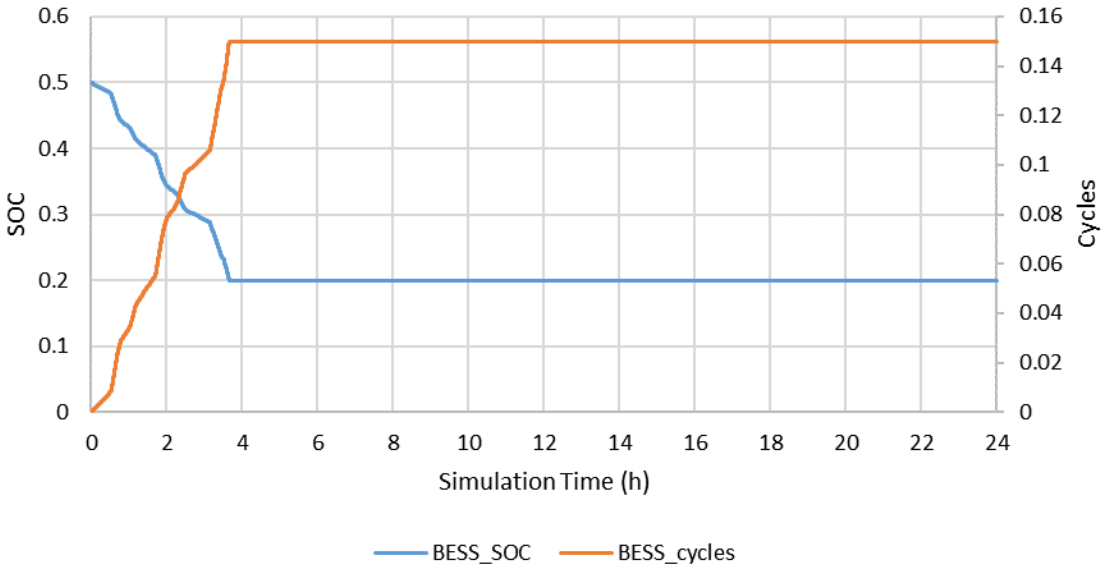

Figure 5.3 Simulation results for Scenario 1: Load profile 2

Figure 5.4 presents the results from the 24-hour simulation of Scenario 2 with load profile 1. It was determined that the microgrid is capable of operating in islanded mode for 79 941 seconds or 22h 12min 21sec and the battery performs ~0.517 full cycles before the BESS reaches the minimum setpoint of 20% SoC.

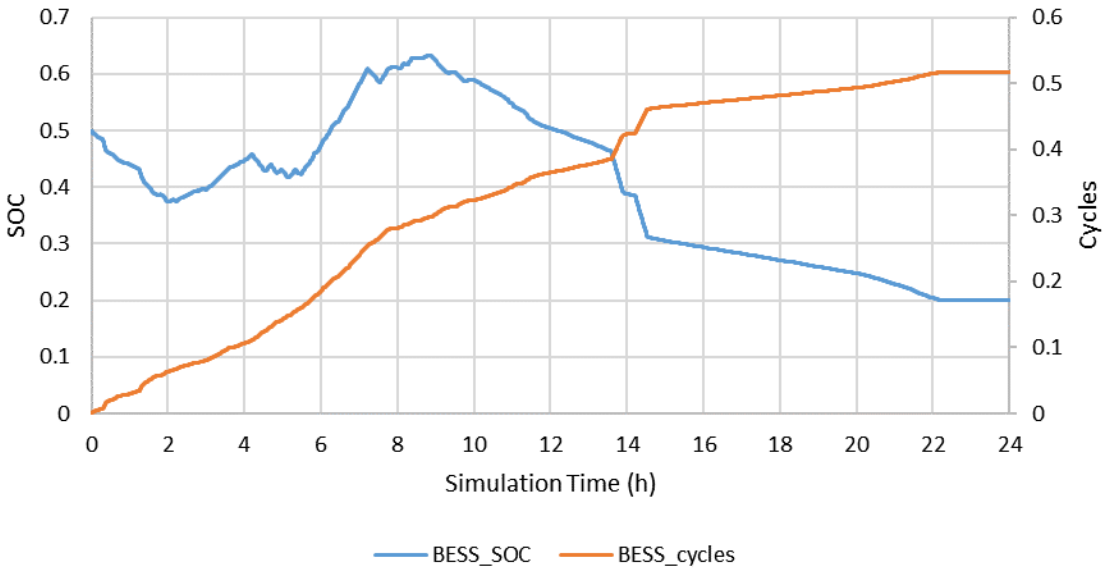

Figure 5.4 Simulation results for Scenario 2: Load profile 1

Figure 5.5 presents the results from the 24-hour simulation of Scenario 2 with load profile 2. It was determined that the microgrid is capable of operating in islanded mode for 52 363 seconds or 14h 32min 43sec and the battery performs ~0.538 full cycles before the BESS reaches the minimum setpoint of 20% SoC.

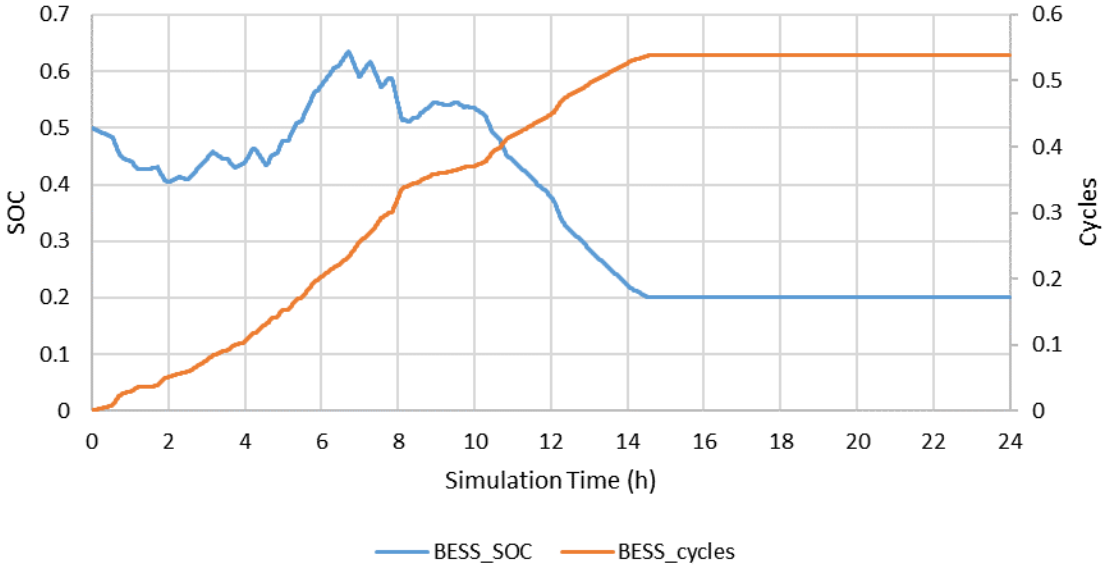

Figure 5.5 Simulation results for Scenario 2: Load profile 2

Figure 5.6 presents the results from the 24-hour simulation of Scenario 3 with load profile 1. It was determined that the microgrid is capable of operating in islanded mode for 39 352 seconds or 10h 55min 52sec and the battery performs ~0.173 full cycles before the BESS reaches the minimum setpoint of 20% SoC.

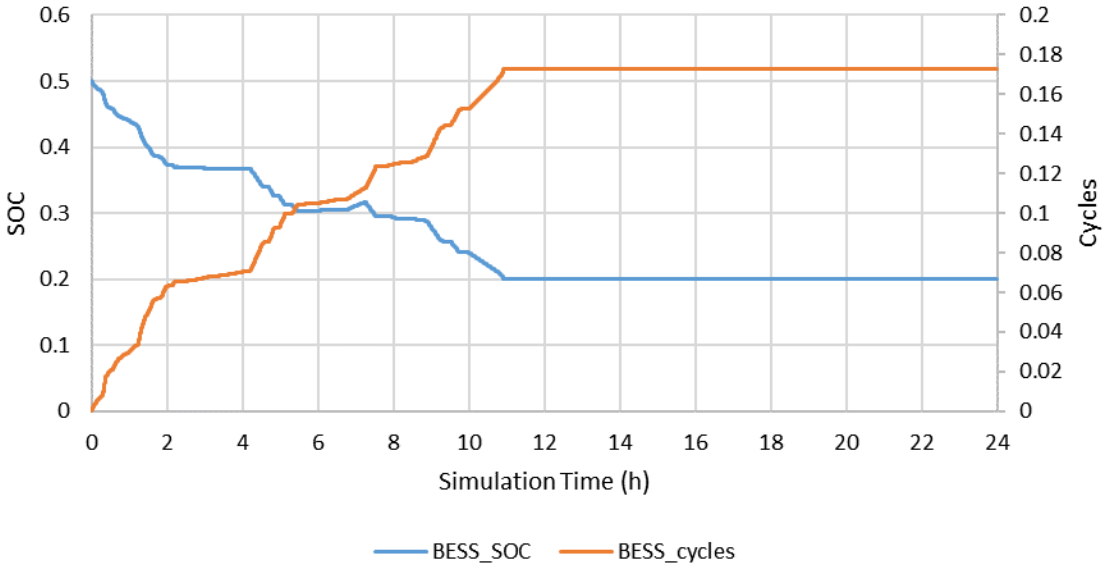

Figure 5.6 Simulation results for Scenario 3: Load profile 1

Figure 5.7 presents the results from the 24-hour simulation of Scenario 3 with load profile 2. It was determined that the microgrid is capable of operating in islanded mode for 29 040 seconds or 8h 4min and the battery performs ~0.174 full cycles before the BESS reaches the minimum setpoint of 20% SoC.

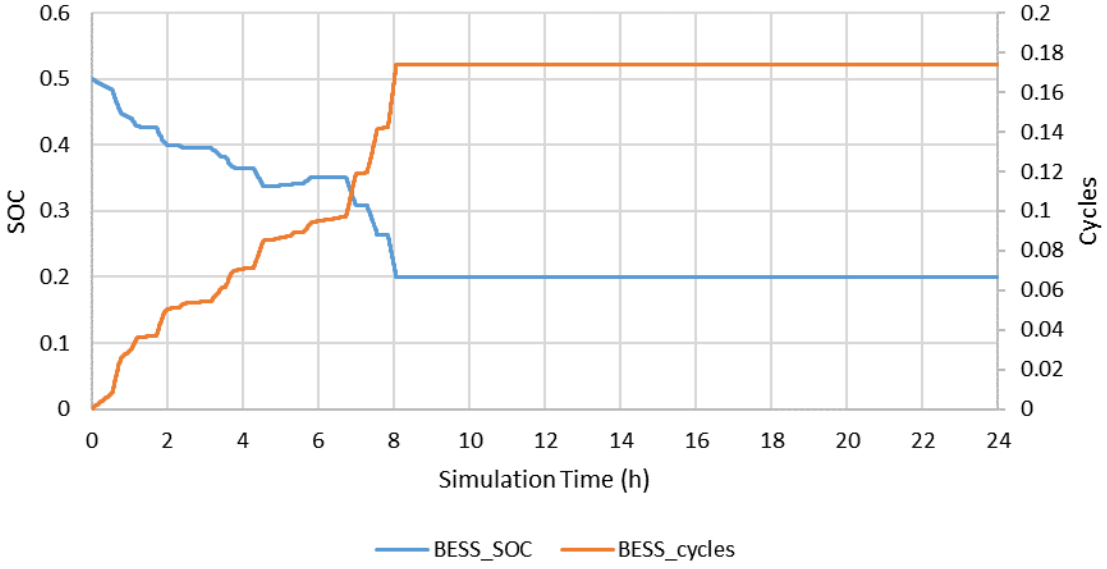

Figure 5.7 Simulation results for Scenario 3: Load profile 2

The results of the scenarios are summarized in Tables 5.1 and 5.2. Table 5.1 presents the microgrid islanded time duration and the number of cycles the BESS performed obtained through Matlab/Simulink simulations. Table 5.2 presents the PHIL-simulation results of researched Scenarios.

Table 5.1 Simulink simulation results

Simulink	**Islanded mode duration**		**BESS cycles/kWh throughput**	
	Load 1	**Load 2**	**Load 1**	**Load 2**
Scenario 1	3h 41min 6sec	3h 39min 43sec	0.15/2.88 kWh	0.15/2.88 kWh
Scenario 2	22h 16min 15sec	14h 36min 23sec	0.52/9.98 kWh	0.54/10,37 kWh

Table 5.2 PHIL simulation results

Simulink	**Islanded mode duration**		**BESS cycles/kWh throughput**	
	Load 1	**Load 2**	**Load 1**	**Load 2**
Scenario 1	3h 41min 6sec	3h 39min 43sec	0.15/2.88 kWh	0.15/2.88 kWh
Scenario 2	22h 12min 21sec	14h 32min 43sec	0.517/9.93 kWh	0.538/10.33 kWh
Scenario 3	10h 55min 52sec	8h 4min 0sec	0.173/3.32 kWh	0.174/3.34 kWh

The scenario featuring FESS is not simulated in Matlab/Simulink, as FESS was not modelled as part of this thesis. To determine the potential of FESS, power reference figures for the 24-hour simulations were investigated instead.

5.2 Comparison of results

Matlab/Simulink and PHIL-simulation result errors of Scenario 1 and Scenario 2 are shown in Table 5.3. In Scenario 1, the Simulink and PHIL simulations output the exact same results. This is because there are no external influences as this is a pure software simulation.

For Scenario 2, there are small differences due to the difference between the modelled PV-generation profile and the actual output of the PV-inverter. This affects both the microgrid islanded mode time duration and the number of cycles the battery must perform. Over the course of the simulated 24 hours, the islanded mode duration and BESS cycles have an error of 0.35% and 0.47% compared to Simulink simulation. The percentages are for the load profile 1 and 2, respectively. The PHIL-simulation results can thus be considered accurate, and the error is caused by the PV-system. PV-system is set to generate 8,85 kWh but the real measured PV-system generated a little over 8,83 kWh. The reason for this is described in chapter 4.1.1.

Table 5.3 24h Simulink and PHIL simulation error

Error	Islanded mode duration		BESS cycles	
	Load 1	Load 2	Load 1	Load 2
Scenario 1	0	0	0.0	0.0
Scenario 2	0h 3min 54sec	0h 3min 40sec	0.003	0.002

The simulation results for load profiles 1 and 2 are almost identical as a result of the similarity of the first few hours of the load profiles, as can be seen in Figure 3.7.

The microgrid system is capable of operating in islanded mode with both load profiles for a similar amount of time (3h 40min). With the added PV-system in Scenario 2, the islanded mode duration increases noticeably due to additional power generated by the PV-system. The large ~8h difference between Scenario 2, load profile 1 and 2 is caused by the differences in load profiles after the first 4 hours. The number of full battery cycles is nearly identical with both loads in both scenarios as the power generated from PV-system was prioritized to power the load and the generated energy from the PV-system was near-identical.

PHIL simulation results with load profile 1

As determined from Scenario 1: based on the Base scenario, the microgrid is initially capable of operating in the islanded mode for 3h 41min and 6sec. The addition of a PV-system increases the islanded time duration of the microgrid noticeably. The downside is that the BESS must perform more cycles as the battery is used as the buffer to store excess power generated by the PV-system and balances the power mismatches should they occur. However, incorporating FESS reduces the islanding time duration but also decreases the number of cycles the battery must perform. The effect of FESS and PV-system on the islanded mode duration and the cycles performed by the BESS in a microgrid with Load profile 1 are visualized in Figure 5.8 and 5.9.

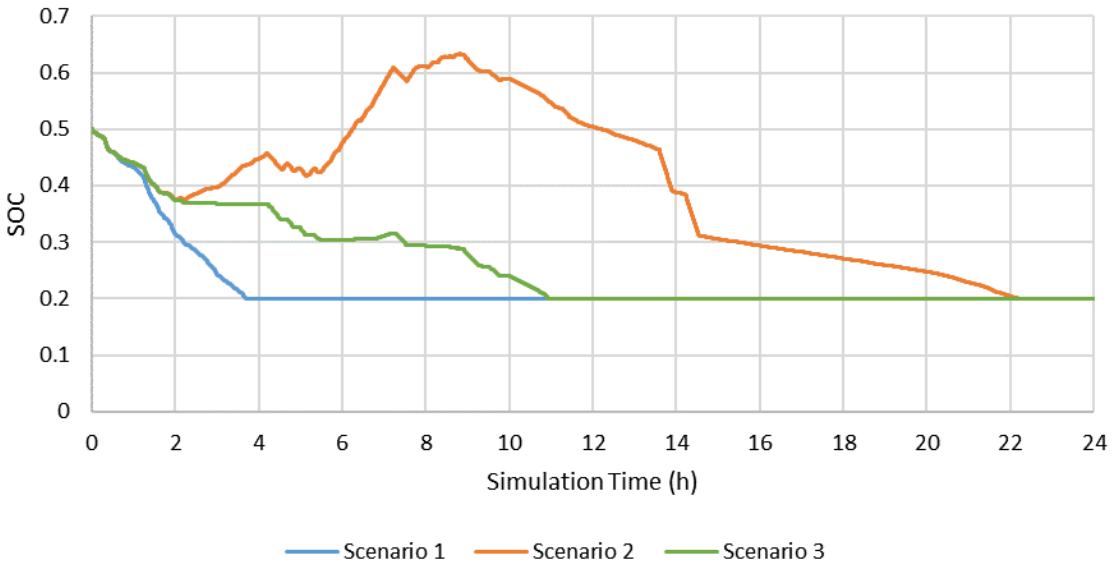

Figure 5.8 PHIL-Simulation results comparison: Load profile 1 – BESS SOC

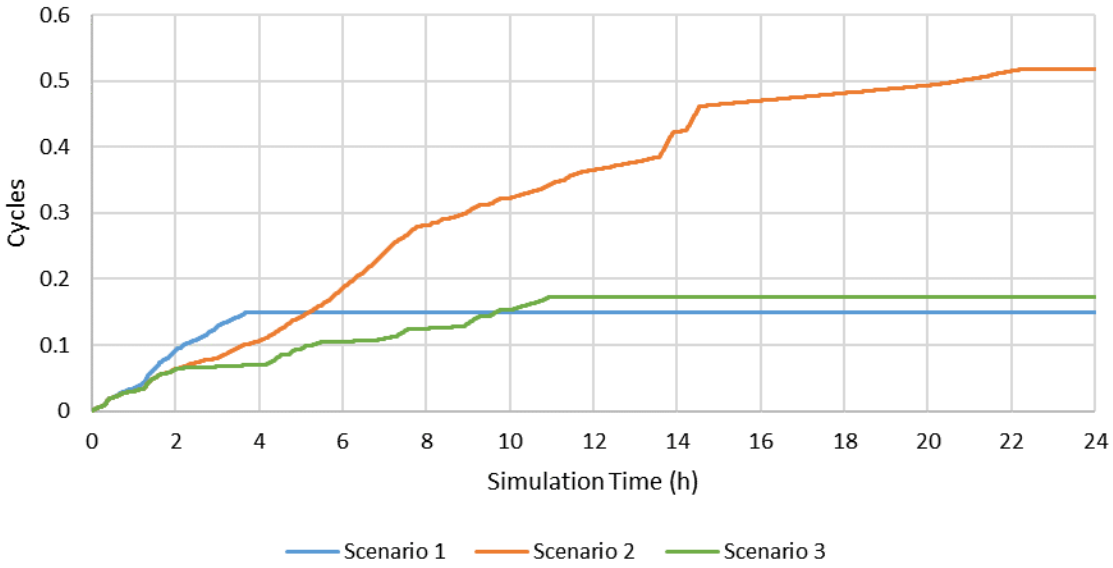

Figure 5.9 PHIL-Simulation results comparison: Load profile 1 – BESS cycles

In Scenario 1, the base islanded time duration, and the number of cycles the BESS must perform are determined. In Scenario 2, with added PV-system affects the system increases the islanded time duration of the microgrid but BESS must perform more cycles as the system has higher uptime. In Scenario 3, the added FESS has a negative effect on the islanded time duration due to high losses but helps to decrease the number of BESS cycles. This is because the FESS soaks up most of the excess PV-generated power, and thus BESS is simply charged less during the simulation. The reason for higher BESS cycles with the FESS is caused by the small inaccuracies of the FESS control. The BESS acts as the system balancer during the time when PV-generation

exceeds load consumption and FESS is prioritized to charge/discharge. This means that the BESS will be charging/discharging with low power during most of this time. The BESS performs fewer cycles as almost all the excess PV-generation is stored in the FESS, totalling 3.67 kWh. The downside is that only 0.1 kWh or 2.7% of stored energy is discharged again during the 24-hour simulation. Therefore, the FESS is responsible for 'wasting' 3.57 kWh or 97.27% of the energy used to charge the FESS. Compared to Scenario 2, adding FESS decreases the islanded time duration by 11hours 16minutes and 29 seconds, or 51%. On the positive side, FESS decreases the number of cycles that BESS must perform by 0.34 or 66% during the simulation.

PHIL simulation results with load profile 2

As determined from Scenario 1: Base scenario, the microgrid is capable of operating in the islanded mode for 3h 39min 43sec. The addition of a PV-system affects the microgrid islanded time duration and BESS cycles similarly as with load profile 1. The PV-system affects the islanded time duration of the microgrid less due to the specifics of the load profile. Adding FESS affects the system as with the previous load profile. The effect of FESS and PV-system on the islanded mode duration and the cycles performed by the BESS in a microgrid with Load profile 2 are visualized in Figure 5.10 and 5.11.

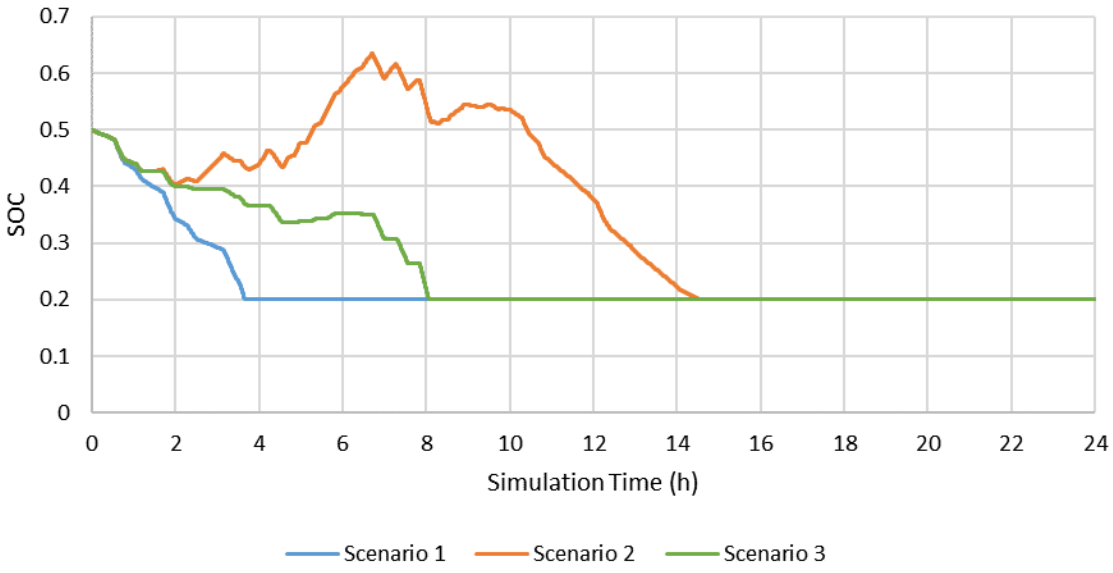

Figure 5.10 PHIL-Simulation results comparison: Load profile 2 – BESS SOC

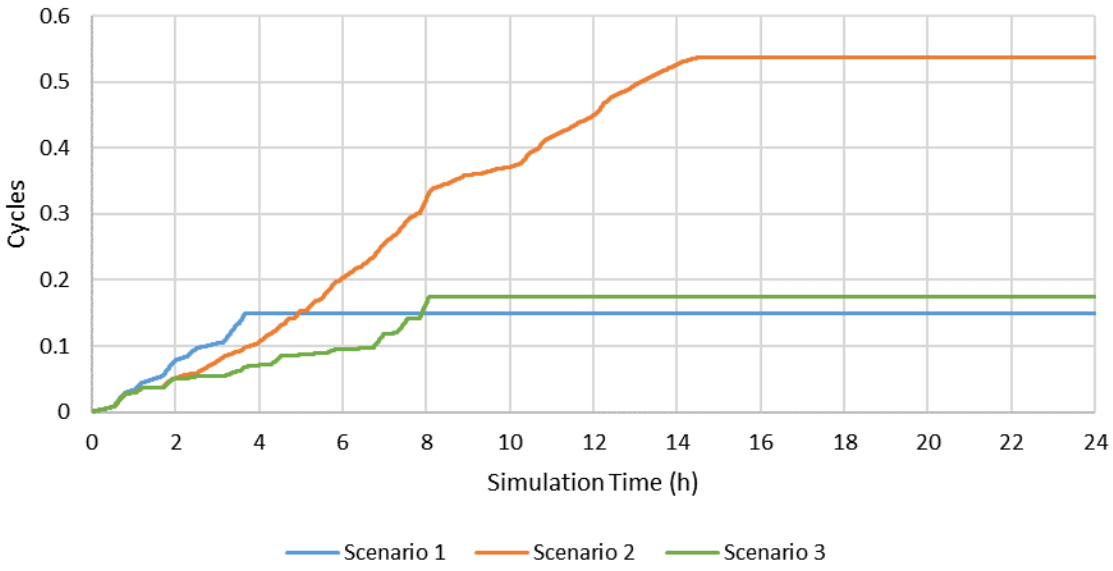

Figure 5.11 PHIL-Simulation results comparison: Load profile 2 – BESS cycles

The BESS performs fewer cycles as almost all the excess PV-generated power is stored in the FESS, totalling 3.39 kWh. The downside is that only 0.09 kWh or 2.74% of stored energy is discharged again during the 24-hour simulation. Therefore, the FESS is responsible for 'losing' 3.3 kWh or 97.25% of the energy used to charge the FESS. Compared to Scenario 2, adding FESS decreases the islanded time duration by 6hours 28minutes and 43 seconds, or 44%. On the positive side, FESS decreases the number of cycles that BESS must perform by 0.364 or 68% during the simulation.

As these PHIL simulations have different islanded mode duration, the simulation results were used to calculate the number of cycles the BESS must perform in 24 hours to better understand the effect of PV-system and FESS. The calculation results are shown in Figure 5.12. There is a clear trend that both the PV-system and FESS help to reduce the number of cycles the BESS must perform. The PV-system helps to reduce the number of cycles the BESS must perform on average by ~26% and FESS reduces the number of cycles performed by additional ~36%.

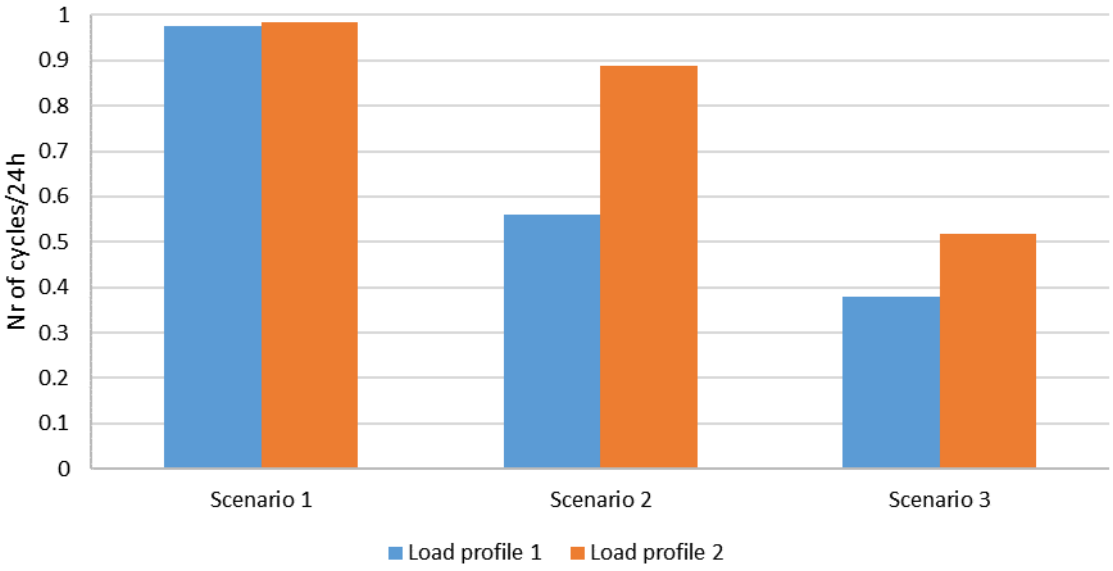

Figure 5.12 BESS number of cycles per 24h

5.3 Conclusions

The developed PHIL setup can accurately run PHIL-simulations with 1 second time-step based on the Matlab/Simulink and PHIL-simulation results comparison. However, implementing control strategies for the existing FESS is possible, but there is only very little benefit to it due to the parameters and characteristics of the FESS.

The PV-system can be accurately controlled, and it affects the islanded microgrid in a positive way by noticeably increasing the islanded time duration of the microgrid. The exact effect depends on the daily load consumption power generated from the PV-system. During the 24-hour simulations performed with the PHIL setup, the PV-system increased the islanded mode duration of the microgrid on average by ~15 hours. The number of cycles the BESS must perform decreased on average by ~26%.

The FESS affects the islanded microgrid in a negative way by noticeably decreasing the islanded time duration of the microgrid. There is great potential in using FESS in islanded microgrids as the FESS helped to reduce the number of cycles the BESS must perform by additional ~36%. The FESS reduced the number of cycles that the BESS must perform only because the FESS is charged instead of the BESS. In essence, FESS acts as a parasite that helps to reduce the number of cycles the BESS must perform at the cost of islanding mode duration. During the 24-hour PHIL-simulations, the FESS lost 97.27% and 97.25% of energy used to charge, respectively. Existing FESS cannot store enough energy and has too high power losses to be viable in the medium- or long-term for any other use than power quality regulation regarding microgrids. For short term,

the FESS can be used to provide power to high start-up devices such as motors by previously charging the FESS to a suitable SOC. Any medium- or long-term (minutes) usage of the FESS should be considered too energy inefficient for use in islanded microgrid if the goal is to increase the islanding time duration or reduce the number of cycles a BESS must perform. A modernised flywheel energy storage system that could store several kWh and has low power losses would be necessary for different control strategies and energy management purposes in islanded microgrids. A demonstration of the problem with the current FESS is shown in Figure 5.13.

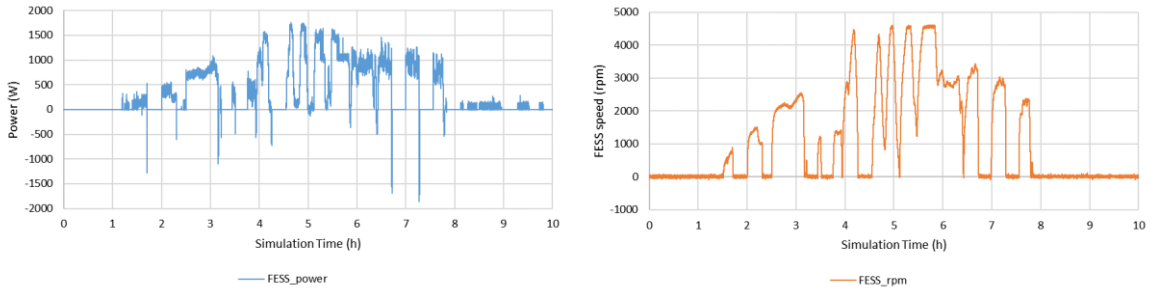

Figure 5.13 The measured power and rpm of the FESS

Although the FESS can successfully charge to considerable rpm/SOC, the maximum energy storage capacity of the FESS is so low (~0.1 kWh) that it can only discharge power for very limited time. Also, due to the considerable self-discharge losses, the FESS will quickly trend towards 0 rpm/SOC if not charged with at least several hundred watts (~500W). Existing FESS must be charged with at least 1kW and discharged almost instantly to avoid great energy losses due to self-discharge.

Increasing the load/PV-generation power would lead to increased charging/discharging power for the FESS but due to the high losses of the FESS, there would be no differences in the results. For load levelling, MA filters with various window lengths were simulated in Simulink and tested with the PHIL setup. Load-levelling with the current FESS is not possible in islanded microgrid due to the low energy capacity and high losses. The FESS can act as the load to increase power consumption during load-levelling based on PV-generated power but virtually all the stored energy is lost before discharging and as a result there is no capability to discharge power in case of load increase. Based on the main and additional short simulations it was clear that the existing FESS is not suitable for any medium- or long-term energy management related control scenarios.

The existing FESS can have a positive effect on the microgrid islanded time duration in a scenario where the BESS is fully charged, and current PV-generation exceeds load consumption. This however has very minimal effect as well as the energy storage capacity of the FESS is very low.

SUMMARY

The aim of the thesis was to develop a Power Hardware-In-The-Loop Setup (PHIL) that enables to study the effects of flywheel energy storage (FESS), PV-system, and different loads on islanded mode duration and battery's (BESS) cyclic lifetime in a microgrid. To achieve this aim, firstly, the state-of-the-art regarding microgrids, renewable energy sources and energy storage systems used in microgrids was analysed. Additionally, an overview of power hardware-in-the-loop (PHIL) setups was given. It was determined that the combination of BESS and FESS would be the optimal choice for energy storage system in a small microgrid. BESS can store energy for extended periods but have limited cyclic lifetime. FESS, on the other hand, has a long cyclic lifetime but cannot store energy for extended periods due to self-discharge.

Consecutively, the existing TalTech PHIL setup is described, and an upgraded PHIL setup based on the state-of-the-art analysis findings is proposed. The proposed setup consists of FESS, programmable PV-system, BESS, electrical load, and power metering devices. As part of this chapter, the electrical schematics of the proposed PHIL setup were developed.

The third chapter focuses on the development of Matlab/Simulink object models for the developed PHIL setup. BESS, PV-generation, and load consumption profiles were modelled in Matlab/Simulink. The BESS was modelled after the datasheets of a real LFP battery (SunGrow SBR096) to research how the PV-system and FESS affect the cyclic lifetime of BESS. PV-generation profile was modelled from 1-minute real measured data into 1-second data via interpolation. Load profiles with a 1-second time-step were modelled with LoadProfile Generator.

In the fourth chapter, the control and communication of the devices (LXI TCP/IP, Modbus TCP/IP) was implemented in the PLC and control scenarios for the devices could be developed. Ringing of FESS measurements was reduced with a moving average filter for the 1-second time-step simulations. The control accuracy of the programmable PV-system was improved to match the reference power with ~99% accuracy during 24-hour simulations. The root mean square error (RMSE) of PV-system was found to be ~8W based on the simulations. The developed scenarios include a base scenario consisting of a load and BESS, a scenario with additional PV-system and a scenario with additional PV-system and FESS. With these scenarios it was possible to investigate the influence on islanded mode duration and battery's (BESS) cyclic lifetime.

In the fifth chapter, the results of Matlab/Simulink and PHIL setup simulations are presented. The simulation results are compared, and conclusion were drawn. The

developed PHIL setup can successfully run PHIL-simulations with a 1 second time-step based on the comparison of Matlab/Simulink and PHIL-simulation results.

The PV-system affects the islanded microgrid in a positive way by noticeably increasing the islanded mode duration of the microgrid. The exact effect depends on the daily load consumption and power generated by the PV-system. During the simulations performed in this thesis, the PV-system increased the islanded mode duration of the microgrid by 11 to 19 hours. It was found that the PV-system can also help reduce the number of cycles the battery must perform on average by ~26%.

The FESS affects the islanded microgrid in a negative way by reducing the islanded mode duration of the microgrid. PHIL-simulation results showed that the FESS helps to reduce the number of cycles the BESS must perform on average by additional ~36%. This value however does not consider the fact that the FESS helps to reduce the number of cycles by operating as a parasite and thus this "good" effect should be disregarded until validated with a modern FESS. The FESS used in this thesis lost on average ~97.26% of the energy used to charge. Of the ~3.53 kWh used to charge the FESS, only ~0.097 kWh could be used again while discharging. The used FESS has very high self-discharge and low energy capacity. This FESS cannot be used in islanded microgrid if the aim is to increase the time duration of islanded mode or extend the lifetime of BESS by reducing the number of cycles the BESS must perform.

A modern FESS with higher energy capacity and lower losses is required to accurately research different scenarios and study how FESS affects the cyclic lifetime of BESS and the time duration of islanded microgrid.

KOKKUVÕTE

Magistritöö eesmärgiks oli luua reaalajasimulaatori (*Power hardware-in-the-loop, PHIL*) katsesüsteem, mis võimaldab uurida kuidas mõjutab hooratasenergiasalvesti ja PV-süsteem erinevate koormuste korral mikrovõrgu akusalvesti (LFP) tsüklilist eluiga ja saartalitluse võimekuse ajalist kestust. Töö eesmärgi saavutamiseks uuriti mikrovõrkude kohta ning analüüsiti mikrovõrkudes kasutatavaid energiaallikaid ja energiasalvestussüsteeme. Lisaks tehti ülevaade PHIL reaalajasimulatsiooni süsteemidest. Leiti, et väikses mikrovõrgus on energiasalvestuseks optimaalseim kasutada keemilise akusalvesti ja hooratasenergiasalvesti hübriidlahendust. Akusalvestid suudavad energiat salvestada pikaajaliselt, aga neil on piiratud tsükliline eluiga. Hooratasenergiasalvestid on seevastu väga pika tsüklilise elueaga, kuid nad ei suuda isetühjenemise tõttu energiat salvestada pikaajaliselt.

Järgnevalt kirjeldatakse olemasolevat TalTech PHIL katsesüsteemi ning tehtud analüüsi tulemuste baasil pakutakse välja olemasoleva katsesüsteemi täiendus. Välja pakutud täiendatud PHIL katsesüsteem koosneb hooratasenergiasalvestist, juhitavast PV-süsteemist, akusalvestist, elektrilisest koormusest ja võimsuse mõõteseadmetest. Selle peatüki osana loodi kavandatud PHIL katsesüsteemi elektriskeemid.

Kolmandas peatükis keskenduti vajalike Matlab/Simulink mudelite arendamisele. Matlab/Simulink keskkonnas modelleeriti akusalvesti, PV-süsteemi toodangu ja koormuse tarbimise profiilid. Aku modelleeriti reaalse LFP aku (*SunGrow SBR096*) andmelehtede järgi, et uurida, kuidas PV-süsteem ja hooratasenergiasalvesti mõjutavad akusalvesti tsüklilist eluiga. PV-toodangu profiil modelleeriti 1-minutilise ajasammuga andmetest 1-sekundilise ajasammuga andmeteks kasutades interpolatsiooni. 1-sekundilise ajasammuga koormuse tarbimise profiilid loodi kasutades LoadProfile Generator rakendust.

Neljandas peatükis loodi tööstuskontrollerile programmid seadmetega suhtlemiseks ja nende juhtimiseks (*LXI TCP/IP, Modbus TCP/IP*). Antud peatüki raames vähendati hooratasenergiasalvesti mõõteandmete müra 1-sekundilise ajasammuga simulatsioonide jaoks kasutades liikuva keskmise (*moving average*) filtrit. Programmeeritava PV-süsteemi juhtimistäpsust parendati ning 24 tunnise simulatsiooni kestel saadi süsteemi täpsuseks ~99%, ruutkeskmise veaga (*RMSE*) ~8W. Loodud stsenaariumid hõlmasid baas-stsenaariumi, mis koosnes koormusest ja akusalvestist, täiendavast stsenaariumist, kus lisati PV-süsteem ning lisaks stsenaarium, kus lisati PV-süsteem ja hooratasenergiasalvesti. Nende stsenaariumite abil oli võimalik uurida mõju saartalitluse pikkusele ja akusalvesti tsüklilisele elueale.

Viiendas peatükis kirjeldati Matlab/Simulink ja PHIL katsesüsteemi simulatsioonitulemusi. Simulatsioonitulemuste põhjal tehti võrdlused ja järeldused. Matlab/Simulink ja PHIL-simulatsioonide tulemuste võrdluse põhjal suudab arendatud PHIL katsesüsteem edukalt jooksutada 1-sekundilise ajasammuga PHIL-simulatsioone.

PV-süsteem aitab märgatavalt pikendada mikrovõrgu saartalitluse ajalist kestust. Täpne ajaline mõju sõltub täpsest päevasest PV-süsteemi toodangu ja tarbimise suhtest. Antud magistritöö raames tehtud 24-tunniste PHIL-simulatsioonide ajal aitas PV-süsteem suurendada mikrovõrgu saartalitluse ajalist kestust 11 kuni 19 tunni võrra. Leiti, et PV-süsteem võib aidata vähendada ka akusalvesti poolt tehtavata tsüklite arvu ~26% võrra.

Kasutatud hooratasenergiasalvesti vähendab mikrovõrgu saartalitluse ajalist kestust. PHIL simulatsioonide tulemused näitavad, et hooratasenergiasalvesti aitab akusalvesti poolt tehtavate tsüklite arvu vähendada veel täiendavalt ~36% võrra. See tulemus aga ei võta arvesse seda, et antud hooratasenergiasalvesti toimib parasiidina ning antud tulemust ei saa arvestada enne valideerimist modernsema hoorattaga. Kasutatud hooratasenergiasalvesti energiakaod olid 24-tunniste PHIL-simulatsioonide käigus keskmiselt ~97.26%. Hooratasenergiasalvesti laadimiseks kasutatud keskmiselt ~3.53 kWh-st sai uuesti kasutada kõigest ~0.097 kWh. Kasutatud hooratasenergiasalvestil on suur isetühjenemine ja väike energiamahtuvus. Antud hooratasenergiasalvestit ei ole seega võimalik kasutada saartalitluses mikrovõrgus, kui eesmärgiks on pikendada saartalitluse ajalist kestust või pikendada aku eluiga akusalvesti tsüklite arvu vähendamisega.

Moderne hooratasenergiasalvesti suurema energiamahtuvuse ja väiksemate kadudega on vajalik, et täpsemalt uurida, kuidas hooratasenergiasalvesti suudab mõjutada mikrovõrgu saartalitluse ajalist kestust ja mõju akusalvesti elueale.

LIST OF REFERENCES

[1] European Commission, "European Commission - A European Green Deal," [Online]. Available: https://ec.europa.eu/info/strategy/priorities-2019-2024/european-green-deal_en. [Accessed 05 02 2022].

[2] IRENA - International Renewable Energy Agency, "Climate Change and Renewable Energy - National Policies and The Role Of Communities, Cities and Regions," 2019. [Online]. Available: https://www.irena.org/-/media/Files/IRENA/Agency/Publication/2019/Jun/IRENA_G20_climate_sustainability_2019.pdf. [Accessed 04 02 2021].

[3] IEA (2021), "Global Energy Review 2021," 2021. [Online]. Available: https://www.iea.org/reports/global-energy-review-2021. [Accessed 03 01 2022].

[4] C. Lyu, "Real-Time Operation optimization of Islanded Microgrid with Battery Energy Storage System," 2020 IEEE Power & Energy Society General Meeting (PESGM), 2020.

[5] E. &. S. J. &. M.-C. J. &. P. J. García-Martínez, "A Review of PHIL Testing for Smart Grids—Selection Guide, Classification and Online Database Analysis," 2020.

[6] C. Y. Hirsch, "Modeling and Simulation of Three-Phase AC Microgrid," Calhoun, 2020.

[7] Q. &. D. K. &. s. s. Tran, "Isolation Microgrid Design for Remote Areas with the Integration of Renewable Energy: A Case Study of Con Dao Island in Vietnam," Clean Technologies, 2021.

[8] B. Lab, "Microgrids - What Are They and How Do They Work?," Berkeley Lab, 2019.

[9] Microgrid Resources Coalition, "Features and Benefits of Microgrids," [Online]. Available: https://www.districtenergy.org/microgrids/about-microgrids97/features. [Accessed 18 12 2021].

[10] M. Brumfield, J. Ferdelman and D. Hess, "gb&d - How Microgrids and Electrification Will Help Prevent the Next Natural Disaster," 01 06 2021. [Online]. Available: https://gbdmagazine.com/how-microgrids-prevent-natural-disasters/. [Accessed 18 12 2021].

[11] H. Alamgir, R. P. Hemanshu, H. Jahangir and B. Frede, "Evolution of microgrids with converter-interfaced generations: Challenges and opprtunities," International Hournal of Electrical Power & Energy Systems, 2019.

[12] M. Ahmed, L. Meegahapola, A. Vahidnia and M. Datta, "Stability and Control Aspects of Microgrid Architectures - A Comprehensive Review," IEEE, 2020.

[13] M. A. &. P. H. &. H. M. &. B. F. Hossain, "Evolution of Microgrids with Converter-Interfaced Generations: Challenges and Opportunities," International Journal of Electrical Power and Energy Systems, 2018.

[14] B. Ponstein and C. Muller, "An Introduction to Microgrids: Combining Multiple Power Sources for Maximum Efficiency and Uptime," Rolls Royce, 2019.

[15] N. M. Kumar and S. S. Chopra, "Hybrid Renewable Energy Microgrid for a Residential Community: A Techno-Economic and Environmental Perspective in the Context of the SDG7," Sustainability, 2020.

[16] T. R. McJunkin and J. T. Reilly, "Net-Zero Carbon Microgrids," 2021.

[17] HOMER Energy, [Online]. Available: https://www.homerenergy.com/. [Accessed 05 05 2022].

[18] E. Wood, "Microgrid Knowledge - What is a Microgrid?," 28 03 2020. [Online]. Available: https://microgridknowledge.com/microgrid-defined/. [Accessed 18 12 2021].

[19] Asian Development Bank, Handbook on Microgrids for Power Quality and Connectivity, Asian Development Bank, 2020.

[20] "Global Wind Atlas," [Online]. Available: https://globalwindatlas.info/. [Accessed 18 12 2021].

[21] Trading Economics, "Trading Economics - EU Natural Gas," [Online]. Available: https://tradingeconomics.com/commodity/eu-natural-gas. [Accessed 18 12 2021].

[22] M. Sterner and I. Stadler, "Handbook of Energy Storage Demand, Technologies, Integration," Springer, 2019.

[23] Asian Development Bank, "Handbook on Battery Energy Storage System," Asian Development Bank, 2018.

[24] Battery University, "Battery University - BU-205: Types of Lithium-Ion," 22 10 2021. [Online]. Available: https://batteryuniversity.com/article/bu-205-types-of-lithium-ion. [Accessed 17 01 2022].

[25] Battery University, "Battery University BU-216: Summary Table of Lithium-based Batteries," 25 10 2021. [Online]. Available: https://batteryuniversity.com/article/bu-216-summary-table-of-lithium-based-batteries. [Accessed 17 01 2022].

[26] W. Jianxue, "Life Cycle Planning of Battery Energy Storage System in Off-grid Wind-Solar-Diesel Microgrid," IET Generation, Transmission & Distribution, 2018.

[27] L. Link, "Research and Development of Power Hardware In The Loop Test Setup For Simulation Of Flywheel Control Scenarios," TalTech Department of Electrical Power Engineering and Mechatronics , 2022.

[28] Rosetta Technik GmbH, "Flywheel Storage system T3-15," Technical documentation.

[29] S. Choudhury, "Flywheel energy storage systems: A critical review on technologies, applications, and future prospects," Electrical Energy Systems Volume 31, Issue 9, 2021.

[30] G. Ramy, "Review on Energy Storage Systems in Microgrids," Electronics 2021, 10, 2134, 2021.

[31] F. Plaum, R. Ahmadihangar and A. Rosin, "Power Smoothing in Smart Buildings using Flywheel Energy Storage," 2020 IEEE 14th International Conference on Compatibility, Power Electronics and Power Engineering (CPE-POWERENG), 2020.

[32] R. Sabzeghar, "Overview of Technical Challenges, Available Technologies and Ongoing Developments of AC/DC Microgrids," 2017.

[33] T. Wu, G. Bao, Y. Chen and J. Shang, "A Review for Control Strategies in Microgrid," 37th Chinese Control Conference (CCC),, 2018.

[34] Y. Zaharaoui, I. Alhamrouni and S. Mekhilef, "Energy Management System in Microgrids: A comprehensive Review," Sustainability, 2021.

[35] K. Sidwall and P. Forsyth, "A Review of Recent Best Practices in the Development of Real-Time Power System Simulators from a Simulator Manufacturer's Perspective," Energies, 2022.

[36] OPAL-RT Technologies, "OPAL-RT Technologies," [Online]. Available: https://www.opal-rt.com/. [Accessed 04 12 2021].

[37] F. Ebe, "Comparison of Power Hardware-in-the-Loop Approaches for the Testing of Smart Grid Controls," Energies, 2018.

[38] M. O. F. K. S. C. D. A. V. a. J. L. G. F. Lauss, "Characteristics and Design of Power Hardware-in-the-Loop Simulations for Electrical Power Systems," IEEE Transactions on Industrial Electronics, 2016.

[39] O. Tremblay, "Contribution to the design of the closed-loop control of a real-time power simulator," 2020.

[40] H. Kikusato, T. S. Ustun and M. Suzuki, "Integrated Power Hardware-in-the-Loop and Lab Testing for Microgrid Controller," IEEE Innovative Smart Grid Technologies - Asia (ISGT Asia), 2019.

[41] C. Seitl, Kathan, Johannes, G. Lauss and F. Lehfuss, "Power Hardware-in-the-Loop Implementation and Verification of a Real Time capable Battery Model," Industrial Electronics (ISIE), 2014.

[42] H. Fakham, T. Qoria, M. Legry, O. Ducarme and F. Colas, "Development of a power hardware in the loop simulation of an islanded microgrid," IECON 2019, 2019.

[43] E. &. G. R. &. V. P. &. C. P. &. R. A. &. L. F. &. L. G. &. K. P. &. G. F. de Jong, "European White Book on Real-Time Power Hardware-in-the-loop testing," 2012.

[44] Siemens AG, "ET 200SP Open Controller," 2018.

[45] Control Techniques, "Unidrive SP - Short Form Guide," 2011.

[46] M. Kesküla, "Planning and design of the electrical installation of the microgrid laboratory," Tallinna Tehnikaülikool - Department of Electrical Power Engineering and Mechatronics , Tallinn, 2020.

[47] VACON, "VACON 3-phase photovoltaic inverters for connection to mains supply drives nxv0010 user's manual," 2011.

[48] Magna-Power Electronics, Inc., "TS Series Documentation - Release 1," 2022.

[49] Siemens AG, "Power Monitoring Device SENTRON PAC3200 manual," 2008.

[50] T. Häring, "Research and Development of Thermal Storage Control Models," Tallinna Tehnikaülikool - Department of Electrical Power Engineering and Mechatronics, Tallinn, 2018.

[51] N. Cinay, "Research and development of control strategies for energy storages in an islanded microgrid," Department of Electrical Power Engineering and Mechatronics, Tallinn, 2020.

[52] N. Pflugradt, "LoadProfileGenerator," [Online]. Available: https://www.loadprofilegenerator.de/. [Accessed 05 02 2022].

[53] VACON, "ARFOFF08 Power generation with general grid codes application manual," 2019.

[54] VACON NX, "OPTCI Modbus TCP option user manual," 2015.

APPENDICES

Appendix 1 Electrical drawings

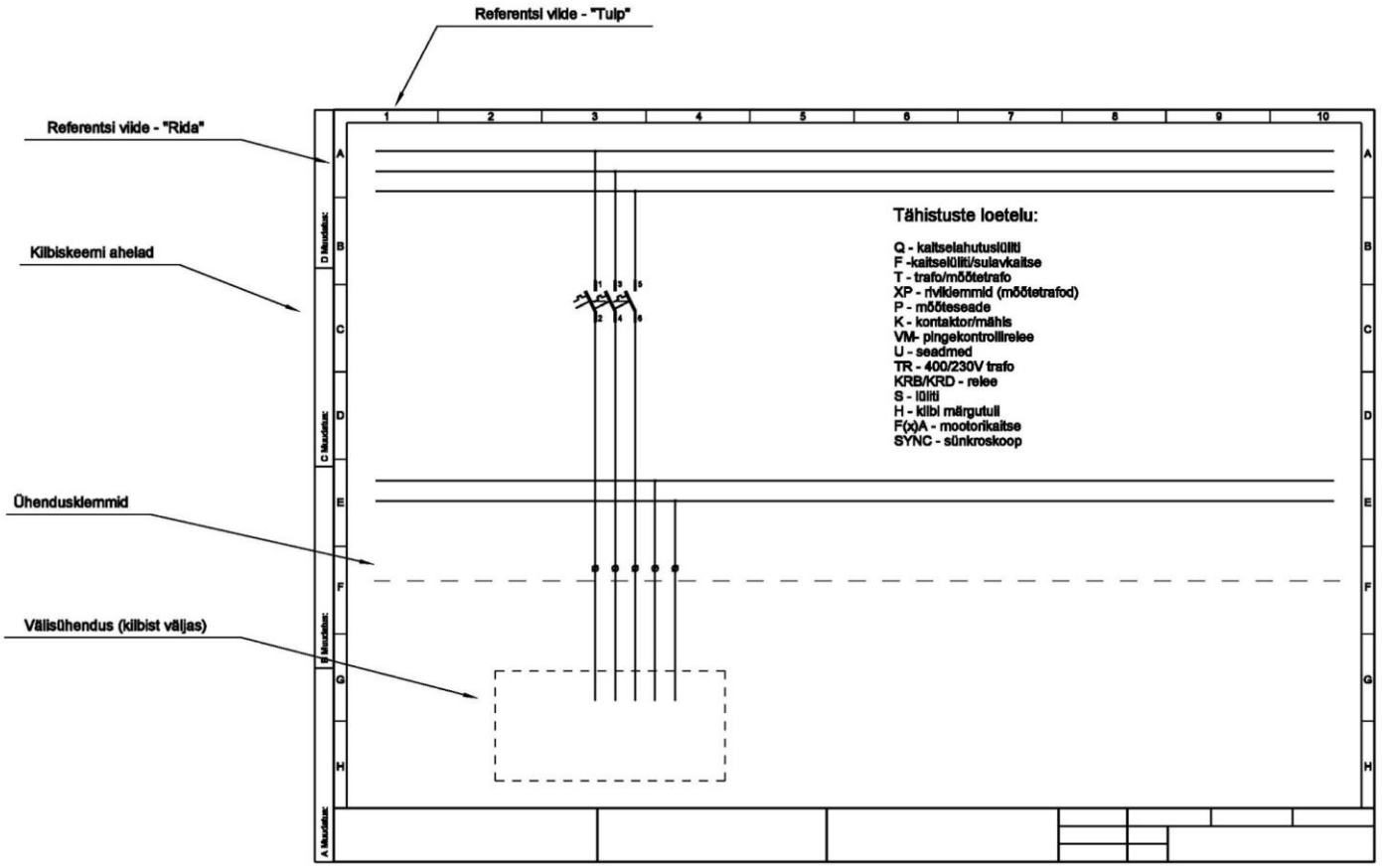

JOONISTE LUGEMINE

Plan. J.Lepik / 14.02.2022	Object ID	Electrical position	Job no.
Draw.	Sheet 2 / 11	Drawing no.	
Check 19.02.2022			

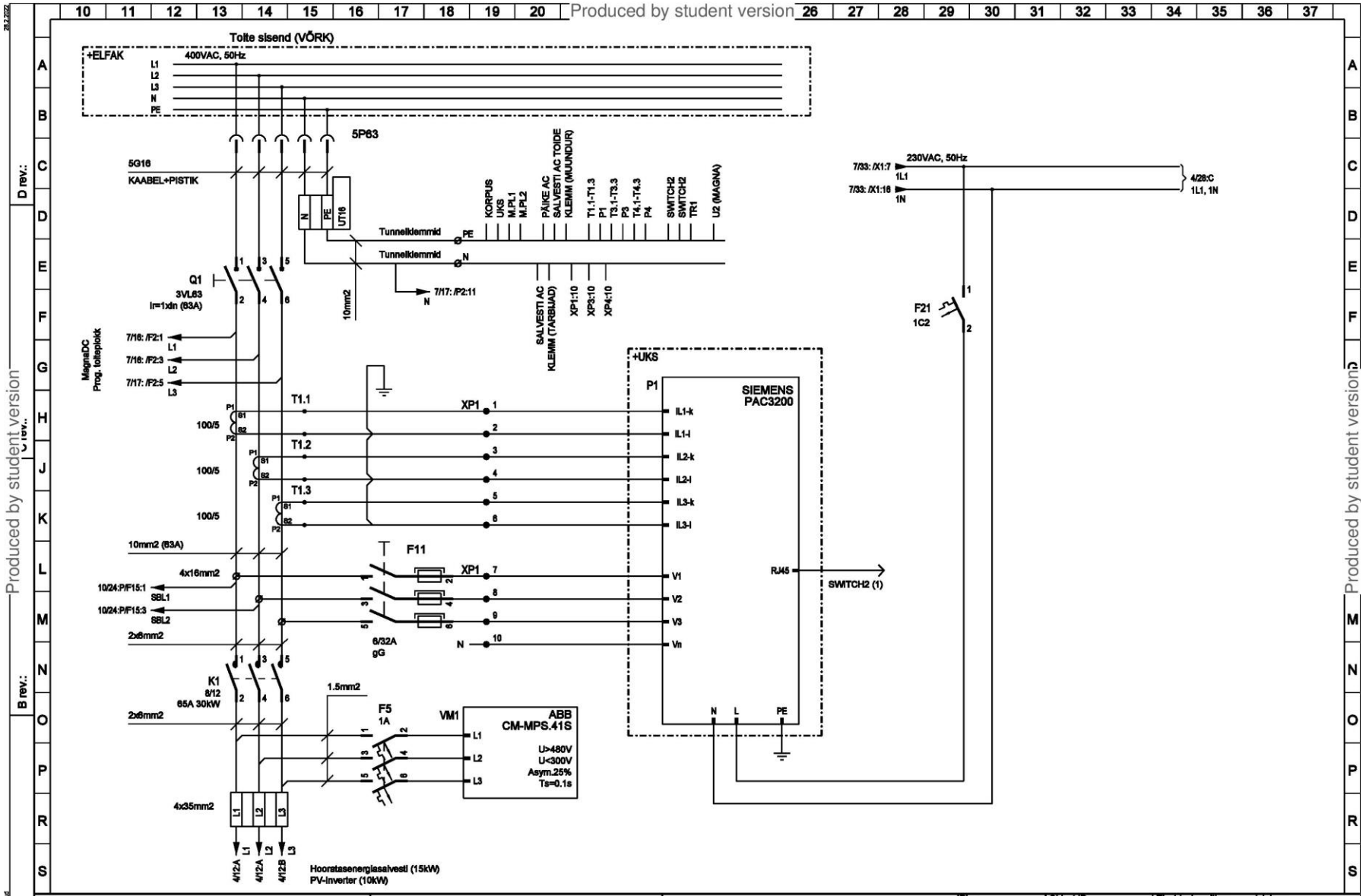

ELEKTRIVÕRK (UTILITY)

Plan. J.Lepik / 14.02.2022	Object ID	Electrical position	Job no.
Draw.	Sheet 3 / 11	Drawing no. 1.1	
Check 19.02.2022			

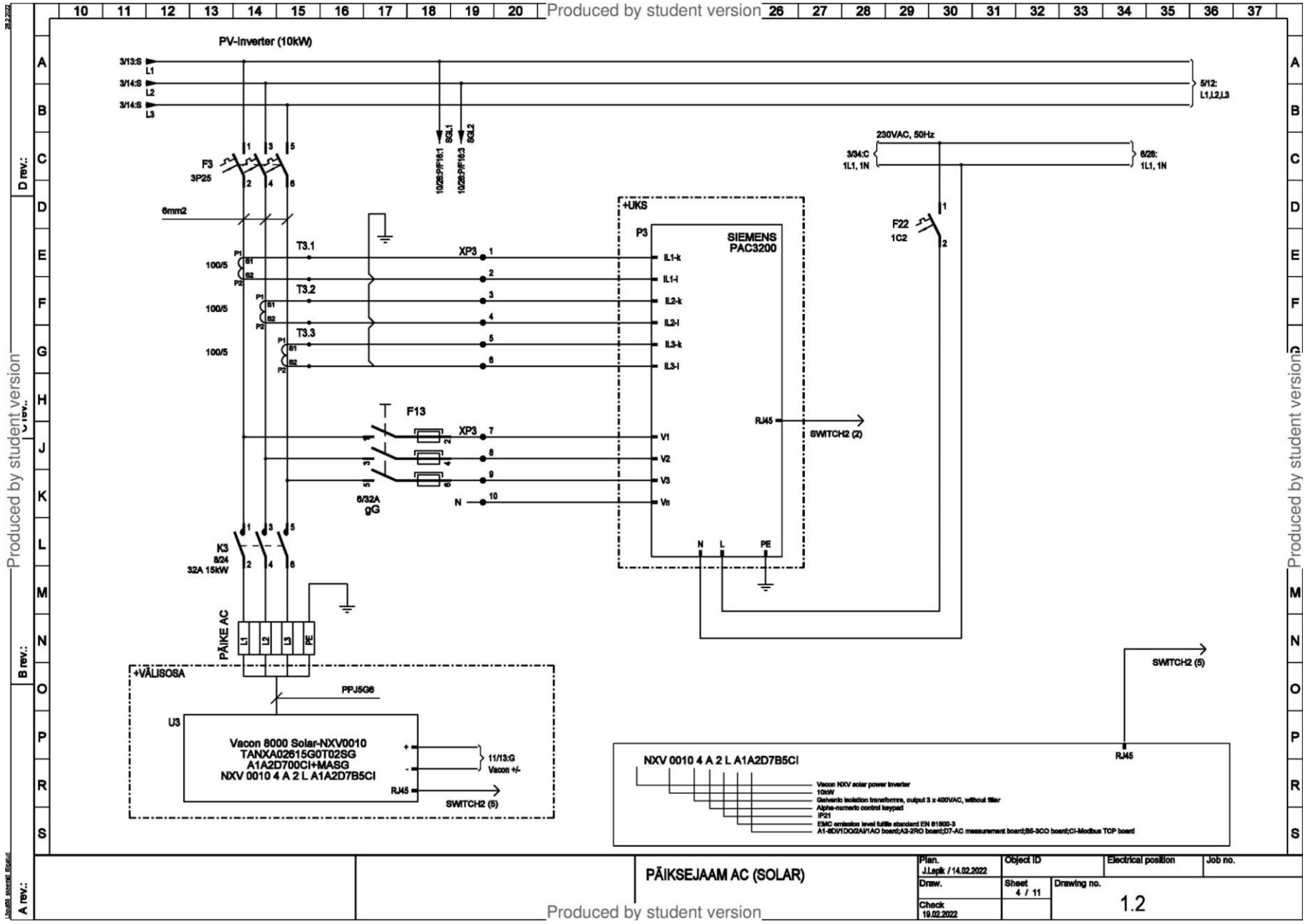

PÄIKSEJAAM AC (SOLAR)

Plan. J.Lepik / 14.02.2022	Object ID	Electrical position	Job no.
Draw.	Sheet 4 / 11	Drawing no. 1.2	
Check 19.02.2022			

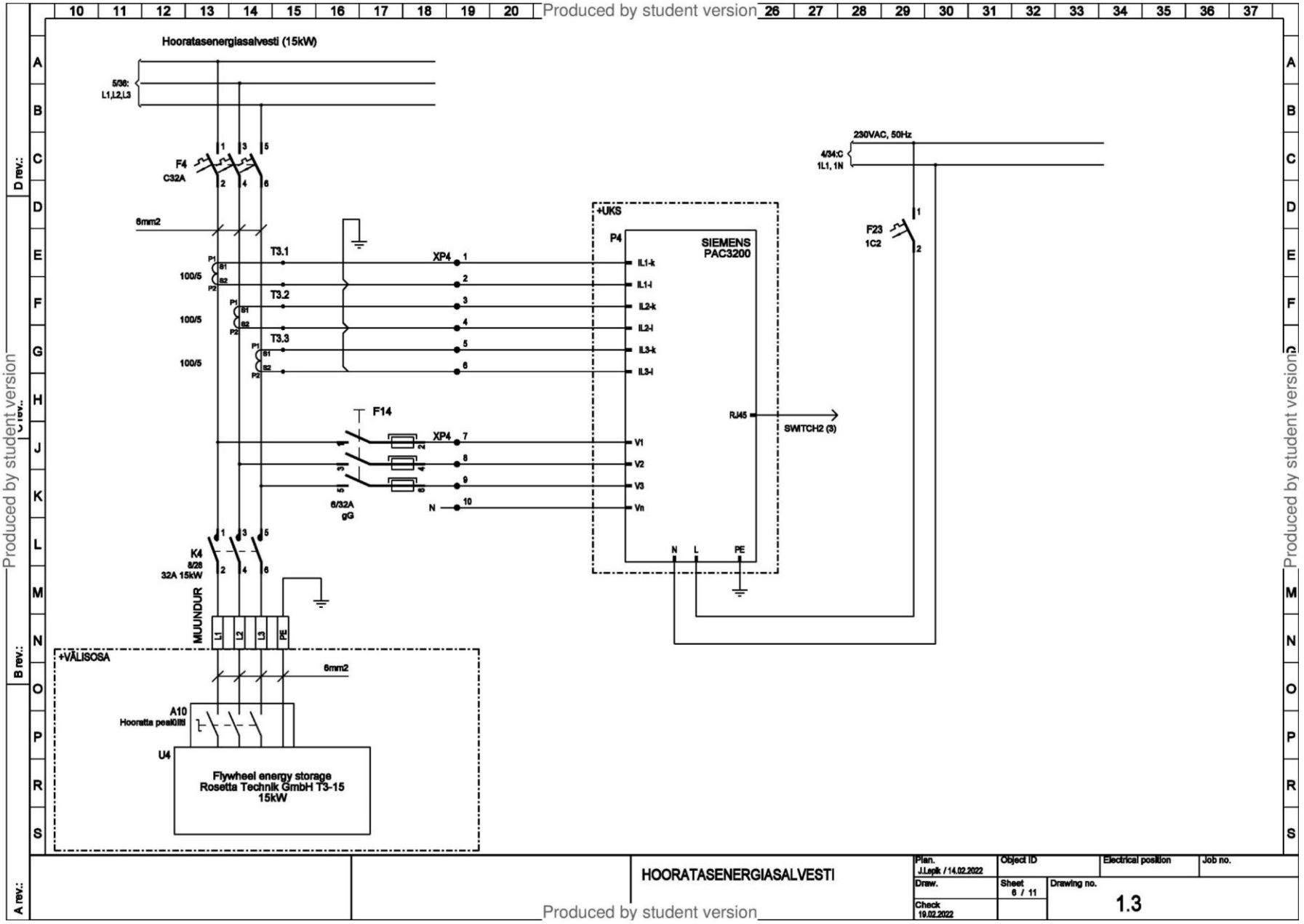

	HOORATASENERGIASALVESTI	Plan. J.Lepik / 14.02.2022	Object ID	Electrical position / Job no.
		Draw.	Sheet 6 / 11	Drawing no. 1.3
		Check 19.02.2022		

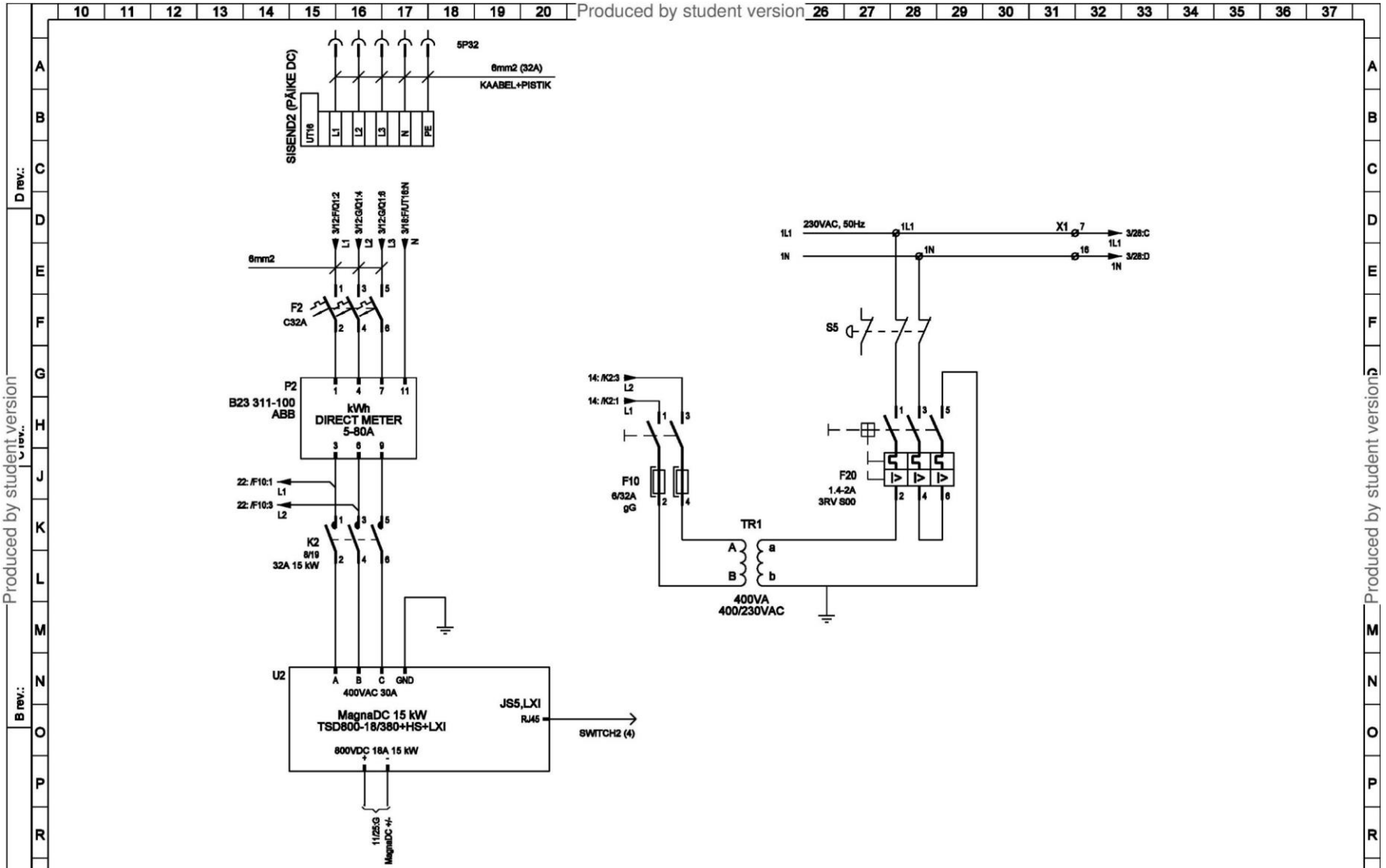

PÄIKSEJAAM DC (SOLAR)	Plan. J.Lepik / 14.02.2022	Object ID	Electrical position	Job no.
	Draw.	Sheet 7 / 11	Drawing no. 1.4	
	Check 19.02.2022			

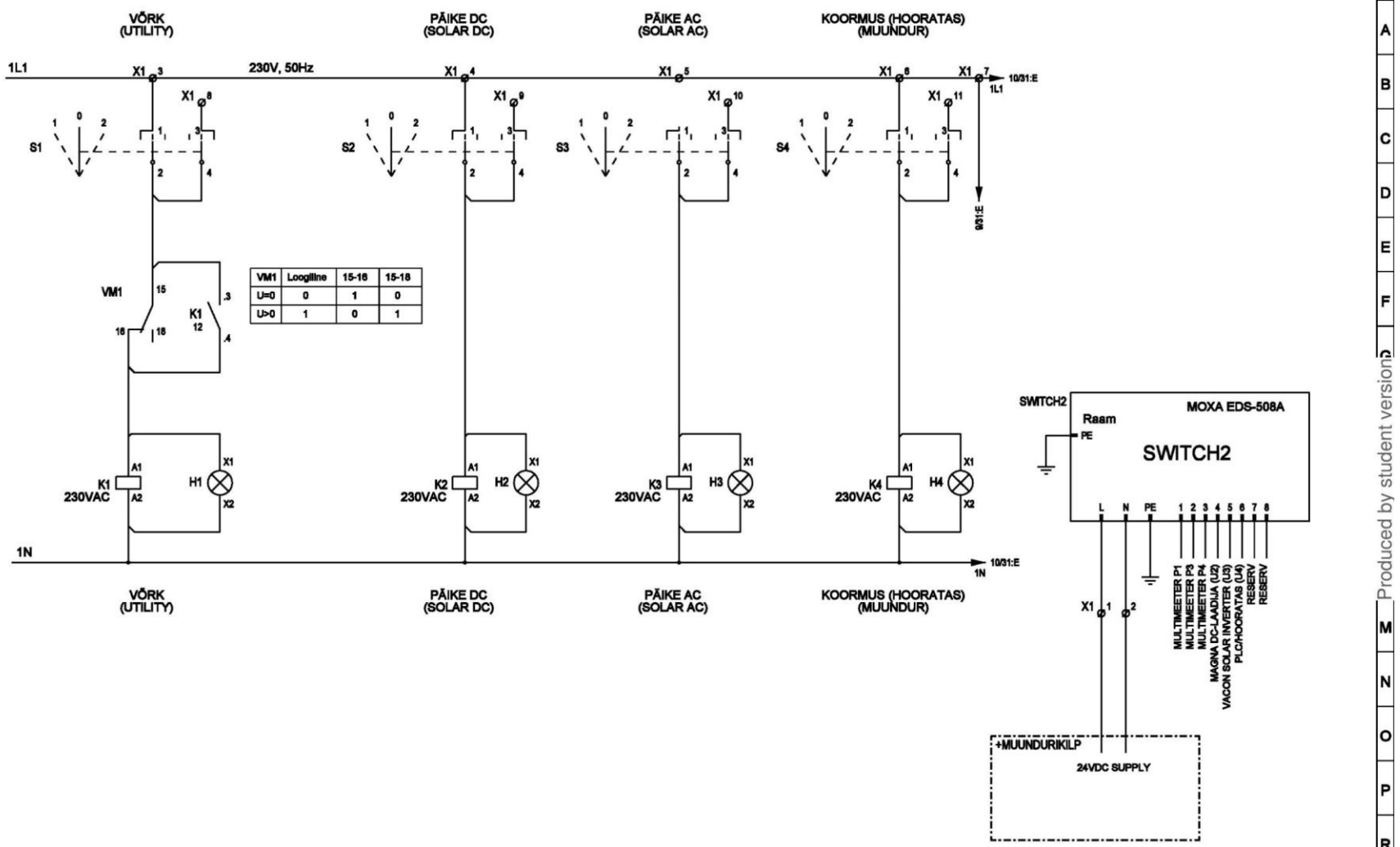

JUHTSIGNAALID

Plan. J.Lepik / 14.02.2022	Object ID	Electrical position	Job no.
Draw.	Sheet 8 / 11	Drawing no. 1.5	
Check 19.02.2022			

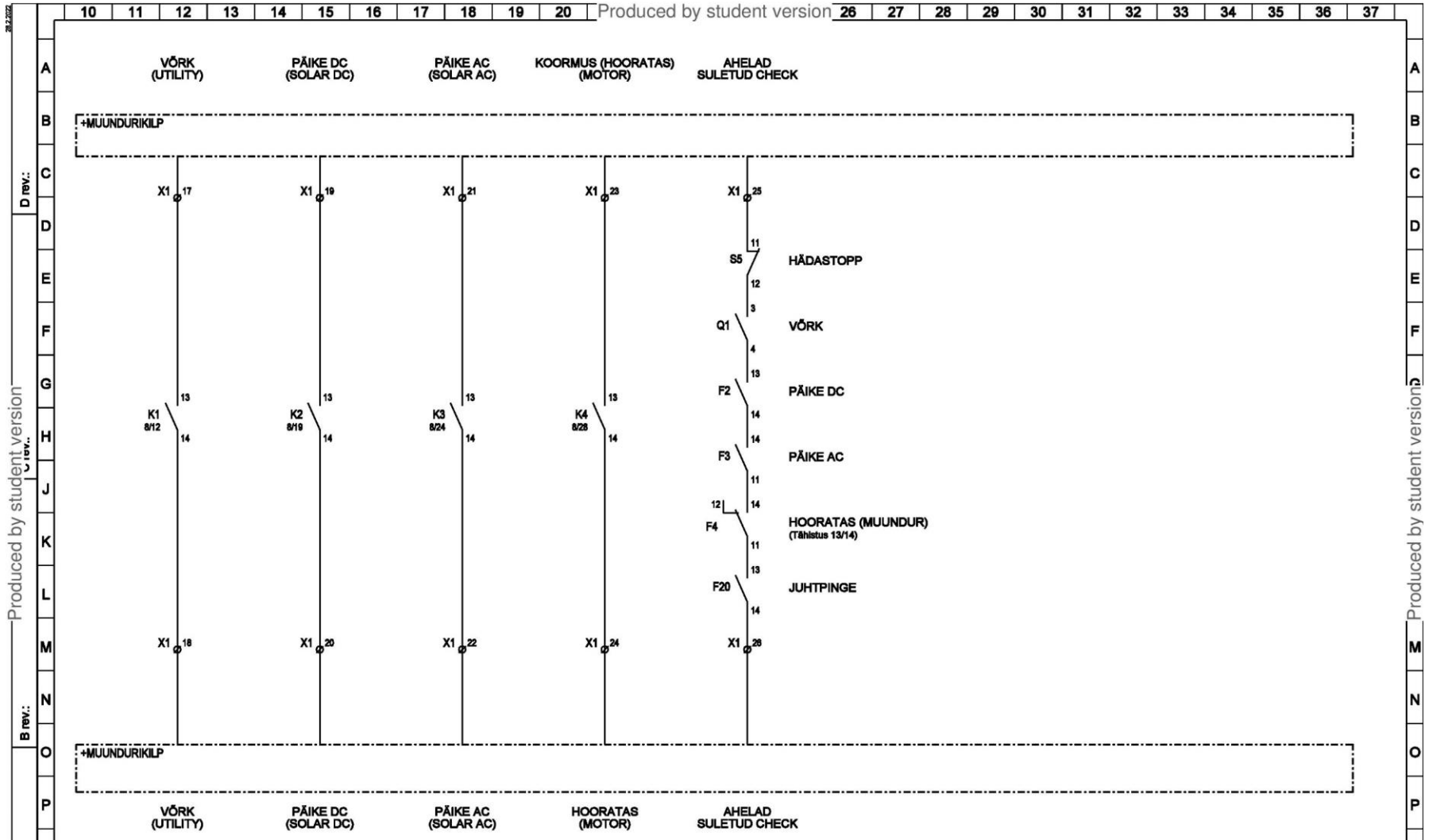

ASENDISIGNAALID

Plan. J.Lepik / 14.02.2022	Object ID	Electrical position	Job no.
Draw.	Sheet 9 / 11	Drawing no. 1.6	
Check 19.02.2022			

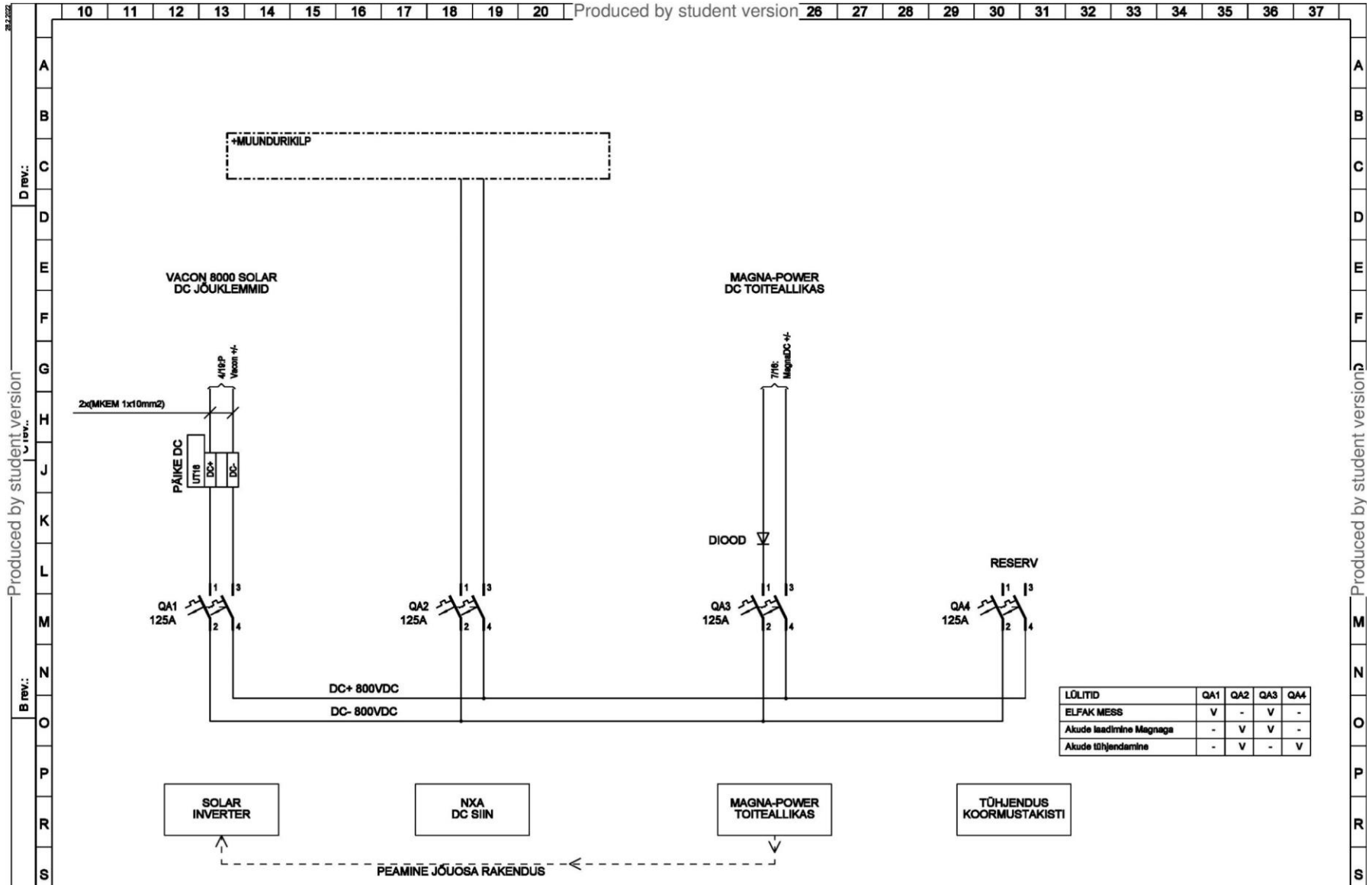

LÜLITID	QA1	QA2	QA3	QA4
ELFAK MESS	V	-	V	-
Akude laadimine Magnaga	-	V	V	-
Akude tühjendamine	-	V	-	V

LISA DC SIIN

Plan. J.Lepik / 14.02.2022	Object ID	Electrical position	Job no.
Draw.	Sheet 11 / 11	Drawing no. 1.8	
Check 19.02.2022			

Appendix 2 Pictures of devices

Flywheel energy storage system

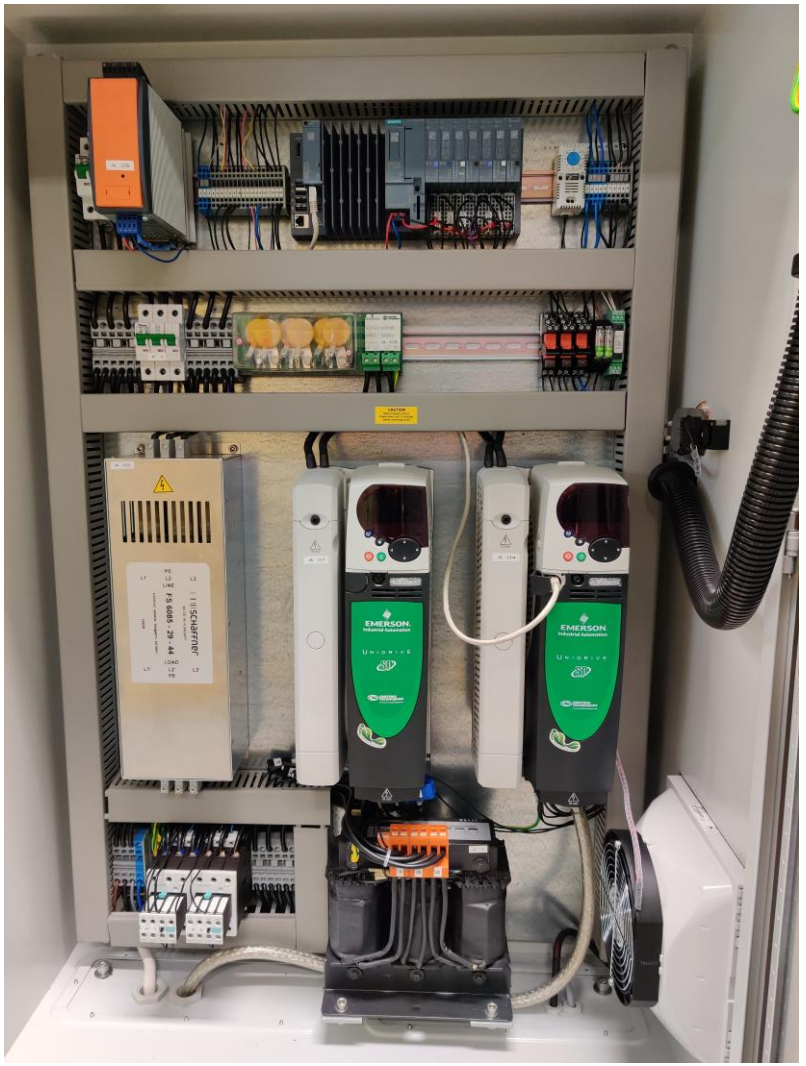

MagnaPower programmable DC power supply

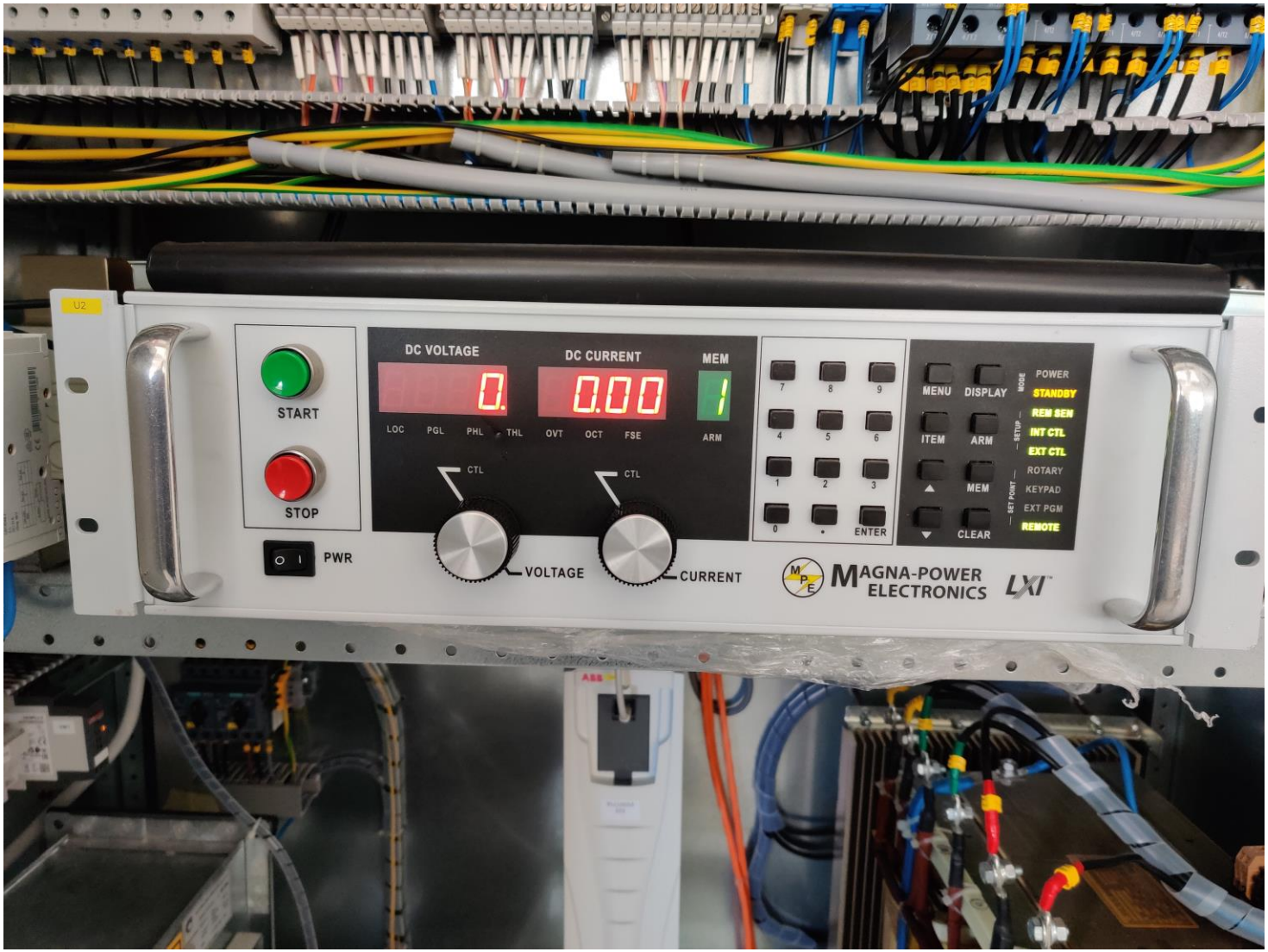

VACON 8000 SOLAR PV-inverter

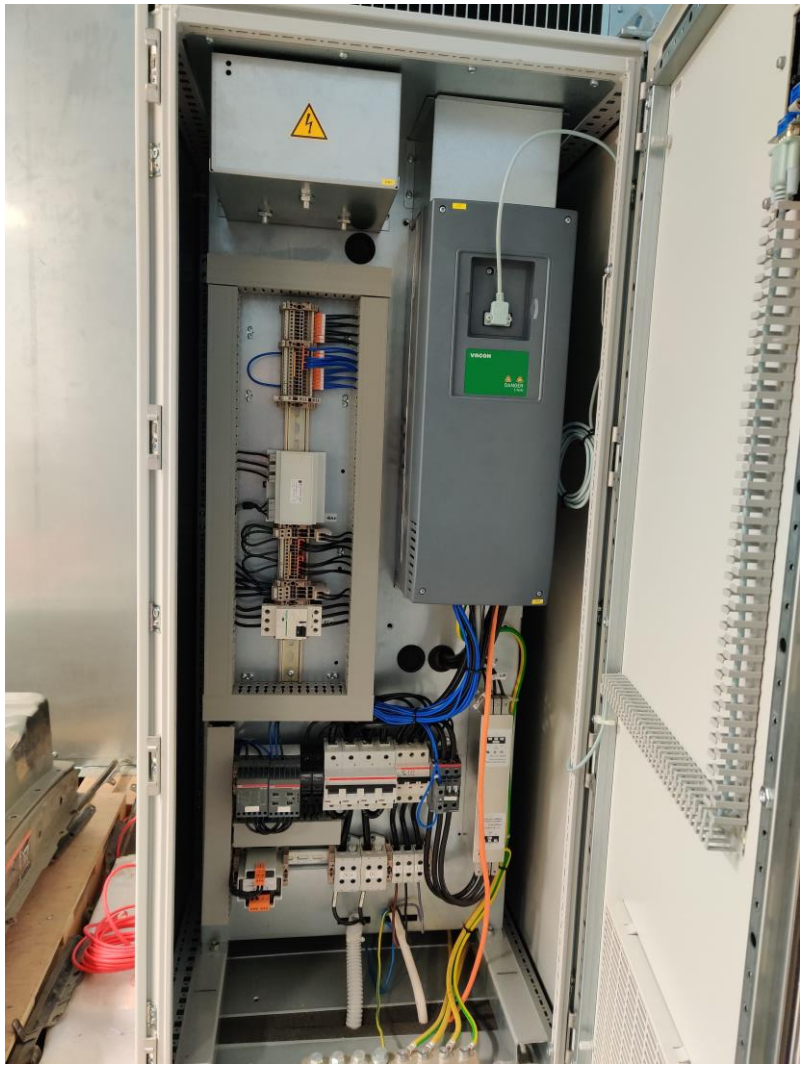

Microgrid main electrical panel; PAC3200 power metering devices